SLAC – PUB – 3726
July 1985
(M)

IRON DOMINATED MAGNETS*

G. E. Fischer
Stanford Linear Accelerator Center, Stanford University, Stanford, CA 94305

TABLE OF CONTENTS

* Work supported by the Department of Energy, contract DE-AC03-76SF00515.

Lectures presented at the 1985 SLAC Summer School on the Physics of High Energy Particle Accelerators, Stanford, California, July 15-26, 1985

IRON DOMINATED MAGNETS

G. E. Fischer
Stanford Linear Accelerator Center, Stanford University, Stanford, CA 94305

ABSTRACT

These two lectures on iron dominated magnets are meant for the student of accelerator science and contain general treatments of the subjects design and construction. The material is arranged in the categories: General concepts and Cost Considerations, Profile Configuration and Harmonics, Magnetic Measurements, a few examples of "special magnets" and Materials and Practices. An extensive literature is provided.

1. GENERAL CONCEPTS AND COST CONSIDERATIONS

1.1 INTRODUCTION

It is quite difficult to give a general lecture since the field of magnet design is limited only by the imagination of the designer and obedience to Maxwell's equations. Still, there are some general principles that can be listed and illustrated by examples so that you can get an overall feeling at what has been done in several laboratories. The theory is of the 19th Century, the practice is today.

These lectures are for students of magnet design and construction - not for the experts, and much of what I am going to say will, I hope, be common sense. I hope at times to be intensely practical, because cost is always an overriding consideration. The key to holding costs under control is simplicity, simplicity, simplicity.

I will concern myself in these talks with iron bounded, that is iron dominated magnets used for and around high energy accelerators. The burgeoning field of superconducting magnets as well as the exciting field of "special magnets", including kickers, rare earth permanent magnets and the like will be treated by experts next week. My own involvement with magnets goes back to my student days now some 35 years ago, just at the time when strong focussing was discovered, and I have never been able to get away from the subject. Being always more interested in their uses and applications, magnets are not my profession and I will therefore give you a generalists impression of this very necessary field. It has taken me through beam lines for experiments, bubble chamber magnets, injection and extraction systems, SPEAR, the Mark I and Mark II detector magnets, PEP, a damping ring and now some 1000 magnets for the SLC arcs.

There is no textbook in this field that I know of, but the next best thing are the proceedings of the first "International Symposium on Magnet Technology" held in 1965 at Stanford University. Symposia were held thereafter about every three years, in Oxford, Hamburg, Brookhaven, Rome, Bratislava, Karlsruhe and Grenoble. The next conference MT-9 will be in Zurich, 9th September 1985.

Another rich source of available information is the "Particle Accelerator Conferences" held every two years in the U.S., whose Transactions are published under the auspices of Nuclear and Plasma Science Society of the Institute of Electrical and Electronics Engineers (IEEE). These meetings have become quite international in character. The last one, the XIth, was held in Vancouver last month. The regular International Accelerator Conferences,on the other hand, tend to deal more with beam dynamics and systems rather than magnets, per sec. I will mention only two more of the many other magnet-related conferences that take place, and they are: "Compumag," dedicated to the computation of electromagnetic fields – the 5th was held in Fort Collins, Colorado last month and the "Applied Superconductivity Conferences," both published under the auspices of the IEEE Magnetics Society.

In these talks, I will use examples taken from the literature and try in each case to provide you with the reference permitting you to later read about the matter in detail. In some small way this will act as a guide to the literature. In this information transfer, there is one more comment to be made. You will quickly discern that the various laboratories have over the years developed distinctive styles in engineering. CERN, for example, drawing on resources from all over Europe tends to construct devices with the greatest of care and attention to every detail. NAL, on the other hand, has had a tradition of producing hardware faster,perhaps more cheaply and therefore more experimental in nature and initial performance. We at SLAC try to steer a middle course in an attempt to obtain the best from both approaches.

1.2 Goals in Magnets Design

What, then, is the question the Accelerator Magnet Designer faces? By magnet designer, I mean the collective of physicist, engineer, mathematician, programmer, financial planner, production manager, materials specialist, quality control inspector, purchasing officer and worker, each of whom brings his or her special knowledge to bear on the problem.

The goal, as I see it, is to produce a product just good enough to perform reliably when the machine turns on and with a sufficient safety factor to take care of anticipated (and unanticipated) future requirements at the lowest cost and on the most timely schedule. It is in estimating these three factors that magnet design, which is in principle an analytic process, turns into an art based

on experience. What does one mean by "good enough" and "reliably" and "future requirements"?

1.2.1 Good Enough

At the project's beginning, the obvious parameters are more or less clearly specified. Field, aperture, ramprate, acceptable power levels, accessibility for installation, maintenance of components, etc. A more difficult one is tolerances. Tolerances are derived by accelerator theoreticians based on considerations such as acceptable orbit distortions, the width of tune stop-bands, the excitation of non-linear resonances (the modern buzz-word is "dynamic aperture"), acceptable values of horizontal vertical coupling, injection and extraction efficiency and the like. Analytic calculations are difficult to interpret and are now generally replaced by computer tracking simulations which are also difficult to interpret. It is in this area that I believe it very important that the magnet designer and the accelerator theoretician establish a very close working relationship so that they can understand and appreciate each others problems. Because overly tight tolerances lead to wasted money!

1.2.2 Reliability

Pardon me for stating something obvious. If we have in a machine, say, 100 magnets, each of which has an uncorrelated failure probability of 0.1% per day, and it takes a day to repair or replace each magnet, the system will be operational about 90 pct. of the time. But, if the machine contains 1000 magnets, it may never run at all. In actual experience, one deals with the concept of mean time between failure and its root mean square deviation so that probability theory must be applied. These facts are well appreciated by industrial designers of, for instance, washing machines and even more so by airplane manufacturers, but are less well known to physicists who are used to dealing with single pieces of "experimental" apparatus. Since the reliability of a new design is essentially unknown, the engineer must strike a compromise between extreme caution and extreme risk. Model work and what is often called structural and "confirmatory" design analysis by independent engineers is called for before proceeding with final design and manufacture.

1.2.3 Safety Factor

In almost every project that I have worked on, the initial design parameters were raised after a few years of operation. Even if the initial funds are very limited, provisions should be incorporated to run the system at some higher energy, current, etc., at a later date without having to tear out the equipment and start anew. This safety factor also permits operation with less wear and tear at the beginning so that design flaws are not disastrous. This matter becomes a negotiation between the project engineer and his management. It is very important, however, for the project engineer to prevent each of his component designers from inserting their own safety factors, since these may be multiplicative and raise cost arbitrarily.

1.3 Steps in Designing Magnets

The procedure some of us follow is summarized in Figure 1.1.

After the field, aperture and length are determined, as I have already mentioned, the question of tolerances should become a matter of negotiation between theoreticians and the designers. By analytic design, I mean first an estimation of the size of the pole faces in order to obtain the required volume of good field. One must also make allowance for the vacuum chamber and its clearances. As you will see later on, one rarely begins from the very beginning but makes use of and modifies designs that have evolved over the years and develops some rules of thumb. That is why looking through the literature can be very helpful. At this point one may wish to set up a 2-dimensional computer lattice relaxation calculation to see if the analytic design is valid, but I caution you not to resort to the computer too early since magnet design is an iterative procedure. Next come the conceptual, mechanical and electrical outlines. They are determined by the facts that the flux density in iron is limited by saturation, and that the current density is limited by cooling considerations. One can now derive the weights of steel and conductor, see if the magnet can be assembled, and calculate its cost of construction and operation. Useful guides in the process are listed in Figure 1.2. The values listed for costs apply to the U.S. in mid 1985 and you will, of course, need to use values which apply to your own situation. Do not forget to take inflation into account. Since practically all the magnets' cost parameters depend on each other, the next step is to start varying these parameters to minimize total overall cost. This means going back to step B and iterate the design remembering also the capital costs of the power supply and installation.

Before discussing each step in more detail, let us look at some actual magnet profiles designed some 20 years ago. Figure 1.3 shows some bending magnet profiles. These examples are taken from Beam Transport line magnet designs

STEPS IN DESIGNING A MAGNET

(A) Define purpose - develop specifications:
Field,aperture,uniformity tolerances,ramp rate,power,cost accesability etc.

(B) Perform analytic design.

(C) Perform first computer design

(D) Mechanical Design:
Material selection, construction techniques forces, weight, alignement criteria etc.

(E) Electrical Design:
Current density,Current, resistance,voltage, temperature rise,time constant
(go back to D if cooling not adequate)

(F) Cost Optimization
(go back to step B and vary secondary parameters)

(G) Examine Installation requirements
(if necessary go back to F)

8-85
5221A1

Fig. 1.1. Steps in Designing a Magnet.

SOME USEFUL GUIDES FOR DESIGN OF CONVENTIONAL MAGNETS

I. Magnet steel begins to saturate ($\mu < 500$) around 15 Kilogauss.

II. The cost of machined steel is about \$ 1.50/# laminated steel is about .35\$/# + .25/hit.

III. The cost of Aluminum Conductor extruded is: ~\$1.50/# and of copper ~\$3.60/#.

IV. Coils with current density J < 1A/mm may not need cooling.

V. Maximum current density for normal water cooled conductor is < 10A/mm^2 or <6000A/in^2

VI. Water flow should be turbulent v > 4-6 ft/sec
Reynolds No.= $\sqrt{D\rho}/\mu$ >4000
v in ft/sec
D in ft.
ρ in #/cu.ft
μ in # sec./ft^2

VII. Price of Power
(a) WOPA (Bureau of Reclamation) 1.89 cents/KWH + demand charge of about 25%
(b) P G & E 4.588cents/KWH* *Large institutional rate

VIII. Cost of putting magnet into service. ie. measurement, installation, cables, power supply etc. is comparable to the Capital Cost of the magnet (Prices mid '85)

8-85 5221A2

Fig. 1.2. Some Useful Guides for Design of Conventional Magnets.

TABLE 1 Bending Magnets

Type number	1	2	3	4	5	
Air gap	15·2	15·2	20·3	15·2	15·2	cm
Maximum field strength	15·6	15·9	3·40	15·6	15·4	kilogauss
Effective length at maximum field	104·6	166·9	39·8	104·4	117·2	cm
Length of polepiece	91·4	152·4	30·5	91·4	101·6	cm
Weight	15·4	28·0	0·52	24·8	50·0	tons
Maximum Voltage	190	190	95	190	190	volts
Maximum Current	450	450	500	450	500	amps
Number of turns	512	544	112	512	480	-
Water flow at 60 psi differential	6·5	6·5	3·6	6·5	7·2	galls/min.
Number available (April 67)	15	7	12	11	4	-
Number on order	-	6	-	-	-	-

Types 1 and 2 are H magnets of conventional design intended to provide momentum analysis in secondary beams. Type 4 is a C magnet version of Type 1. Optimisation of total cost including running cost and cost of power supplies has led to these magnets being more bulky than is common elsewhere. Type 1 and Type 4 magnets may be fitted with polepieces which have tapered sides. This increases the maximum bending strength by 5% at the expense of losing a 15 cm width of good field. The air gap may be varied by inserting or removing spacers in the return leg of the yoke though naturally this can reduce the maximum field at full current.

Type 3 is a weak vertical steering magnet for use with an early type of electrostatic separator. Type 5 is a basic unit of the Spectrometer Magnet Assembly described in Section 7.

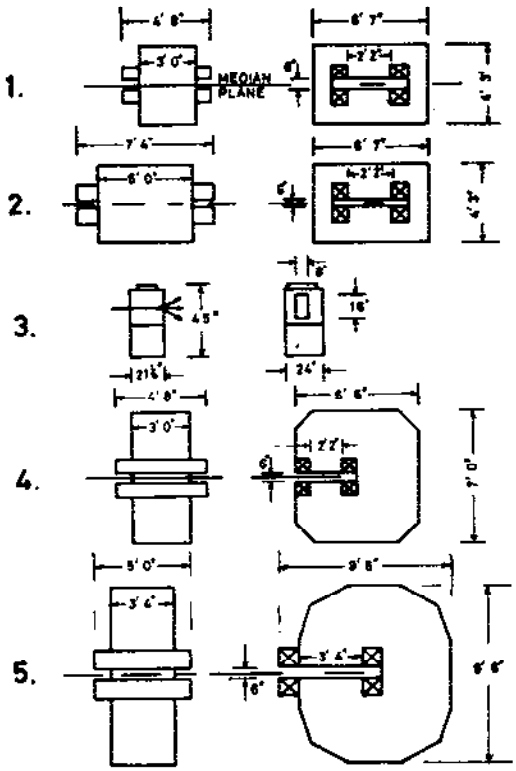

10–95

Fig. 1. Bending Magnets

5221A3

Fig. 1.3. Bending Magnet Design at NIMROD in the Late 1960's.

for experiments at NIMROD England (Ref. 2) and were meant for relatively low energy, large phase space beams (10 cm gaps) and are relatively power hungry for today's times. Figure 1.4 shows the types of quadrupoles that match the

TABLE 2 Quadrupoles

Type number	1	2	3	4	5	6	
Aperture radius	10·2	10·2	10·2	10·2	10·0	10·2	cm
Max. field gradient	1,170	1,015	1,010	965	1,050	1,000*	gauss/cm
Effective length at max. gradient	85·3	49·5	49·3	86·9	85·7	49·5*	cm
Length of polepiece	76·2	38·1	38·1	76·2	75·0	38·1	cm
Overall width of magnet	147·3	114·8	71·9	71·9	50·0	54·6	cm
Weight	6·5	2·0	1·3	2·0	2·2	1·25	tons
Maximum voltage	95	95	95	95	165	106*	volts
Maximum current	500	500	1,000	1,000	850	1,000	amps
Number of turns per pole	121	111	54	43	57	49	-
Water flow at 60 psi differential	5·0	5·0	10·3	10·3	10·0	8·5*	galls/min
Number available (April 1967)	16	30	10	14	6	"	-
Number on order	4	-	-	6	-	"	-

* *Estimated.*

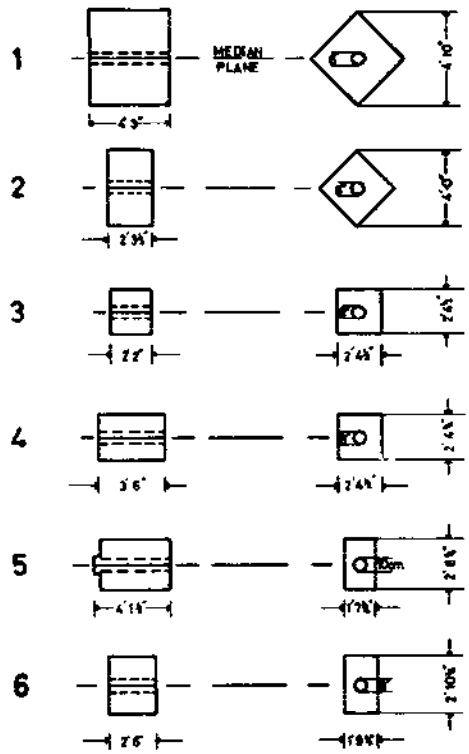

Fig. 2. Quadrupoles

Standard lengths of quadrupole are 76 cm (Types 1, 4, 5) and 38 cm (Types 2, 3, 6). This is the physical length of the polepieces. Quadrupoles of each length have almost identical magnetic parameters. All are of 10·2 cm aperture radius and are fitted with cylindrical end shims. Type 5 is identical to a design used at CERN and its parameters are therefore slightly different.

Types 1 and 2 are designed for minimum total cost and are therefore somewhat bulky. Types 3 and 4 are of smaller overall width and hence higher power consumption. They are intended to be used where the outside dimensions of the Types 1 and 2 are an embarrassment. Their yoke members are arranged to form a square rather than diamond shape. This helps to reduce their width.

Types 5 and 6 are even narrower, being of the Figure-of-Eight configuration described in Section 7. These are intended for use where space is very limited.

10—85

5221A4

Fig. 1.4. Quadrupole Magnet Designs at NIMROD in late 1960's.

bends in aperture. From these pictures you see right away that one is dealing with tens of tons of steel and 50-100 kilowatts of power per magnet. One pays dearly for magnet aperture! In the last few years high quality,large aperture magnets have staged a comeback for use in antiproton coolers (Ref. 21).

1.4 PARAMETERS

1.4.1 Dipole

Let us quickly calculate the current necessary to drive the field across an air gap. In Figure 1.5 we have a magnet that looks like the NAL Bending Magnet.

$$\text{Amperes Law} \oint H \cdot dl = NI \tag{1}$$

is applied – and the integral is evaluated around a flux path enclosing the current so that

$$NI(\text{Ampere Turns}) = \oint \frac{B}{\mu} \cdot dl = \frac{Bg^{\text{air}}}{\mu_0} + \frac{B\ell^{\text{iron}}}{\mu_o}\left(\frac{\mu_o}{\mu_{\text{iron}}}\right) \tag{2}$$

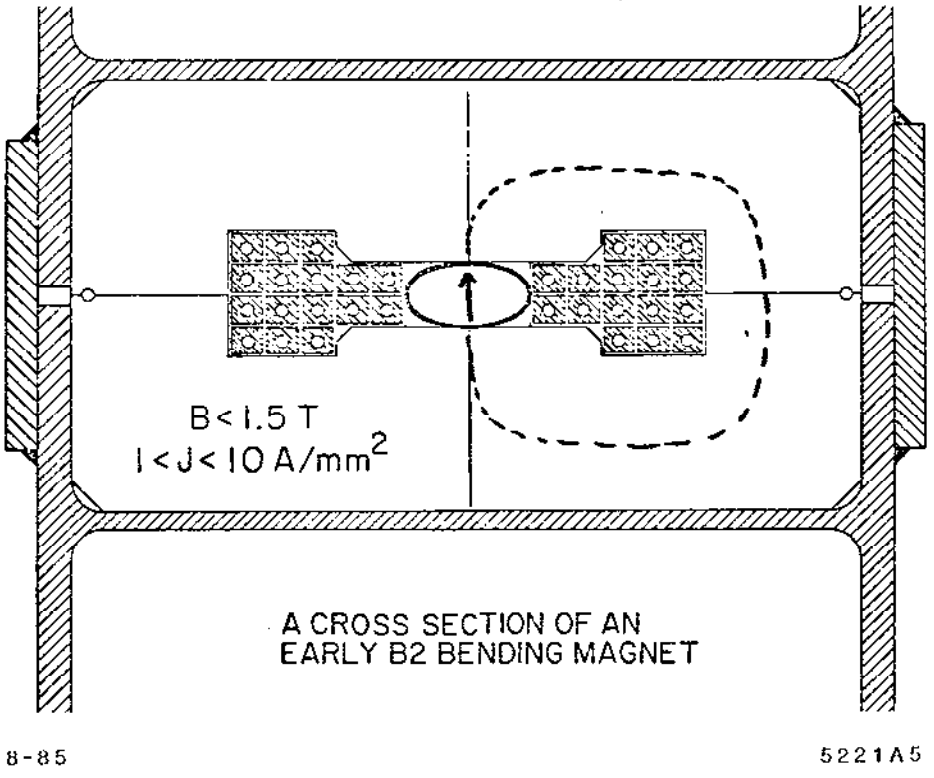

Fig. 1.5. Current vs Field Relationship in a Bending Magnet.

If the iron is not saturated so that

$$\left(\frac{\mu_o}{\mu_{\text{iron}}}\right)\frac{g}{\ell} \gg 1, \tag{3}$$

we can neglect the second term.

$$NI(\text{Ampere}) = \frac{B\left(\text{webers/m}^2\right) g(\text{meter})}{\mu_o = 4\pi \times 10^7(\text{meters/ampmeter})}$$

$$1 \text{ weber/m}^2 = 1 \text{ Telsa} = 10^4 \text{ gauss}$$

Hence the electrical power $P = (NI)^2 R_o$ is proportional to g^2. The effective cross sectional resistance of magnet coil is:

$R_o = \rho\ L/A$

in which ρ is the resistivity of the conductor material

L is the length of the magnet

A is the cross sectional Area of the Coil.

The second term in Eq. (2) leads to an inefficiency due to saturation and is generally kept to less than 10% of the first term by holding the flux density in the iron to less than 1.5 Tesla by providing enough area of steel.

The current density, $J = NI/A$, we will see, is the other critical scaling parameter. Smaller A means smaller magnets, i.e., smaller capital costs but higher power and operating cost. It is also limited by the ability to cool the magnet. Typical values for "standard" applications range from 1 to 10 A/mm^2.

1.4.2 Quadrupole

Let us quickly do the same thing for a focusing magnet. Figure 1.6 shows a 15″ bore quadrupole from the 20-GeV spectrometer at SLAC. Now we wish to evaluate the current to establish a gradient K. The magnet has hyperbolic faces such that the field at a radius r from the axis is $B(r) = Kr$, and we choose the path of integration shown. It is in three parts. Hence

$$NI = \oint H \cdot dl = \int_o^a \frac{B(r)}{\mu^o} dr + [\text{Iron path}] + [\text{path } \perp \text{ to the field}] \tag{4}$$

$$= \int_o^a Krdr = \frac{Ka^2}{2}\ , \text{ ignoring iron} \tag{5}$$

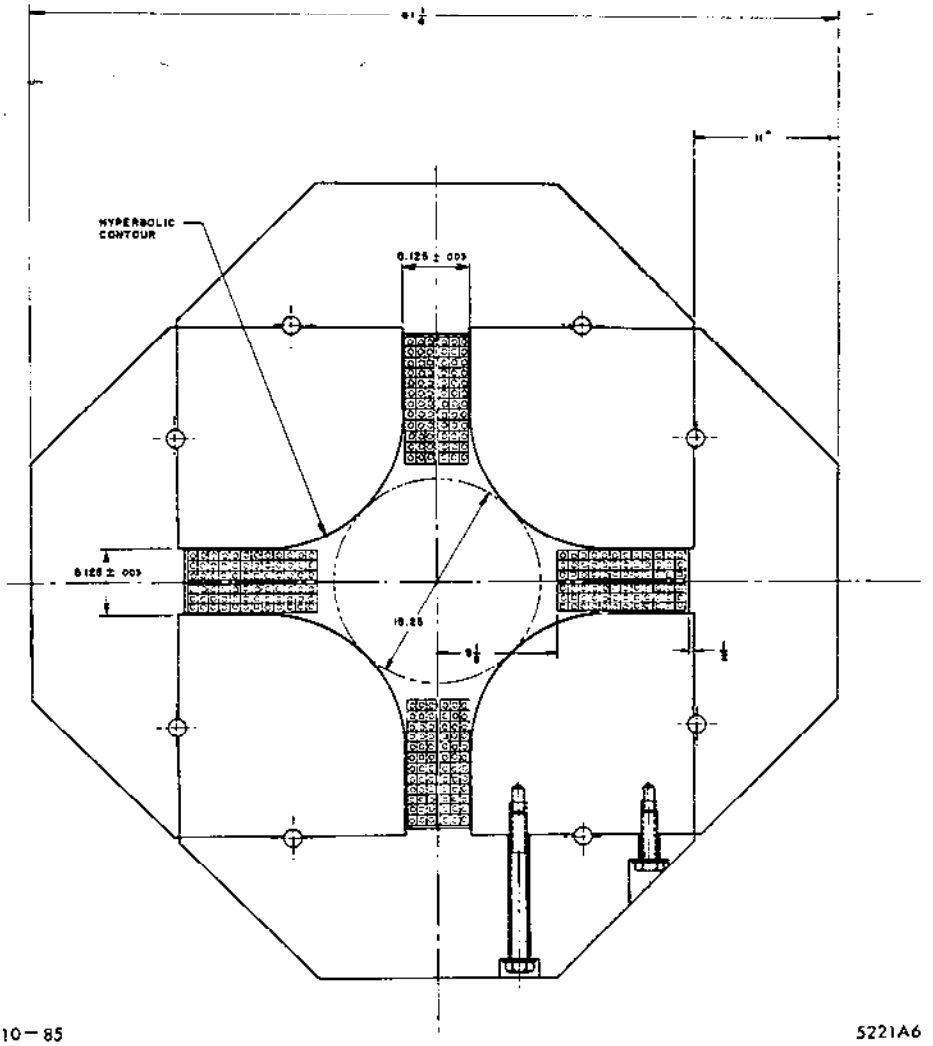

Fig. 1.6. Current vs Field Relationship in a Quadrupole.

path as before. No amp-turns req'd for path $\perp$ to field.

But since $Ka = B_{\text{poletip}}$, we have

$$NI/\text{pole} = \frac{B_{\text{poletip}}(\text{Weber/m}^2) \times a(\text{m})}{2\mu_o = 2(4\pi \times 10^{-7})} \tag{6}$$

very similar to the bending magnet in form except there are 4 poles and the number of Ampere Turns to establish the gradient is proportional to a^2. Hence the Power $\alpha(NI)^2\ \alpha a^4$, i.e. the fourth power of the radius.

Now we have a somewhat more difficult problem getting the coils in. They terminate the hyperbola causing higher order field terms. The more coil area the more problems. This could mean having to increase the aperture, and this

will cost both steel and power. The solutions to these problems are part of the next lecture.

1.4.3 Sextupole

All modern machines and many spectrometers employ sextupoles to cancel or alleviate the effects of chromaticity. By this I mean the fact that the focal lengths of quadrupoles, and hence the tune of a machine (the number of Betatron oscillations/turn), depend on the deviation "dp" of the particles momentum about its central momentum (P_o). In Figure 1.7 are shown some sextupole profiles. If the field $B(r)$ is characterized by a sextupole form, i.e., quadratic in r we have $B(r) = \frac{1}{2}g^1r^2$ and choosing the path as shown

$$NI = \oint H \cdot dl = \oint \frac{B(r)}{\mu} dl = \int_o^a \frac{g^1 r^2 dr}{2\mu_o} = \frac{g^1 a^3}{6\mu_o} \tag{7}$$

or

$$NI/\text{pole} = \frac{B_{\text{poletip}}\ a}{3\mu_o} \tag{8}$$

Incidentally, the equation of the pole is a cubic $3x^2y - y^3 = a^3$.

We note: The power to establish the gradient T/m^2 is proportional to the 6th power of the radius, and it is even harder to squeeze the 6 coils into the cross section.

Fortunately, the sextupolar fields required in most machines are only 10% as strong as quadrupole fields at the edges of the aperture.

1.4.4 Non–Symmetric Profiles

You may have noticed that the sextupole shown in the lower part of the figure is not axially symmetric. It has , in fact, been tailored to fit an elliptic vacuum chamber largely because of power considerations. Let me warn you, however, I think that this sextupole is difficult to build. More usually seen are what have come to be called "Collins" (for Tom Collins), or "Figure 1.8" or "Narrow" quadrupoles. Figure 1.8 shows an early design and flux pattern. Notice that it has no sides and is especially useful in those applications where beams must pass close to each other in one plane. Another example is the NAL main ring quadrupole shown in Figure 1.9. In Refs. 3 and 4 you will find details of a few other examples. If carefully constructed they can have every bit as good field quality as symmetric quads.

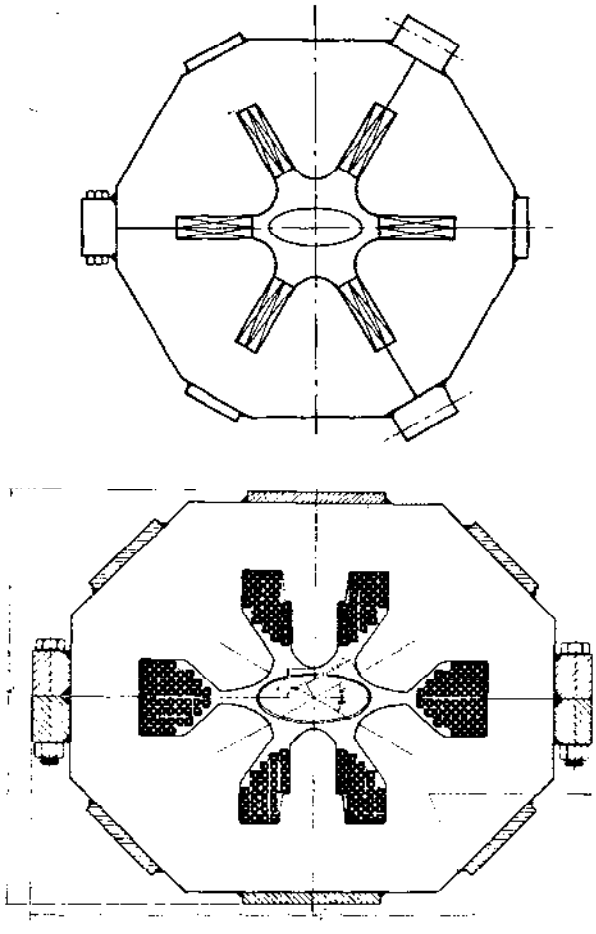

Fig. 1.7. Current vs Field Relationship in a Sextupole.

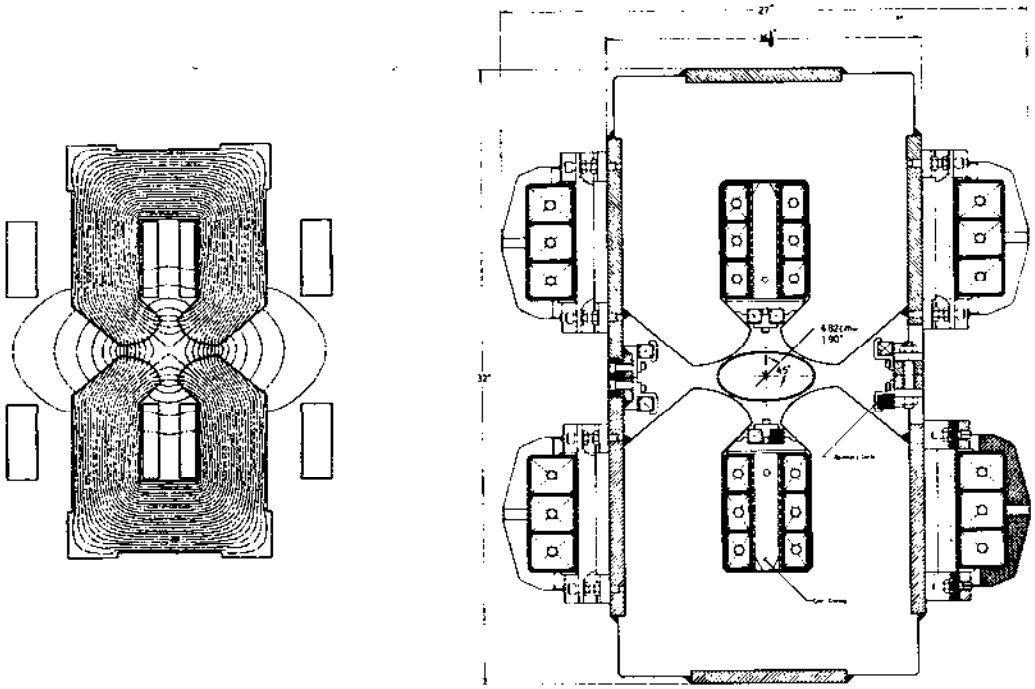

Fig. 1.8. Example of a "Figure 8" or "Collins" Type Quadrupole.

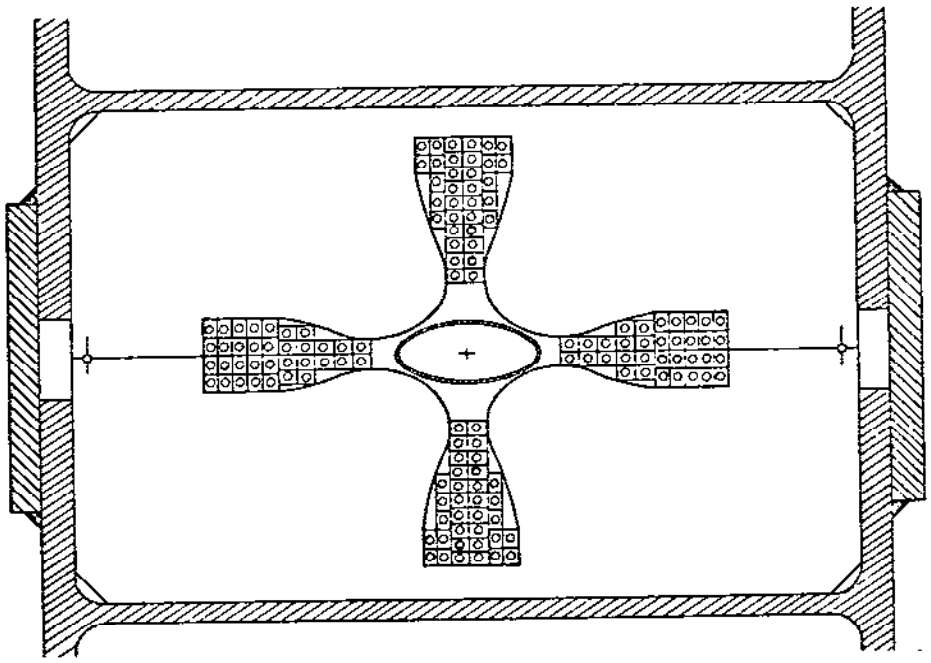

Fig. 1.9. Eliptic Cross Section of an FNAL Main Ring Quad.

1.4.5 Window Frame Designs

In Figure 1.10 are depicted some dipoles that appear to have no poles. These are often used as steering correction elements, and because in this case the coils return outside the iron, are less efficient. Field quality, however, in the absence of saturation is excellent.

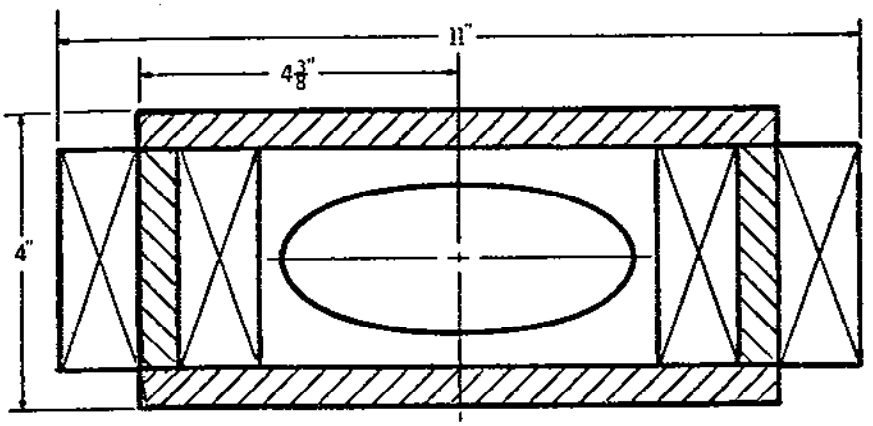

Horizontal Closed Orbit Deflector

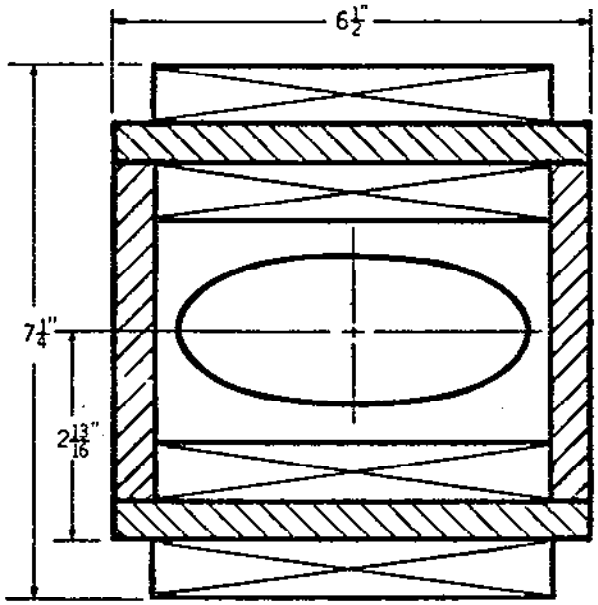

Vertical Closed Orbit Deflector

8-85 5221A10

Fig. 1.10. "Poleless" Dipole Corrector – Profiles.

The quadrupole version of this concept is shown in Figure 1.11 and is often called the Panofsky Quad. It can be made with excellent field quality but is used only as a correction element, because it otherwise consumes too much power. It is really an example of an ironless magnet, and this subject leads naturally into the superconducting field which is beyond the scope of these lectures. Clearly the magnetic field is determined by the placement of the conductor not the steel return yoke.

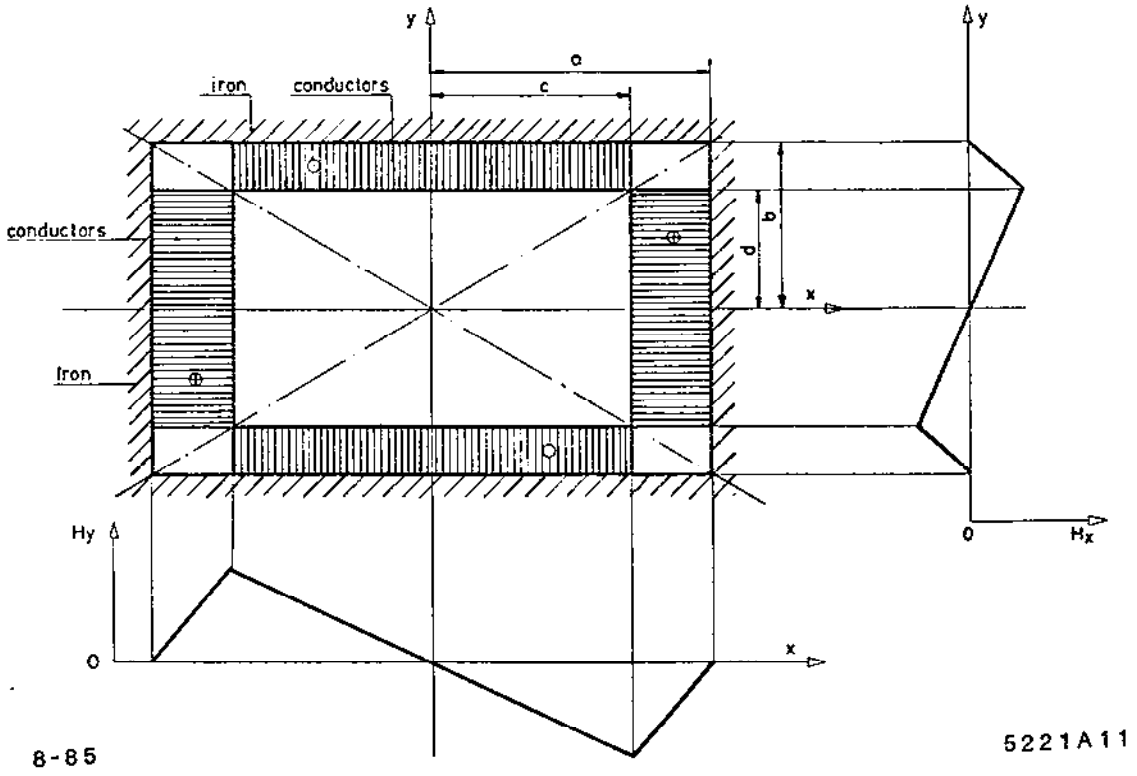

Fig. 1.11. A Poleless "Panofsky" Quadrupole.

1.5 General Review References

At most magnet conferences some distinguished author is called upon to review the state of the field. See for example Refs. 5 and 6. The one by Professor M. Stanley Livingston, Ref. 7, co-inventor of the cyclotron and of strong focussing and one of my former mentors, traces the historical development of accelerator magnets up to 1970 and, I would say, is required reading for the student.

1.6 Examples – Old and New

The rationale of the design and the performance of booster magnets at CERN and NAL and KEK may be of interest to you. References 8, 9 and 10 give details. The CERN Booster is noteworthy in that 4 bending and 4 focusing elements are stacked on top of each other. Figure 1.12 shows how these magnets are realized. References 11 through 14 detail the NAL Main Bends and Quads.

Observe how multiple magnets remain with us. Figure 1.13 depicts the Texas Accelerator Center's entry into the SSC sweepstakes. It shows (life-size) the lamination of the cold iron "superferric" magnet which is energized, however,by superconducting coils (Ref. 20). At low fields this magnet is clearly dominated by the shape of the configuration. Its field uniformity is adjusted over a very wide dynamic range (over 3 Tesla) by varying the current in three separate windings. There are to be 1000 magnets, each 140 meters long!

1.7 Cost Optimization

As stated at the outset, one of the main goals in accelerator design is to design for minimum total cost. Total cost includes not only the capital cost of the magnet but also the capital cost of the power supply, power distribution and cooling system and especially the estimated operating costs of power over the projected life of the project. The procedure given by Brianti and Gabriel at CERN, Ref. 15, for DC and AC magnets is noteworthy. The main scaling parameter they use are the length of the magnets and the DC or peak current density (J) in the coils. Other considerations are listed in Refs. 16 through 18. Here is what the CERN people do:

They consider magnets of the types shown in Figures 1.14 and 1.15 with the dimensions indicated.

A summary of cost expressions is shown in Figure 1.16.

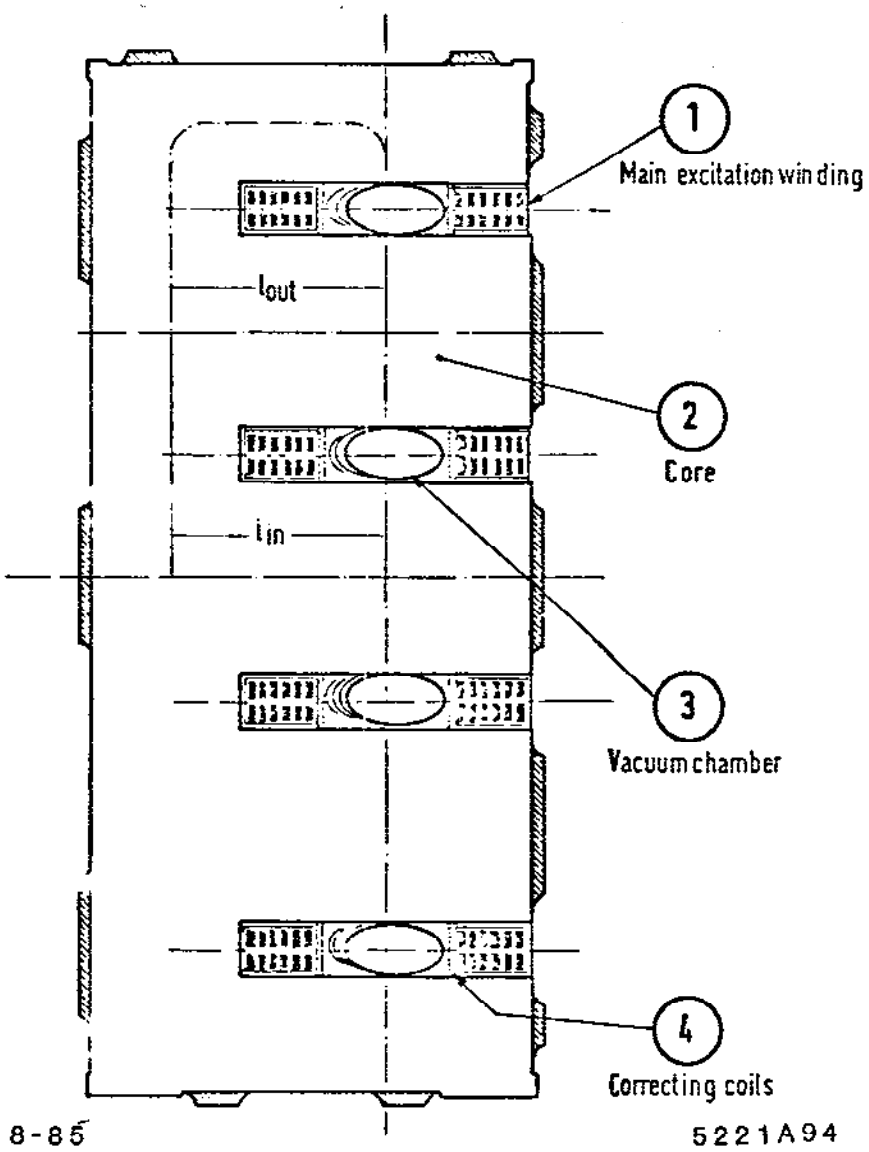

Fig. 1.12. Example of a "Multiple Magnet" at the CERN P.S. Booster.

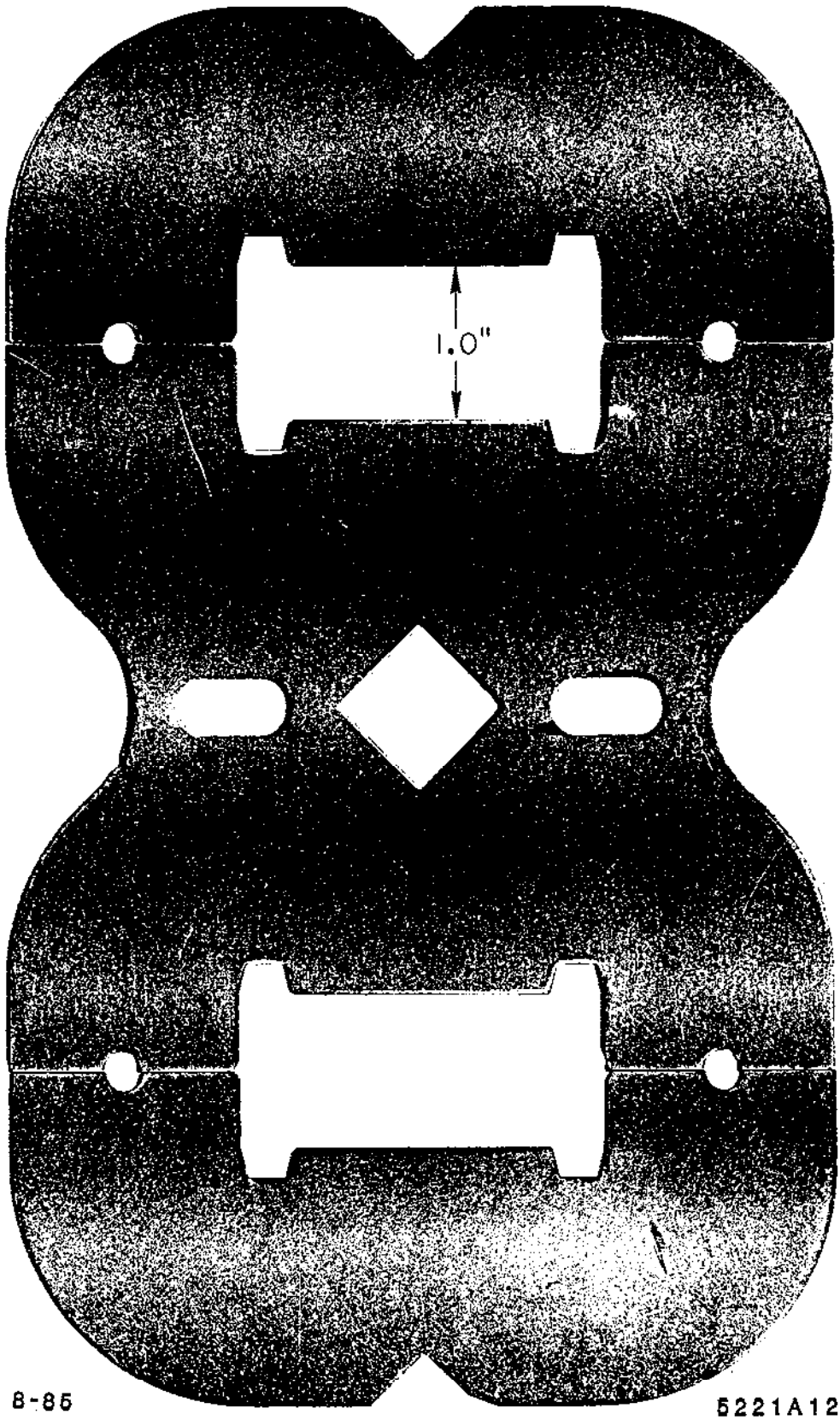

Fig. 1.13. The TAC "Superferric" SSC Bending Magnet Lamination.

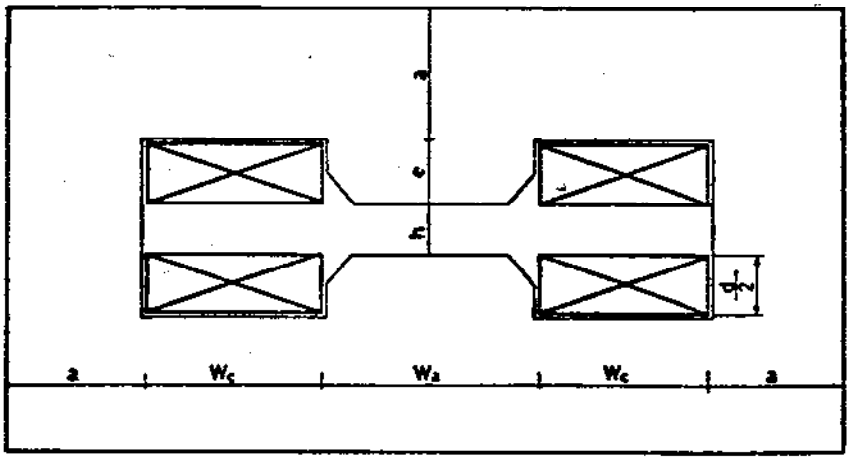

H Magnet with "flat" end connections of coils.

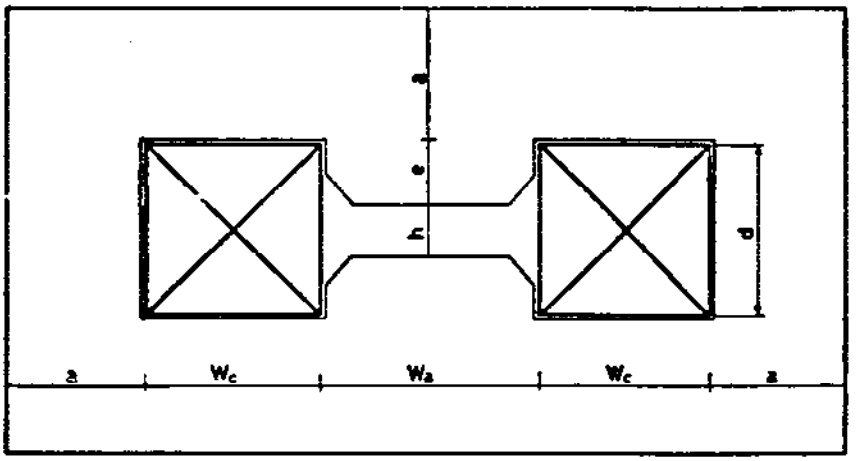

H Magnet with "saddle-shaped" end connections of coils.

8-85 5221A13

Fig. 1.14. Cross Sections Evaluated in Cost Optimizations (A).

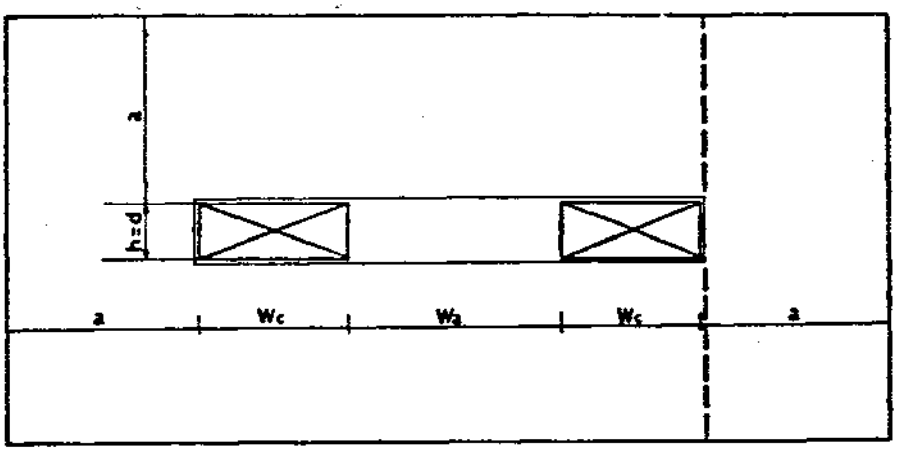

Window-frame magnet (with one or two return yokes).

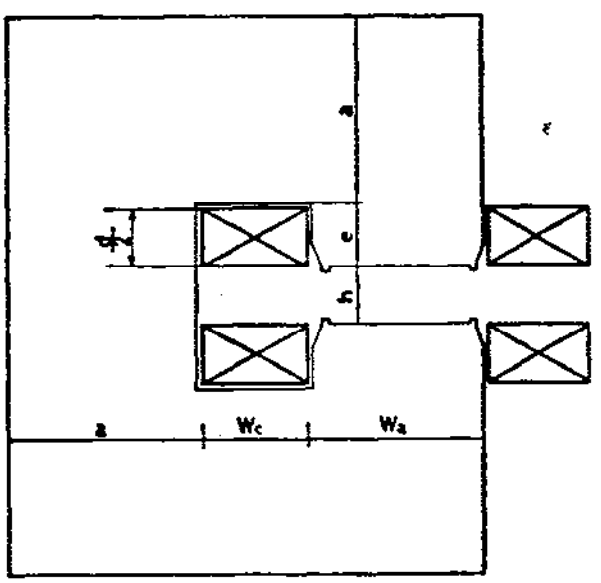

8-85 C magnet. 5221A14

Fig. 1.15. Cross Sections Evaluated in Cost Optimizations (B).

FACTORS THAT DETERMINE SYSTEM COSTS

M_e=Equipment Cost = $M_1 + M_2 + M_3 + M_4 + M_5$

M_1 = Cost of power supply and associated equipment

M_2 = Cost of finished coil mounted in the yoke

M_3 = Cost of finished yoke

M_4 = Cost of AC and DC Power distribution system

M_5 = Cost of cooling system,pumps distribution,towers etc.

M_o=Operating Cost = Cost of power to run magnets,distribution and cooling systems

.....

$M_1 = M_{01}$ = Cost of Equipment that is independent of Power (such as cublicles,controls,regulators etc) + [cost/KW of supply] x Power x $1/\eta$ (where η is efficiency of conversion)

M_2 = [finished cost/m^3] x volume of conductor

M_3 = [finished cost of core/m^3] x volume of core

M_4 = [cost/KW of distribution] x Power

M_5 = [cost/KW of water system] x Power

M_0 = [Cost/KWHr of electricity] x Operating hours x β x Power

(where β takes into account rectifier and distribution losses and the use factor, ie. the system is not always at full power)

8-85 5221A93

Fig. 1.16. Factors That Determine Magnet System Costs.

In this study expressions are then developed for all the coefficients using some set of fixed input parameters.

$$\frac{P\theta}{3} = \text{total bending power in TM req. (5 TM)}$$

$$\theta_m = \text{maximum deflection angle per magnet (.05 rad)}$$

$$h = \text{gap height (5 cm)}$$

$$\frac{\Delta B}{B} = \text{field accuracy } (10^{-3})$$

$$T = \text{running time } 30,000 \text{ hrs. } (\sim 8 \text{ yrs.})$$

Letting the length of magnet and current density be "free" parameters.

One could of course differentiate the total cost with respect to the free parameters to find the minima, but it is more instructive to calculate some cases.

Results for a large set of 5 Tesla Meter Magnets at CERN in 1970 are shown in the following Figures. The conductor material is copper. I infer that a power cost of .03 SF/KW hour was used.

Figure 1.17 shows the obvious – Power varies as J, also longer magnets have less end conductors.

Figure 1.18 shows that Volume of coil varies inversely as the square of J.

Figure 1.19 shows Volume yoke varies inversely as the square of J.

Figure 1.20 cost of various things for fixed length, showing that around 4 A/mm^2, the P.S. + magnet costs are about equal.

Figure 1.21 shows minimum cost for J around 4.3 A/mm^2

Figure 1.22 shows a minimum around 5 A/mm^2 with cost of electricity halved.

The Conclusions

1. Power is very important – it enters into the equipment cost through the P.S. and in cost of electricity.
2. Design fluxes should be in 1.2 to 1.7 Tesla region.
3. Minima in J are broad but around 4 A/mm^2.
4. Try to keep magnets long to minimize end effects.
5. Run many magnets in series to minimize P.S. costs.

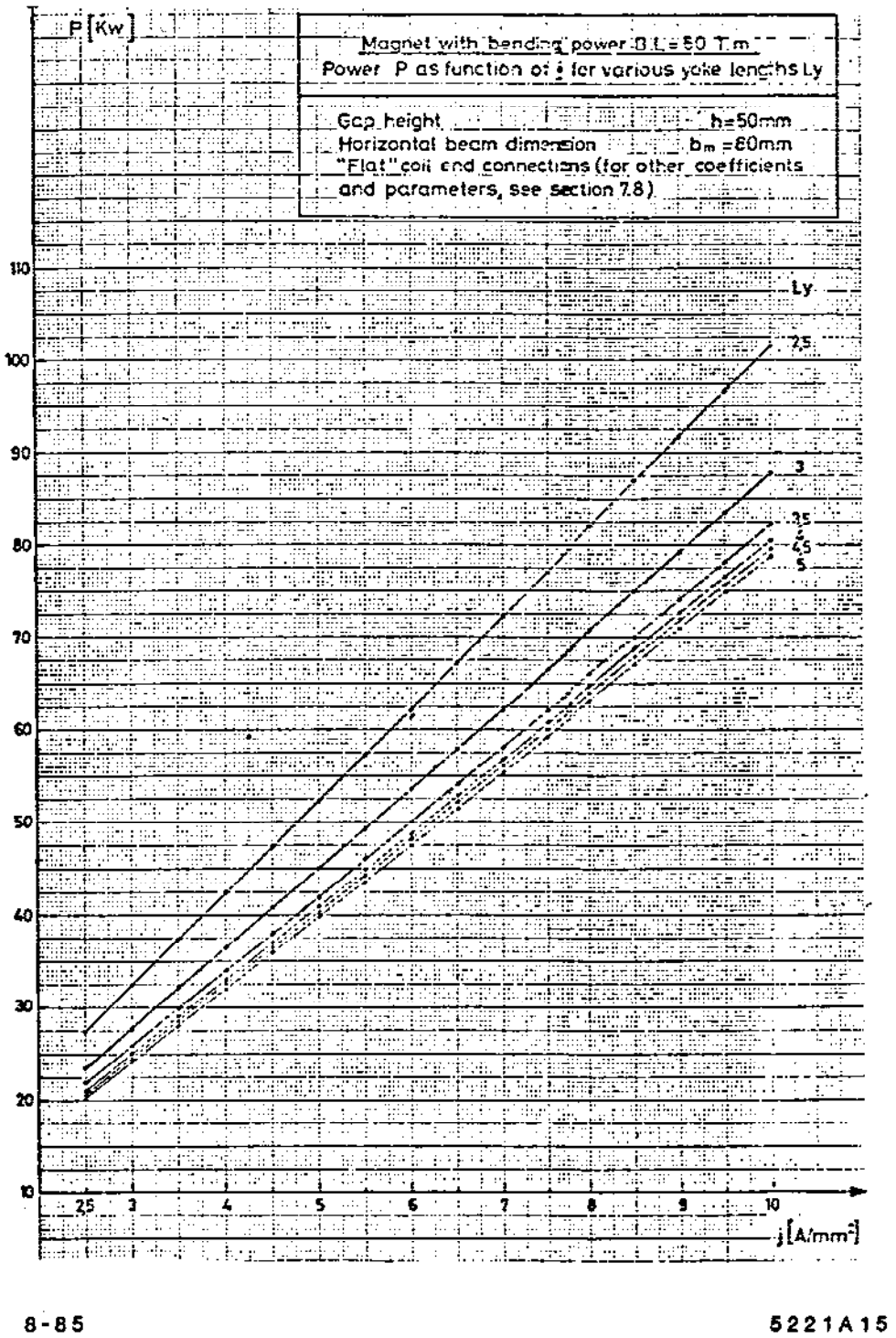

Fig. 1.17. Cost Study – Power vs Current Density (J).

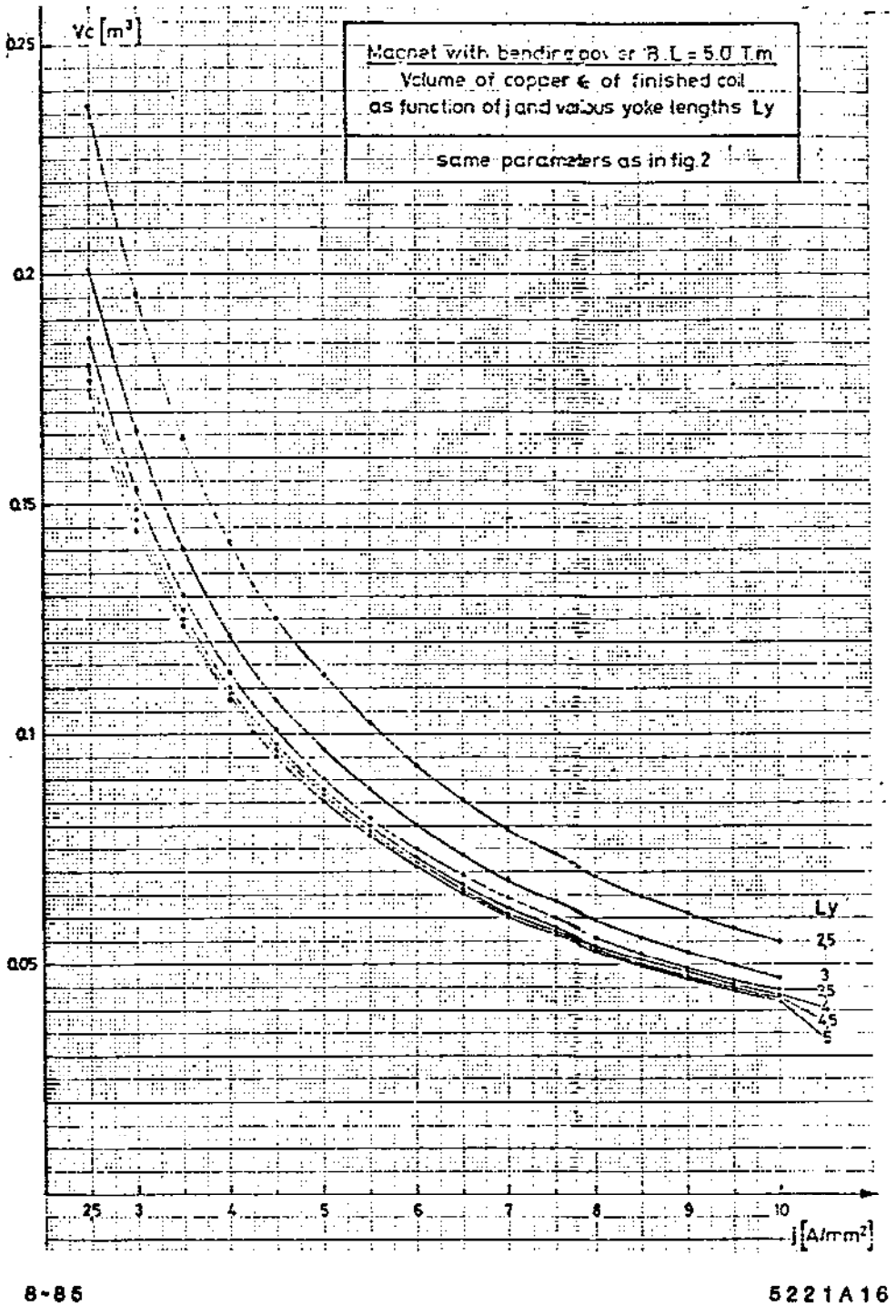

Fig. 1.18. Cost Study – Coil Volume vs Current Density.

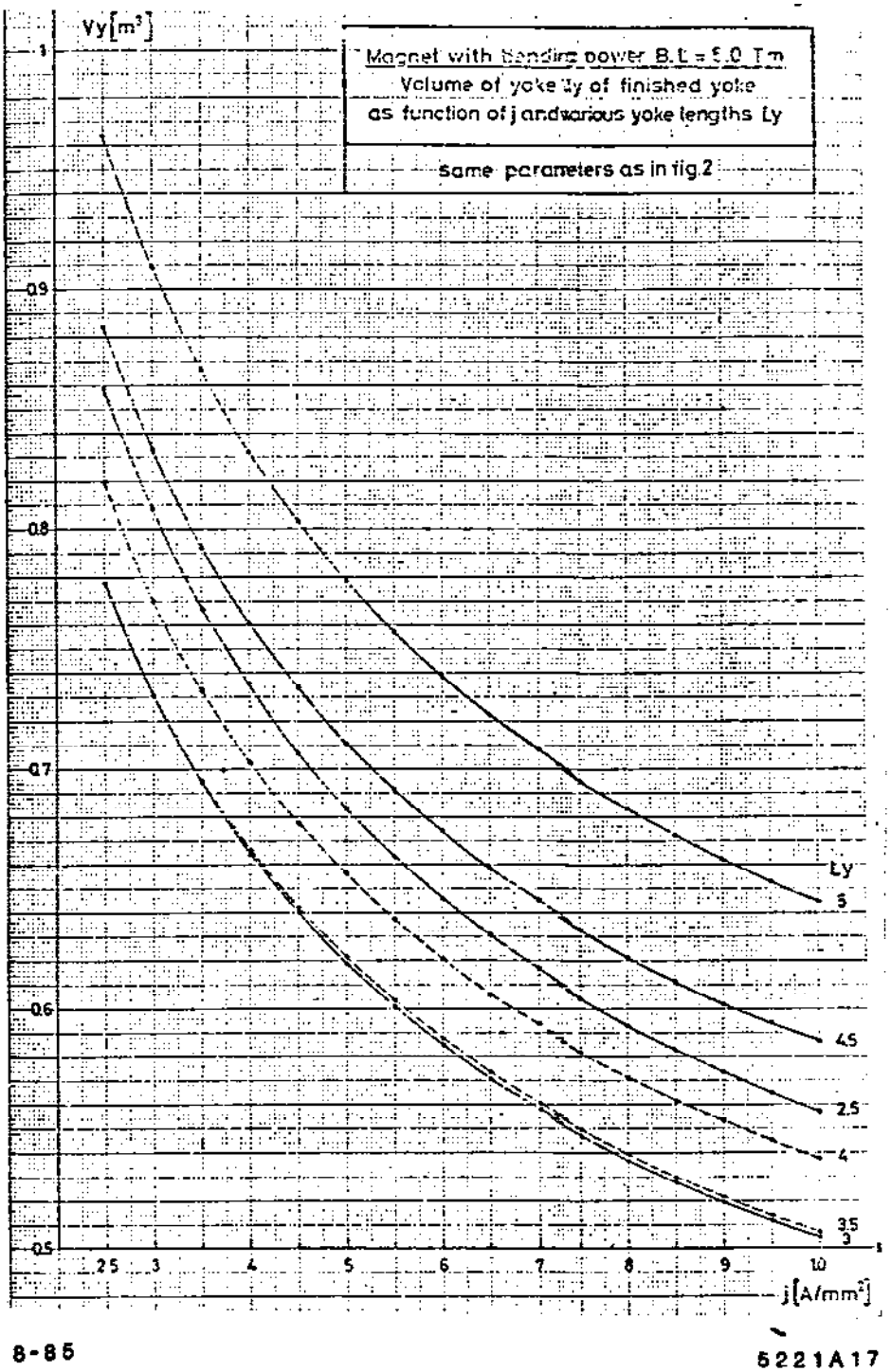

Fig. 1.19. Cost Study – Yoke Volume vs Current Density.

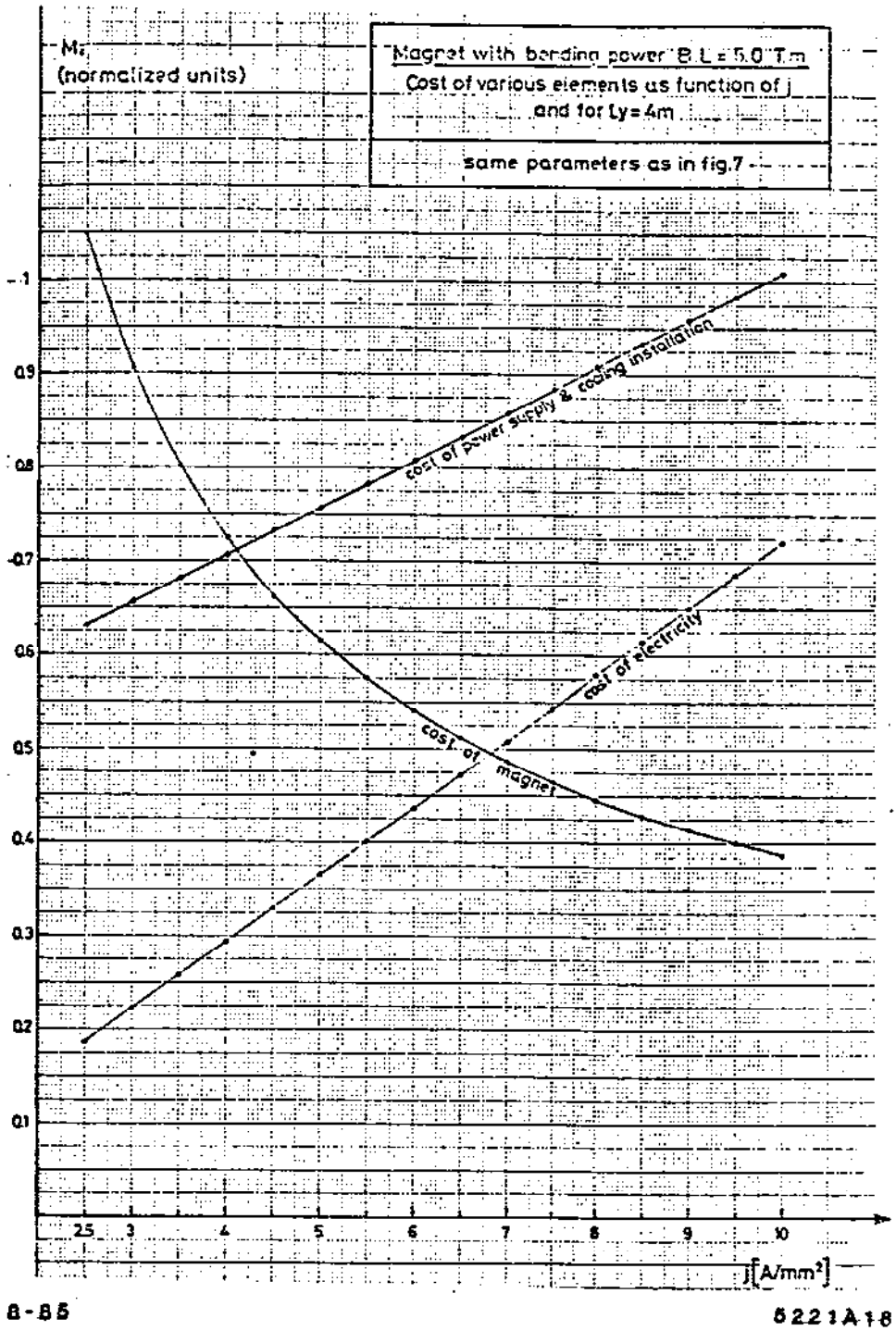

Fig. 1.20. Cost Study – Various Costs vs Current Density.

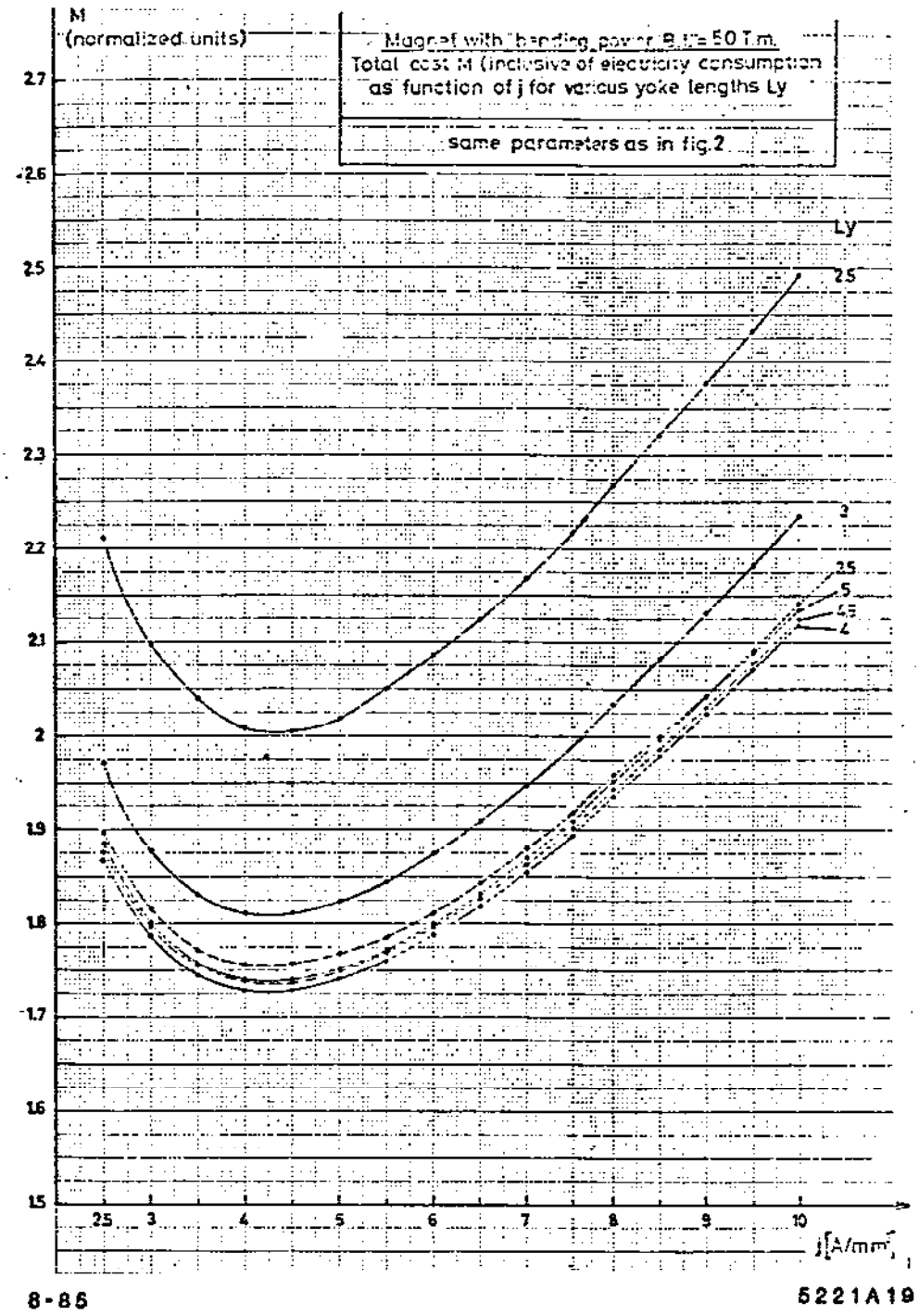

Fig. 1.21. Cost Study – Overall Normalized Cost vs Current Density.

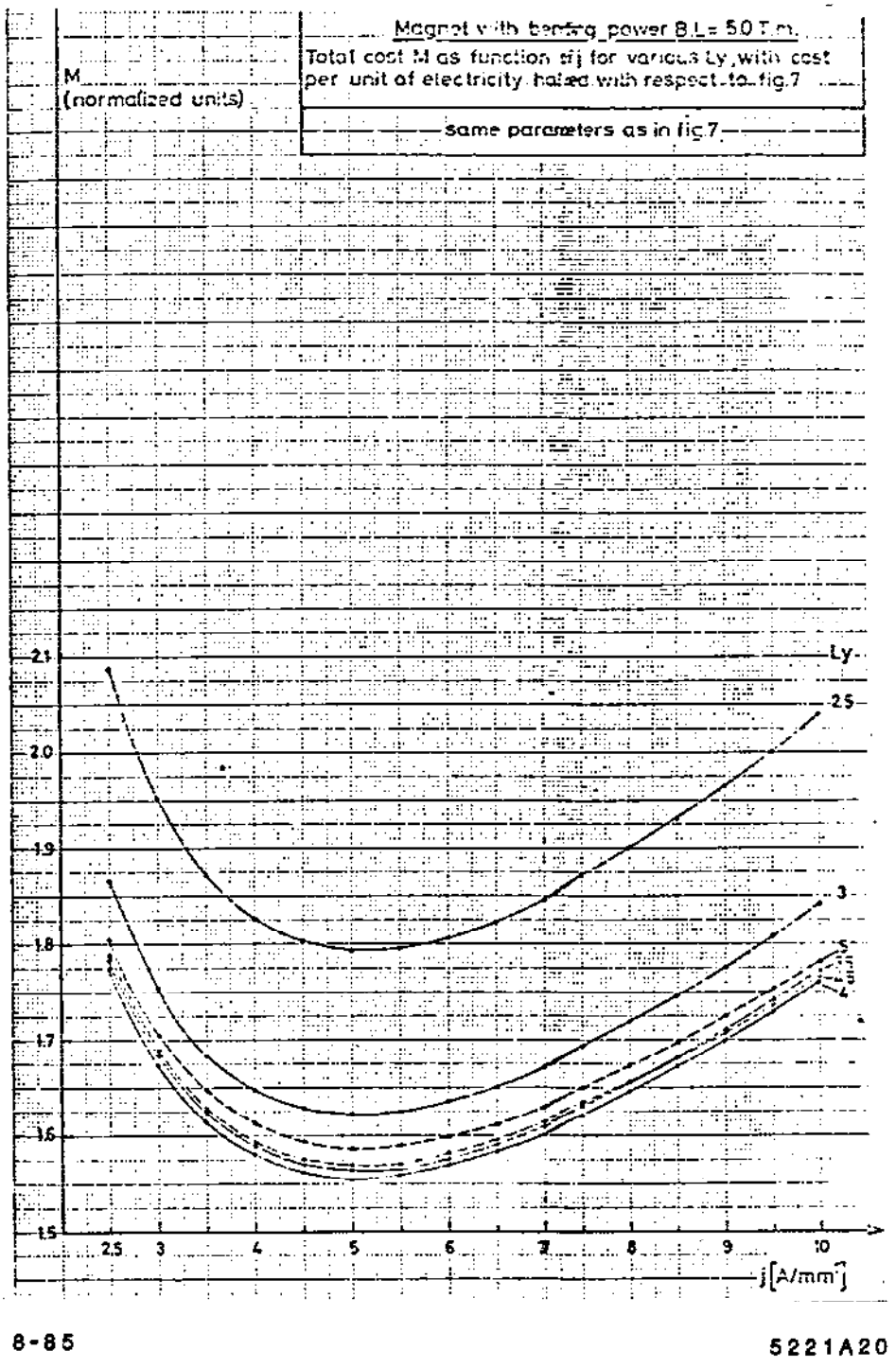

Fig. 1.22. Cost Study – Same as Fig. 1.21 but with Electricity Cost Halved.

PLEASE NOTE: You will get different results if you put in your own values. This is only an example of the procedure.

For instance, at SLAC we use a great deal of aluminum as conductor and this moves the minimum in J to around 1 A/mm^2. We will discuss aluminum in another lecture.

Increasing the cost of power will, of course, move the minimum to even lower values of J.

These types of calculations have also been done for other magnets and are usually set up on a computer program. Figure 1.23 shows the kinds of cross sections calculated even back in 1965 before we all had desk top computers for fiscal analysis. We will see in the next chapter how the profile is influenced by the field level the magnet is to operate at. Let me conclude this subject by saying that the balance between capital and operating cots is a question that must be answered by the laboratories' management, since the designer himself is not generally in a position to know all the details of future funding levels.

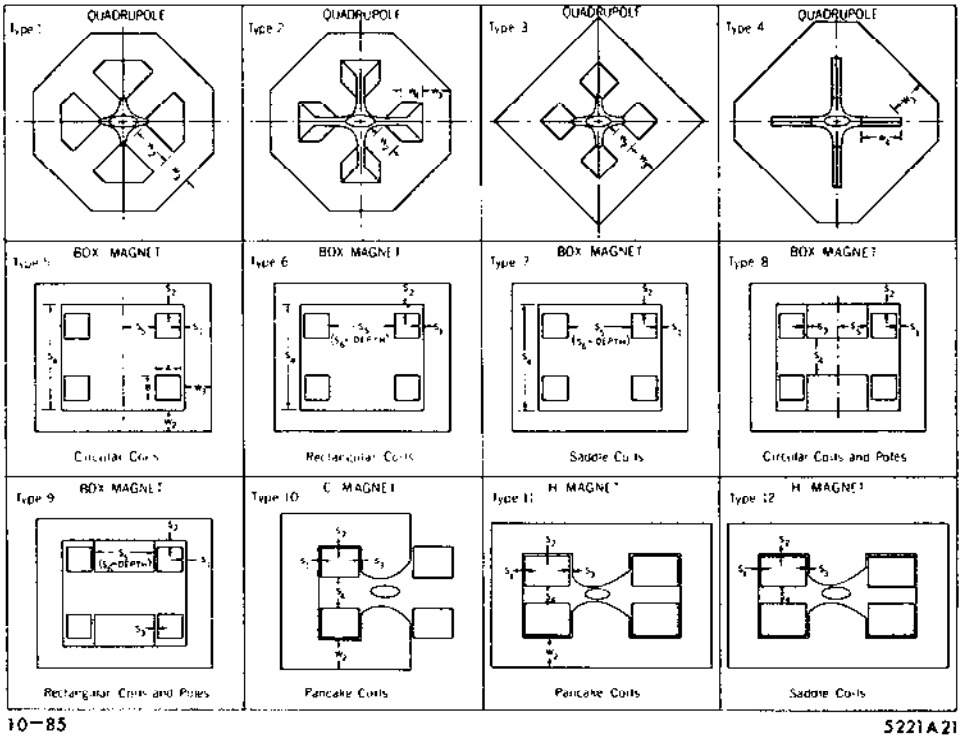

Fig. 1.23. Cross Sections Evaluated for Cost by COMA (1965).

1.8 PEP Magnets and Costs

The PEP magnet system was described by Bob Bell, Chief Mechanical Engineer for PEP in Ref. 19. Figure 1.24 gives a breakdown of actual construction costs when the system was completed in November 1979. I show this table so that you, as future accelerator designers, see that the cost of a magnet SYSTEM has ingredients other than just the cost of the magnets.

PEP MAGNET SYSTEM COSTS Completed Nov 1979

(no conventional facilities)

E.D.&I.

Ring (SLAC)	1,018,517
I.R.Quads (LBL)	287,100
Power Supply (LBL)	511,900
	1,817,517

COMPONENTS

	Number	gap	length	$
Bending Magnets	192	7 cm	5.4 m	2,311,224
Quadrupoles	216	10cm	1.0 m	1,741,915
low field bends	24	10cm	2.0 m	99,040
Sextupoles	192	12cm	.3,.5m	433,469
Multipoles (corr)	24	20cm	.5 m	58,806
Vertical steering	24	10cm	.5m	54,649
I.R.Quads (high qual)	24	16cm	1.5,2.0	1,106,600
Supports	216			663,703
Bussing and Cooling (no towers or pumps)				505,377
Magnet Measuremet (SLAC)				274,822
Transporters				68,602
Tools and misc.				106,606
Handling and Transportation				137,861
Power Supplies (no I & C) (LBL)				.. 889,000
				8,451,674

INSTALLATION : (T & M)

Installation Survey	75,300
Ring Magnet Installation	1,563,600
I.R.Magnet Installation	61,800
P.S. Installation	294,200
	1,994,900

8-85
5221A22

Fig. 1.24. Example of a Magnet "System" Cost.

REFERENCES – CHAPTER 1

1. Proceedings of the International Symposium on Magnet Technology – SLAC, Stanford University, Stanford, California 94305, September 8–10, 1965 Conf–650922, UC–28.
2. MT-2, (1967) p.121. R.G. Bendell et al. (1967) Rutherford labs.
3. NS-18 (1971) p.869. R. Avery and J. Tanabe (LBL).
4. MT-6 (1977) p.419. H. Ikegani (Osaka University, Osaka Japan).
5. MT-2 (1967) p.3 A. Asner, G. Petrucci and L. Resegotti (CERN).
6. MT-5. (1975) p.3. R. Billinge (CERN).
7. MT-3 (1970) p.377. M. Stanley Livingston (NAL).
8. MT-3 (1970) p.418. A. Asner et al.(CERN).
9. MT-3 (1970) p.537. R. Billinge, W. Hanson and P. Reardon (NAL).
10. MT-4 (1972) p.372. H. Sasaki et al. (KEK).
11. MT-3 (1970) p.490. H. Hinterberger and R. Sheldon (NAL).
12. NS-18 (1971) p.853. H. Hinterberger et al. (NAL).
13. NS-16 (1969) p.667. R. Lari and L.C. Teng (Argonne, NAL).
14. NS-18 (1971) p.857. H. Hinterberger et al. (NAL).
15. CERN/SI/Int. DL/70-10. Brianti and Gabriel (CERN).
16. NS-12 (1965) p.354. C. Dols and R. Kilpatrick (LBL).
17. NS-14 (1967) p.377. H. Paul Hernandez (LBL).
18. NS-18 (1971) p.797. J. Allinger, G.T. Dandy, J.N. Jackson and L.W. Smith (BNL).
19. SLAC PUB-2045. M. Anderson, R. A. Bell et al. (SLAC Nov. 1977).
20. Paper S6. R. Huson et al., Particle Accelerator Conf. Vancouver, June 1985. Paper P38. S. Pissanetsky and W.S. Schmidt. PAC, Vancouver, June 1985.
21. MT-9 (1981) p.1591. Autin et al. and p.1860. Pincott et al.

2. PROFILE CONFIGURATIONS AND HARMONICS

2.1 INTRODUCTION

In the previous chapter, we concerned ourselves generally with the size and economics of magnets for a given aperture and field. This portion is about practical methods of shaping the iron and conductors in order to achieve the field uniformities required for machine performance. Beware the accelerator theorist who demands field errors less than 0.01% – one will see that such performance is possible but difficult to achieve and costly.

Two examples of tolerances for the electron-positron storage ring, PEP, are listed in Refs. 22 and 23. Tolerances on storage rings are generally more severe than on accelerators, because the phase spaces of beams have to be maintained for many revolutions (hours) so that either the luminosity is not degraded or so that particles do not leave the machine's orbit and cause background in nearby detectors. One of the most intensely studied problems in the accelerator physics community today (summer 1985) is what the magnetic field tolerances for the SSC, a proton collider, should be (Ref. 24).

It is not difficult to devise perfect mathematical pole configurations for specific fields. The problem is they cannot be built economically. There are always side and end effects. The practical method is in the other direction, you estimate the size of the pole and then derive the resulting field in terms of an expansion of higher order field terms. In other words, one must solve the Laplace or Poisson equation with finite boundary conditions and then expand the error field. Then you move the boundaries until the field quality is good enough. Before the large-scale computer came along, people did this by analytic methods such as conformal mapping or solved the problem with analogue computers, carbon paper, watertanks or, more to the point, magnetic models. Before running to the computer, what can one learn from experience?

2.2 RULE OF THUMB CONTOUR SHAPING

2.2.1 Bending Magnets (H Type)

Consider the bending magnet in Figure 2.1(a). Due to the finite lateral extent of the pole pieces, the field will fall at the sides. Consider a long magnet so that the problem is two dimensional.

For a square corner, a very useful expression for how much overhand (a) is needed to produce a given dB/B at the edge of the good field region is given by

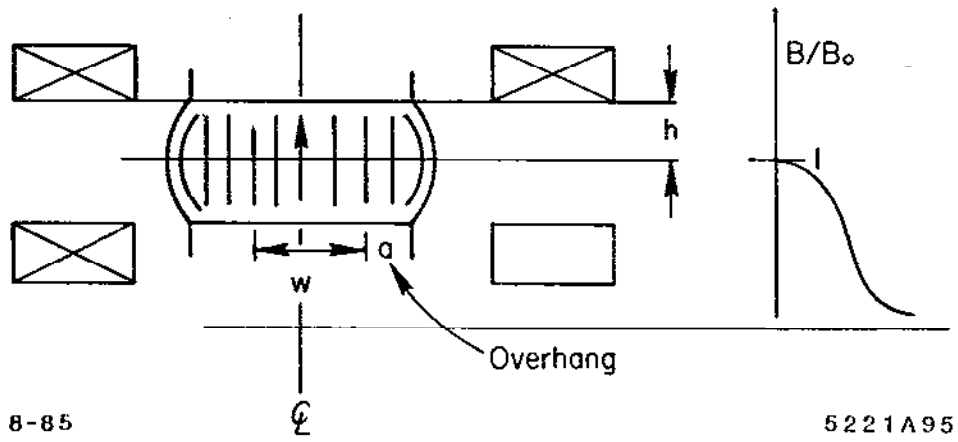

Fig. 2.1. (a) Transverse Fringing Fields of a Bending Magnet.

the engineering relation

$$X = \frac{a}{h} = 0.75 - 0.36\ell_{10}\left(100\,\frac{\Delta B}{B}\right)$$

If, for example, we wish $dB/B \approx$ 10-4, then $a/h \approx 2.4$ or very approximately a distance equal to the total gap. This is a good starting point for the design.

The next step is to make it better. It is natural to assume that since there is insufficient iron on the corner to add some in the gap. This has been known since the days cyclotron magnets were "shimmed". But what happens is that the flux concentration at the corner is too high, and the field rises and then falls. So the next step is to take some iron away to make the concentration flatter. This is still easy to machine with simple machine tools and, therefore, does not cost too much.

However, nature simply abhors sharp corners, and as the magnet is run to higher flux densities, the steel at the corner saturates and the shape of the flux distribution changes. So, let us make the corners round. If the magnet is laminated this is no problem, since the punch and die is machined this way for manufacturing Figure 2.1(b).

This is not the end of the story, however, because the pole must carry all that stray flux that comes in from the side. If the corner saturates, then the root of the pole may saturate even more, and one must give the lines room to be carried away. Therefore, in high field magnets the pole must be tapered. LESSON 1. The remedy for the disease called "pole root saturation" is taper the pole! If the pole is tapered more stray flux must be carried around the backleg. LESSON 2. The remedy for "iron deficiency anemia" is to make the backleg wide enough.

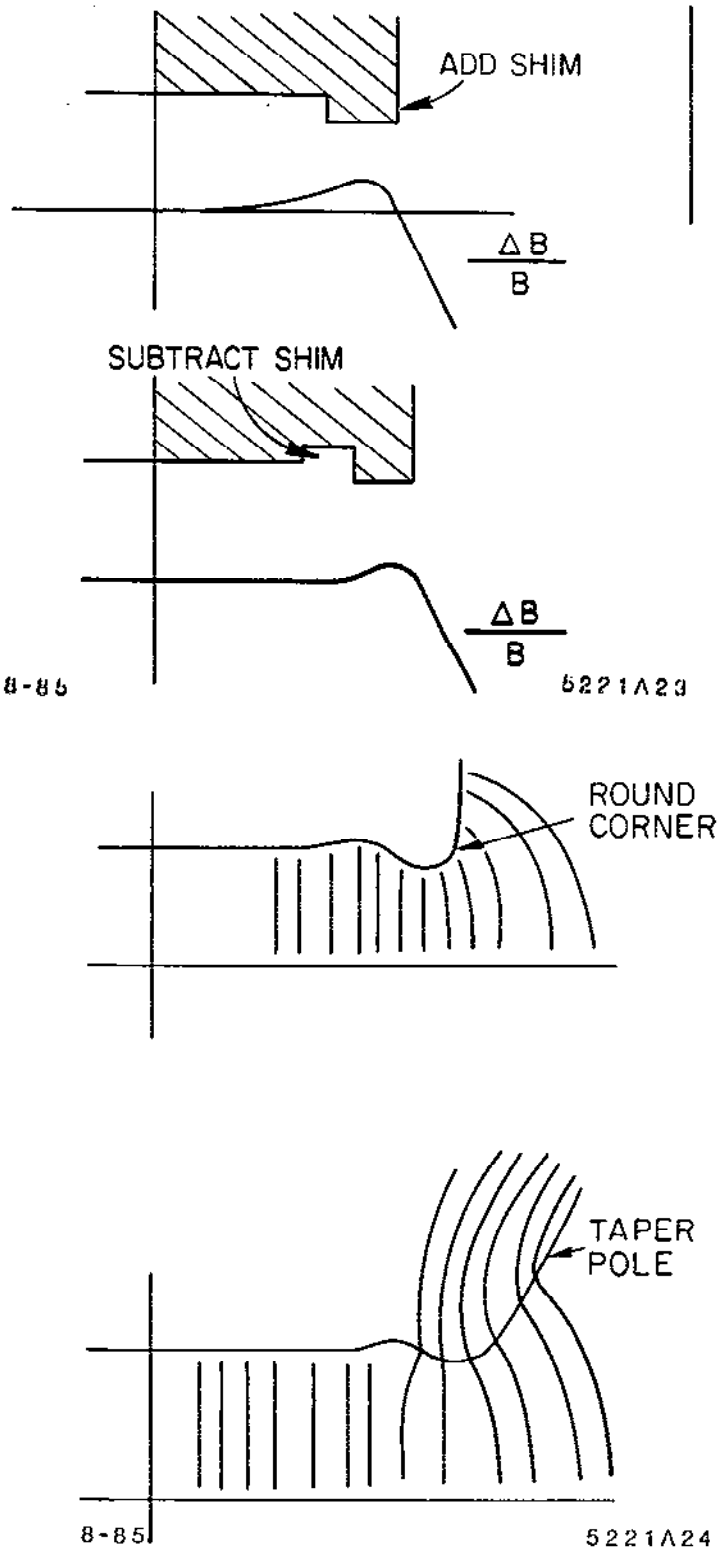

Fig. 2.1. (b) Transverse Corners of a High Field Bend.

In fact, if the shape of the field is to be constant with excitation – it must be a surface of constant magnetic scalar potential! This is called the Rogowsky contour. Now you know as much as I do and can proceed to calculation with a computer. We will discuss end effects later.

2.2.2 Bending Magnets (C Type)

A *C* magnet, often used to permit easier installation and service of vacuum chamber, has an additional problem. The *H* magnet is 2-fold symmetric – i.e. not only about the median plane but also about its center line. The field will, therefore, fall off the same way on both sides. The *C* magnet has only one symmetry plane. Since $\oint H \cdot dl = NI$ is a constant, the contribution to the integral in the iron has different path lengths , and with finite permeability will have a lower *B* field in the gap on the outside than on the inside. In other words, it will have an unwanted gradient and all odd as well as even harmonics of the field. This is shown in Figure 2.1(c). Notice in Figure 2.2 the signs and magnitude of the sextupolar terms and how they change with excitation as *H* and *C* type bends are driven toward saturation. Figure 2.3 shows how the field falls off far from corners out in the coil region. It is only slightly affected by what one does at the corner but all that stray flux must be carried by the back leg.

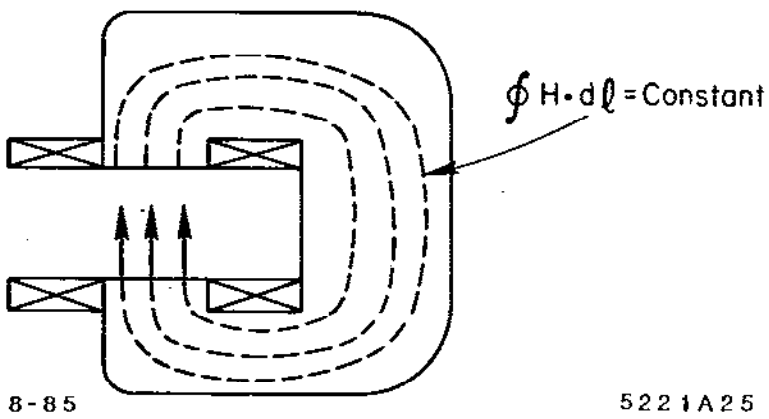

Fig. 2.1. (c) Why a "C" Bending Magnet has a Gradient.

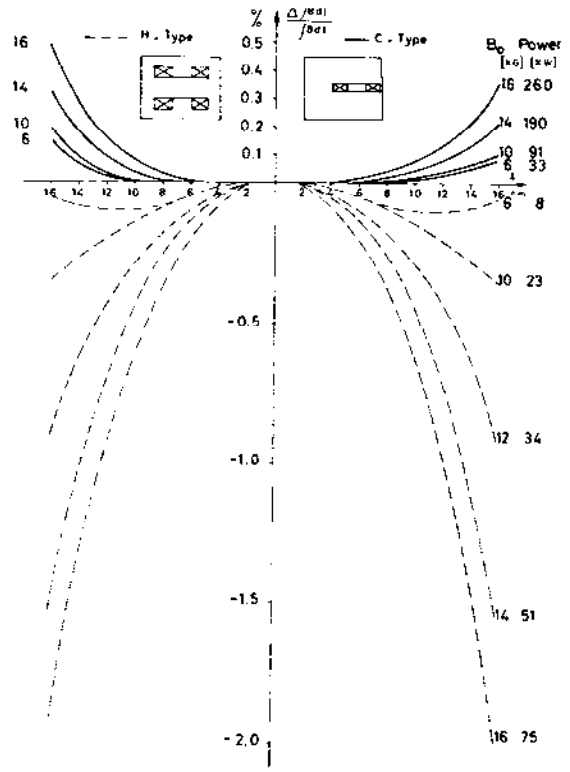

Variation of $\int Bdl$ for two designs of bending magnet. The increase in power consumption for the same field level for the C-type model can be noted. The departure from uniformity in bending length as a function of transverse displacement and field level is related to the different distribution of the conductors in the two magnets. 10-85 5221A26

Fig. 2.2. Example of Sextupolar Field Fall Off.

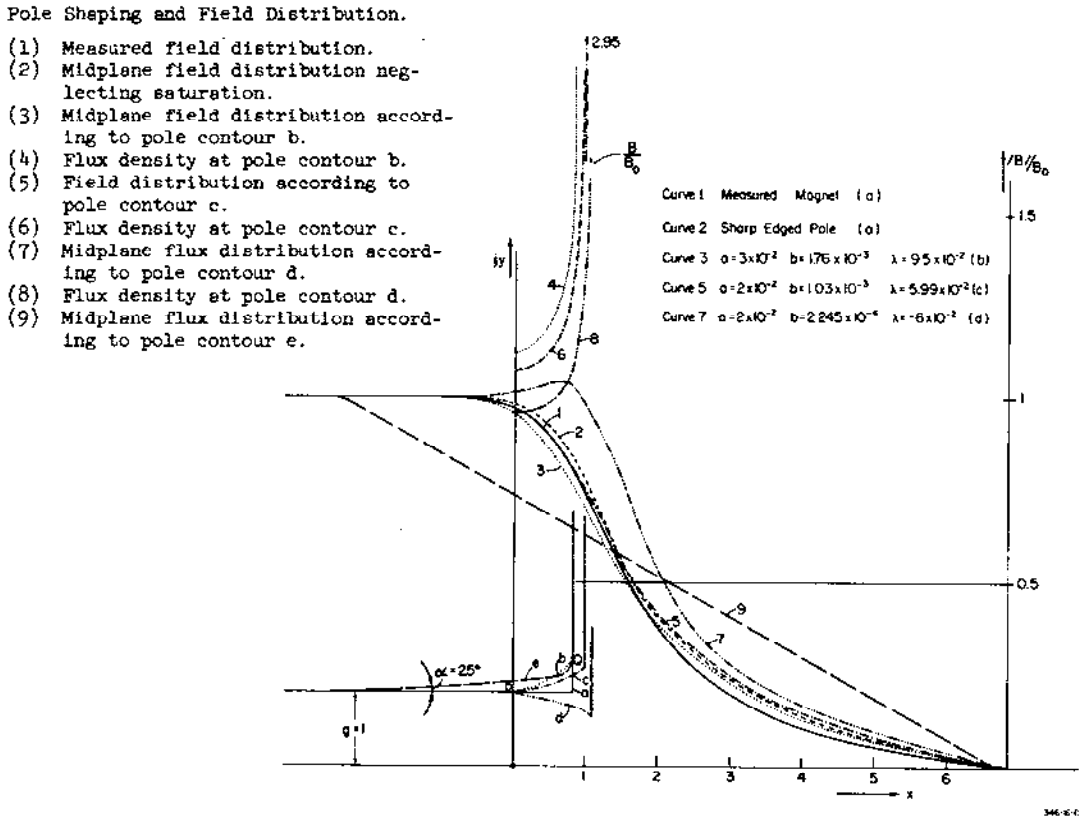

Fig. 2.3. Fields in the Coil Area of a Bending Magnet.

2.2.3 Quadrupoles

Precisely the same kinds of considerations of contour shaping that we have applied in dipole geometry also apply in quadrupole geometry. The first question then is "how wide does the pole have to be?"

In Figure 2.4 the iron of the hyperbola has been cut straight back to put the coil in. We can then resort to a very useful graph calculated by Dr. Helmut Wiedemann in an internal DESY Report H5/71-4, April 1971, shown in Figure 2.5. Let us take an example – for a gradient error $dg/g \approx$ 10-3 at 70% of the bore radius, we find $A/R_o = 0.35$. The pole width $P_1 = 1.5R_o$. If we wish the field to be this good out to 90% of R_o then $P_2 = 1.76R_o$. This clearly is about as wide a pole tolerable since there will be very high fields at the corner. Actually that is a pretty good quadrupole.

The most common thing done in the past,when poles were machined out of solid iron, is to add metal at a tangent point, as shown in Figure 2.4. Since we have learned to laminate magnets the most complicated shapes are easy and all the considerations that we went through for the dipole contours apply here as well.

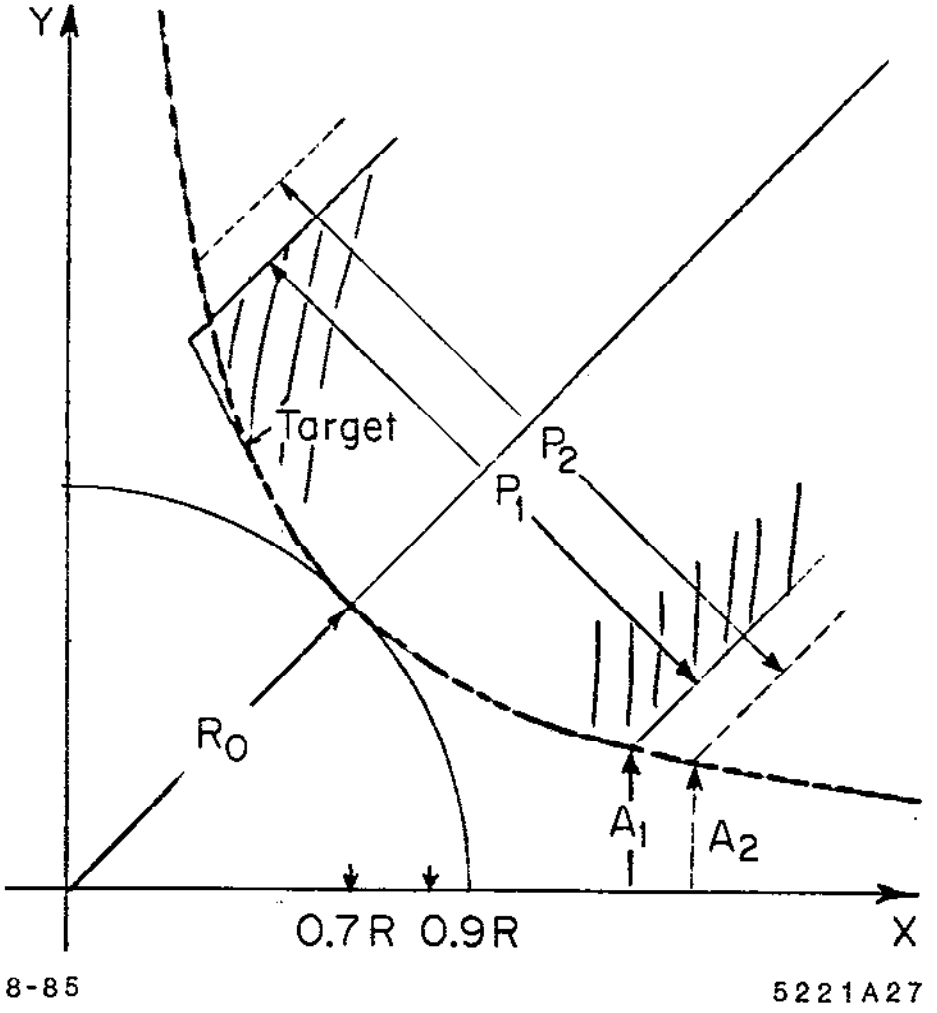

Fig. 2.4. Truncation of the Quadrupole Hyperbola.

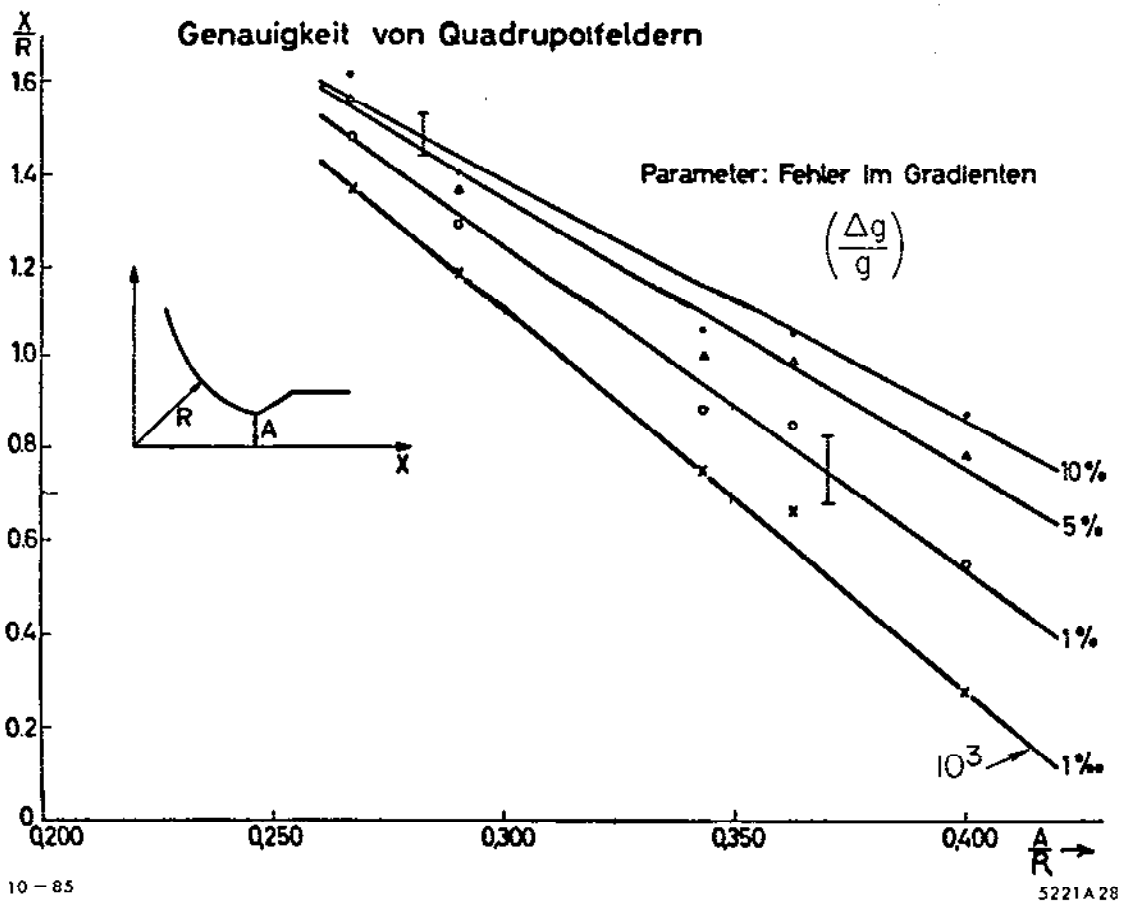

Fig. 2.5. Estimated Pole Width vs Gradient Uniformity.

2.2.4 *Conductor Placement*

Although we are discussing iron dominated magnets, conductor placement does have effects. In the last chapter you probably noticed that the high field NAL bend had a conductor right in the gap. This is very useful (but more complicated) way to force the field back into the gap. In Figure 2.6 we show what a profound effect omitting one conductor can have on the field uniformity of a SLAC Spectrometer Quad.

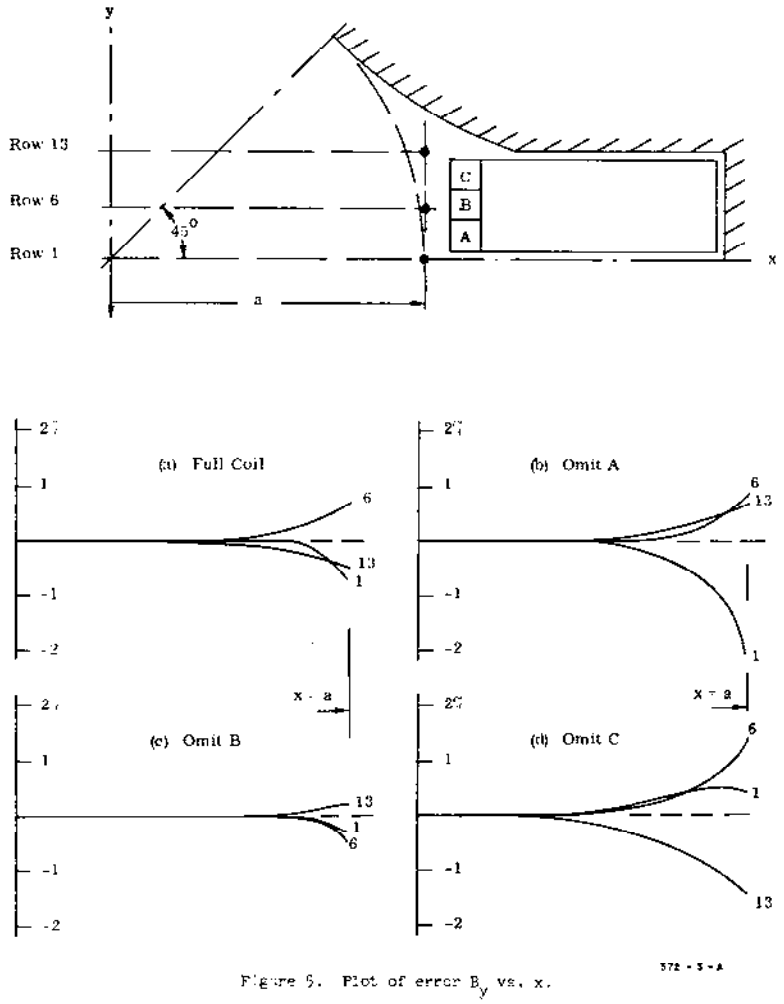

Fig. 2.6. Effect of Conductor Placements in Quadrupoles.

2.2.5 *Sextupole Pole Widths*

Figure 2.7 (also by Helmut Wiedemann) gives you a feeling of how sextupole magnet strength errors scale with pole width. Fortunately, sextupoles generally do not need to be as accurate.

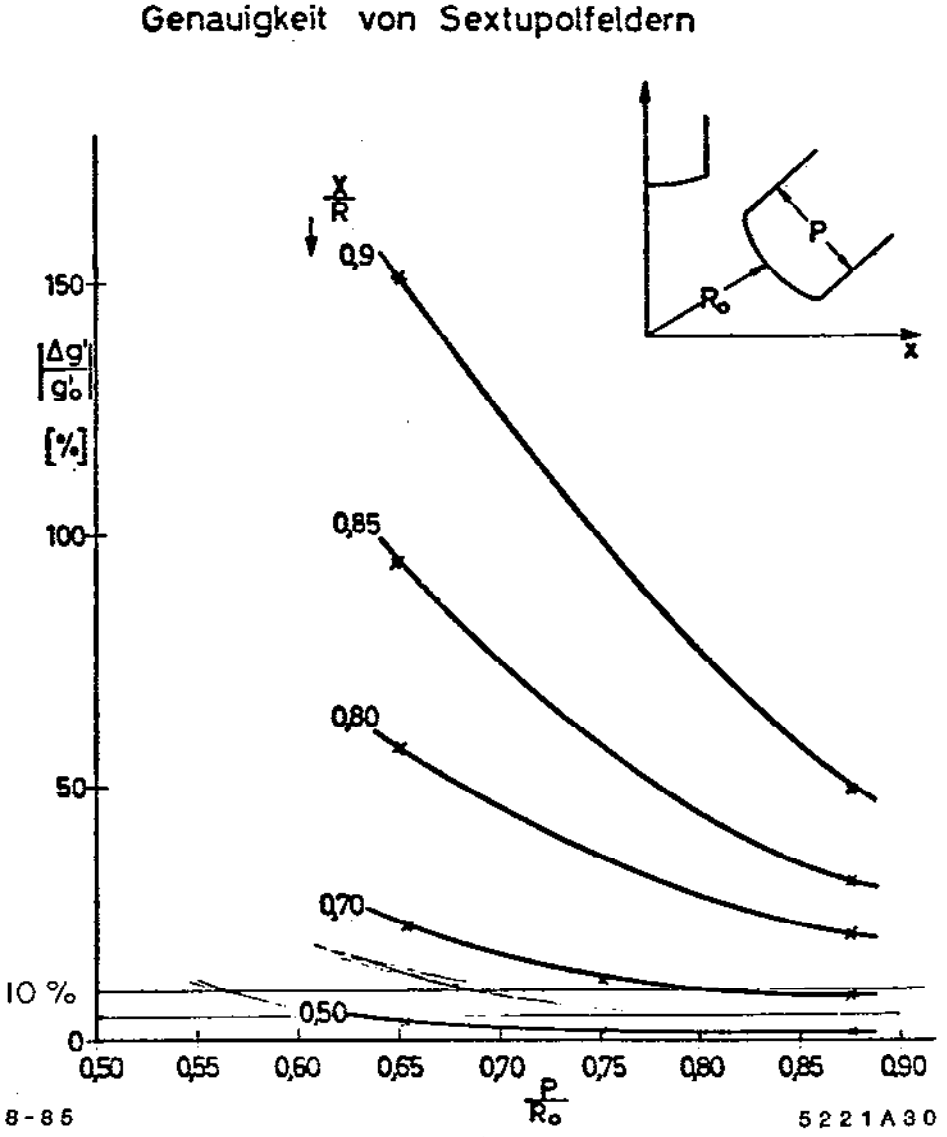

Fig. 2.7. Estimated Pole width vs Sextupole Uniformity.

2.3 Field Computation By Computer

We are now in a position to see how educated our estimates are. This means solving Laplace's or Poisson's equation with the boundary conditions of the problem. Many computer programs have been written for this purpose and are described in the many Refs. 25 through 34 that I have listed for you. Some of the people associated with these programs are Winslow, Colonias, Brechna, Herrmannsfeldt, Trowbridge, Lari, Carpenter, Iselin and, most familiar to me, Klaus Halbach and Ron Holsinger who developed the current versions of "POISSON." Over the last 20 years, the programs have grown very sophisticated and, consequently, less transparent. Most importantly, they are able to calculate the solution in the presence of non-linear iron. Forces on the conductors can be treated. The subroutine MINT analyzes the good field region in terms of harmonics, and the package MIRT actually moves the iron in shim regions to produce the desired field characteristics. Conformal transformations are built in. The work has become a profession, in fact, as I mentioned last chapter, the mathematical troubadours of this trade hold their own conferences, and travel about from laboratory to laboratory setting up their programs (if you pay them) so that others can use their tools.

Most of the application is in 2 dimensions in either rectangular or cyclindrical coordinates. This is fine for most accelerator magnets which are generally much longer than wide. Three dimensional programs are now coming into use (Ref. 38). Since they would consume so much normal computer time, it pays to run them on a CRAY.

As a generalist it is simply not possible for me to go into the details of this work except to show you in the barest of outline what the designer does and how he uses this tool. The interested student might consult Thomas Weiland's recent article, the title page of which is shown in Figure 2.8. For the expert there is C. Iselin's article [MT-7 page 2168 (1981)] which contains many references. How POISSON is used as a black box is given in Ref. 35.

Particle Accelerators
1984 Vol. 15 pp. 245–292
0031-2460/84/1504/0245$18.50/0

ON THE NUMERICAL SOLUTION OF MAXWELL'S EQUATIONS AND APPLICATIONS IN THE FIELD OF ACCELERATOR PHYSICS

THOMAS WEILAND

DESY 2000 Hamburg 52, FRG

(Received June 27, 1983; in final form January 5, 1984)

A discretization ansatz for Maxwell's equations is described that enables treatment of all possible homogeneous and inhomogeneous problems from nonlinear magnetostatics and electrostatics to time-dependent field problems that include charges moving freely at any speed. The same method can be used for magnet design, for cavity-mode investigations and wake-force computations in time and frequency domains, antenna problems, and waveguide structures.

The method makes direct use of the electric and magnetic field as unknowns, thus yielding uniquely defined vectors in combination with a suitable grid definition. This "natural" ansatz avoids problems arising from the use of artificial functions such as vector potentials or Hertz potentials.

Using this ansatz, many computer codes have been developed and applied to various problems. Applications in the field of accelerator physics include magnet and solenoid design; design of accelerating rf-cavities and beam-tracking calculations for instability studies. More recently the method has been used to study the new acceleration principle of wake-field compression.

1. INTRODUCTION

The unified theory of electric and magnetic fields is described by Maxwell's equations[1]

$$\oint_{(A)} \mathbf{E} \cdot d\mathbf{s} = -\iint_{A} \frac{\partial \mathbf{B}}{\partial t} \cdot d\mathbf{A} \tag{1}$$

$$\oint_{(A)} \mathbf{H} \cdot d\mathbf{s} = \iint_{A} \left(\frac{\partial \mathbf{D}}{\partial t} + \mathbf{J} + \rho \mathbf{v} \right) \cdot d\mathbf{A} \tag{2}$$

$$\iint_{(V)} \mathbf{B} \cdot d\mathbf{A} = 0 \tag{3}$$

$$\iint_{(V)} \left(\frac{\partial \mathbf{D}}{\partial t} + \mathbf{J} + \rho \cdot \mathbf{v} \right) \cdot d\mathbf{A} = 0 \tag{4}$$

In these equations **E** and **H** are the electric and magnetic field and **D** and **B** are the electric and magnetic flux densities. The current density is denoted by **J** and ρ denotes

Fig. 2.8. Maxwells Equations.

Figure 2.9 gives the equation to be solved.

THE VECTOR POTENTIAL EQUATION

In the x, y plane:

$$\frac{\partial^2 A}{\partial x^2} + \frac{\partial^2 A}{\partial y^2} - \frac{1}{\mu}\frac{\partial \mu}{\partial x}\frac{\partial A}{\partial x} - \frac{1}{\mu}\frac{\partial \mu}{\partial y}\frac{\partial A}{\partial y} = -\mu J$$

in which $J = J_z$ = the current density within coil

$\mu = \mu(H)$ is given in Table form.

If the solution is $A = \vec{A}_z$ in 2 dimensions

$$\text{then} \qquad B_x = -\frac{\partial A}{\partial y} \qquad \text{and} \qquad B_y = -\frac{\partial A}{\partial x}$$

To each point of the mesh and each boundary point is associated a finite difference equation representing the local approximation of the partial derivative equation. The system of finite difference equations is solved by a relaxation method using extrapolation.

8-85 5221A96

Fig. 2.9. The Vector Potential Equations to be Solved.

Figure 2.10 shows how the problem is set up on a triangular mesh of "logical" coordinates which are distorted to fit the boundaries of the problem.

The lattice sub-routine iteratively generates the mesh shown in the lower diagram.

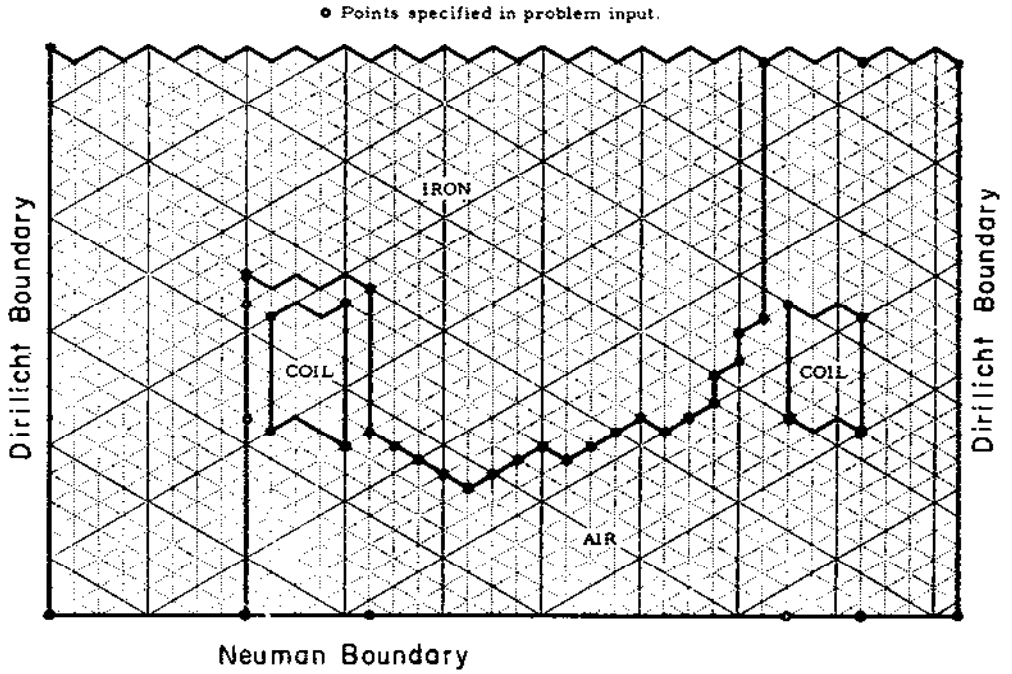

Figure 4. Logical map of C-magnet mesh.

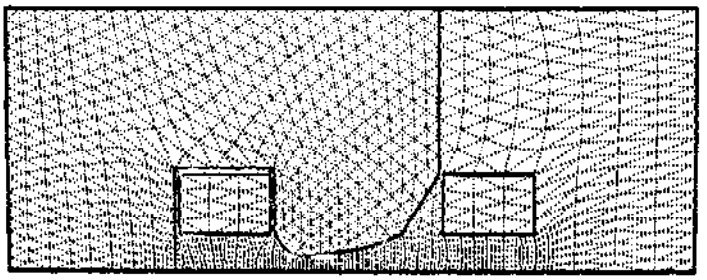

Fig. 2.10. Triangular Mesh Used in Setting Up the Lattice.

Computation of the vector potential then proceeds iteratively for each mesh point. The computation proceeds in the iron region with the determination of vector potential, magnetic induction and permeability at each mesh point. The vector potentials A are first computed at all points by assuming a constant value of permeability, then the components of the induction B are determined

as partial derivatives of A, and the permeability values as a function of the absolute values of B are read from a table. Then, the whole process is repeated with adjusted permeability values: cycling is continued until the changes in permeability are all below a specified value. Finally, the MMF drops between points of the iron contour are computed. The fields B_x, B_y, B_{total} and the gradient are computed and printed in the form of a map.

So that you can see graphically what has been calculated, lines of equal vector potential (i.e., flux lines) are then plotted as shown in Figure 2.11. In rectangular coordinates, the density of lines is proportional to the field intensity. Certain portions can be expanded to show detail.

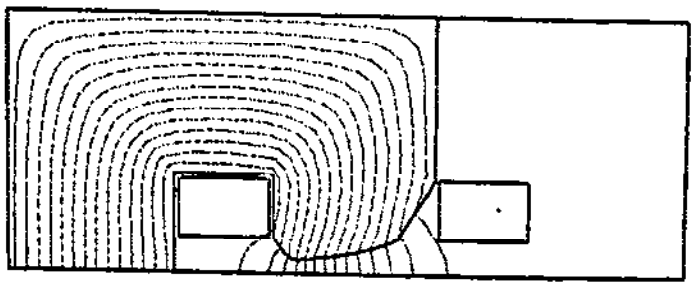

Figure 6. C-magnet showing equipotentials.

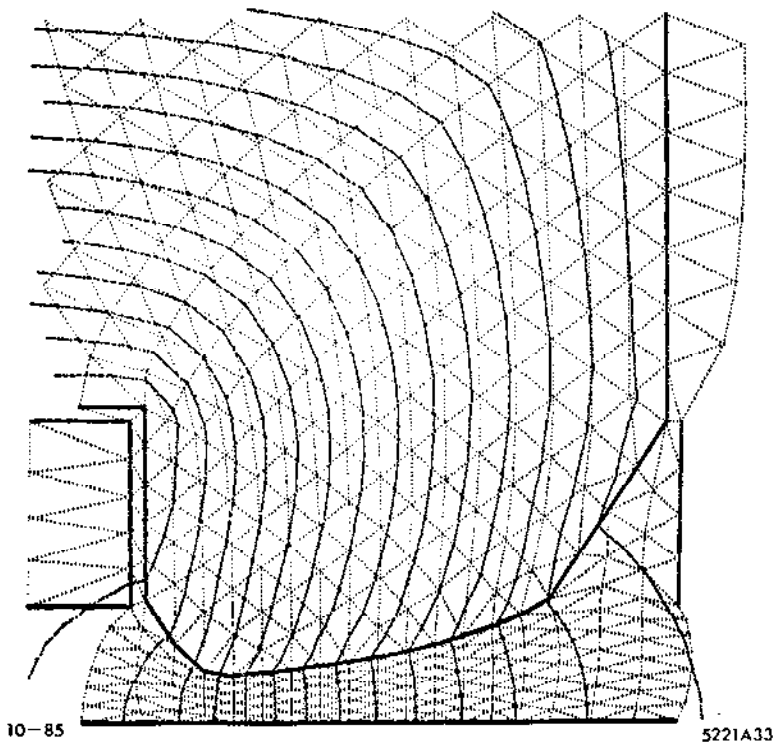

Fig. 2.11. Field Lines Traveling along Lines of Constant Vector Potential.

How accurate is POISSON? In the early 1970's we used to use magnetic measurements to check the calculation, in the 1980's its the other way around. In dipole geometry, given a good table of permeability mu, sufficient mesh points in the region of interest, B is better than $1/10^3$ when compared with magnetic measurement of actual magnets in absolute field, as well as in shape. Note: So far our version cannot handle residual fields. With great care in setting up the lattice, effects as small as $-1/10^4$ can be estimated in relative field shape. Double precision code must be used. In quadrupole geometry, the program is not as reliable, but we can use a trick–conformal mapping.

2.4 Examples of Computer Field Calculations

(a) An extreme case of high gradient quadrupole design (Ref. 36).

Figure 2.12 shows the profile and field distribution of a 1.0 cm bore quadrupole of gradient up to 25 kG/cm. As a rule of thumb it is not possible to have more

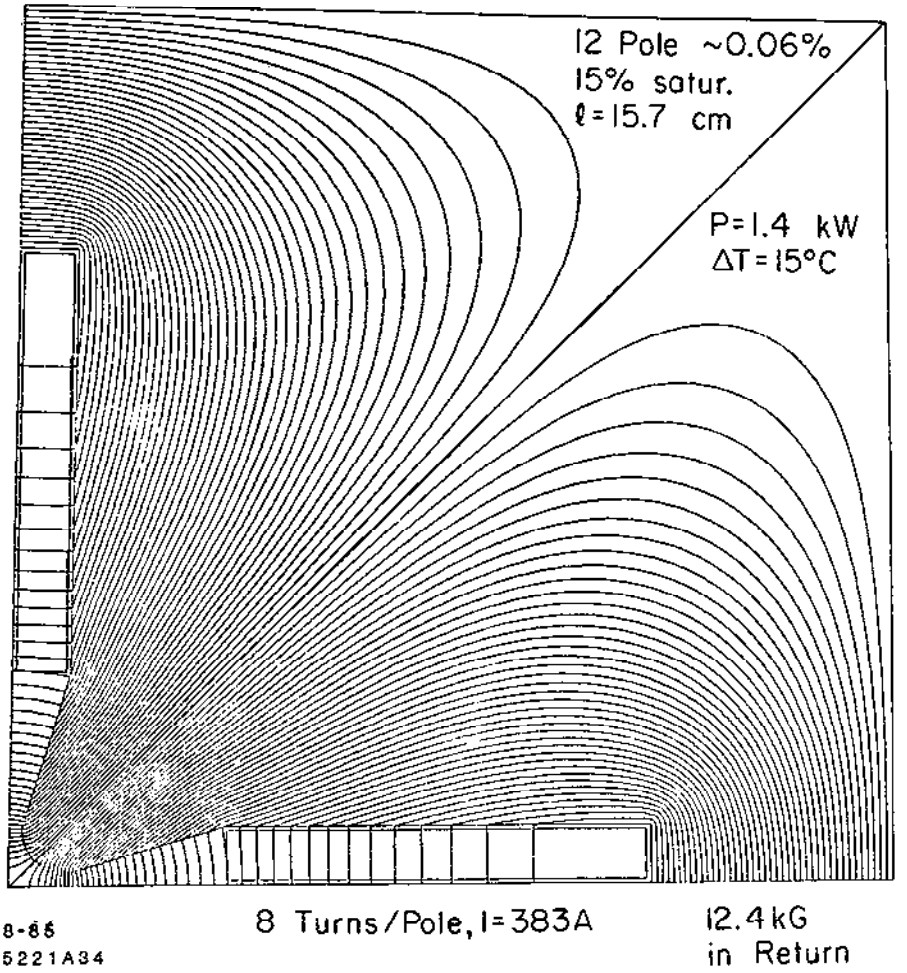

Fig. 2.12. Field Lines of a 1 cm Bore 25 kG/cm Quad.

than 10-12 kG on the poletip because of saturation at the pole root. Small magnets are more difficult to cool because although the required current scales with aperture, the current density scales inversely with the aperture squared. If relative mechanical tolerances are to remain the same, machining tolerances are pushed to the 0.1 mil level! Such tolerances can be achieved with modern computer controlled electric discharge milling (EDM) techniques.

(b) A new 20 kG bending magnet design for the SLC damping ring (Ref. 37).

Figure 2.13(b) show how the sides of this magnet are shaped for high fields. Figure 2.14(a) depicts the 3 dimensional TOSCA (Ref. 38) mesh used to study the ends (which are important in maximizing the synchrotron radiation integrals that are proportional to $\int B^2 \cdot dl$). Figure 2.14(b) shows good agreement between calculation and measurement for the end field fall off.

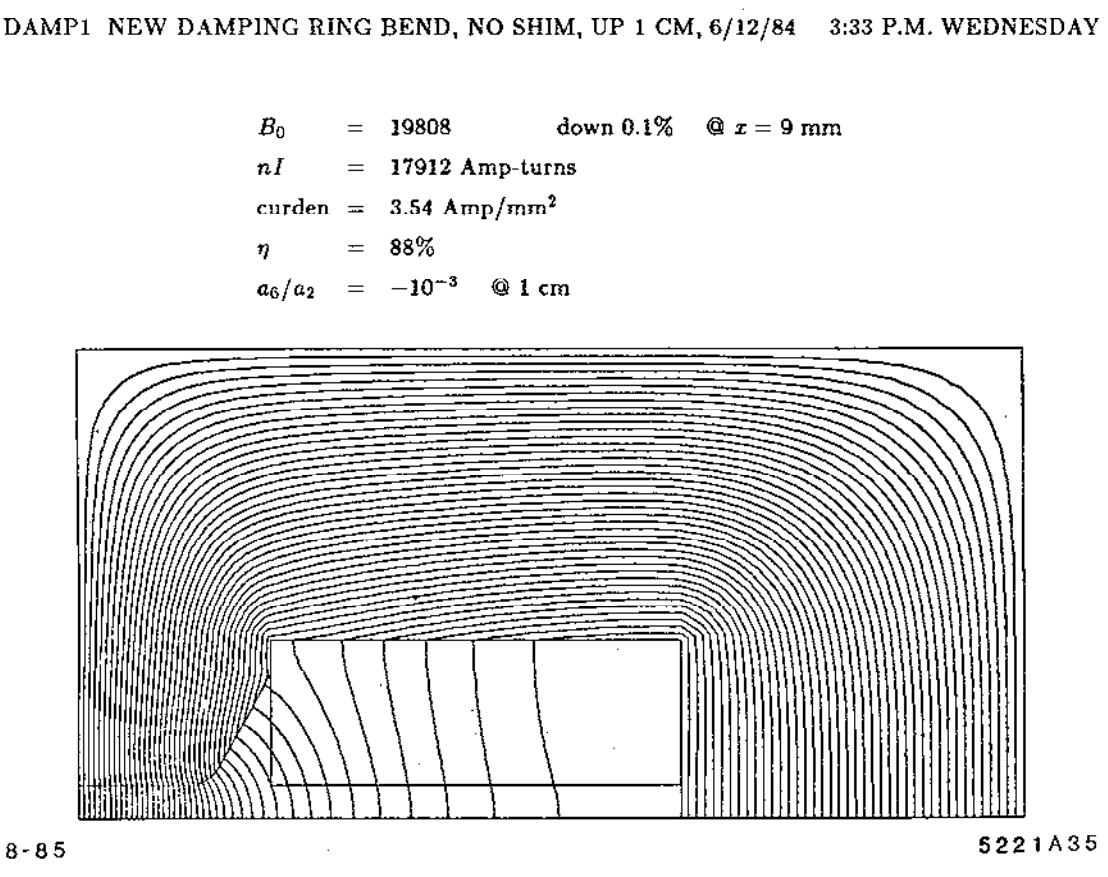

Fig. 2.13. Field Lines and Parameters of a 20 kG Bend.

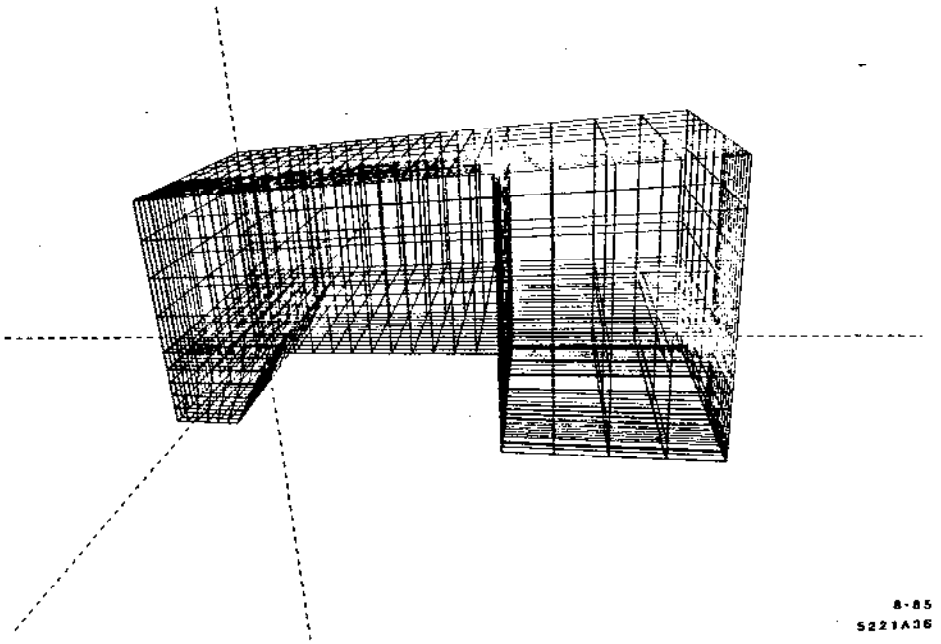

Fig. 2.14. (a) TOSCA 3D Mesh of Magnet in Fig. 2.13.

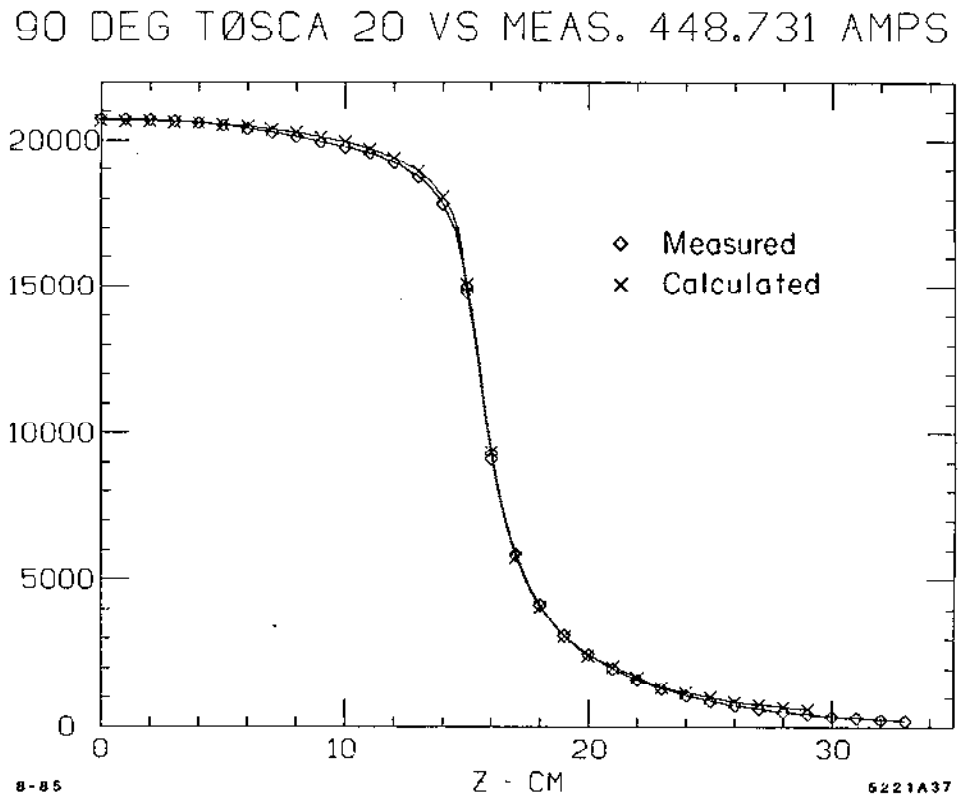

Fig. 2.14. (b) Comparison of TOSCA End Field Calculation with Measurement.

(c) SLC arc transport AG magnets.

50 GeV electrons must be transported in such a way that very little phase space dilution occurs due to synchrotron radiation excitation. This requires very high focussing gradients superimposed on the bending field. The magnet chosen is shown in Figure 2.15. You will recognize it as a half quadrupole with a neutral pole mirror plane. The equilibrium orbit is located 8mm from this pole as indicated by the cross. A POISSON field plot is superimposed. Some care with the profile is indicated since the system is about 2.2 Kilometers long (Ref. 39).

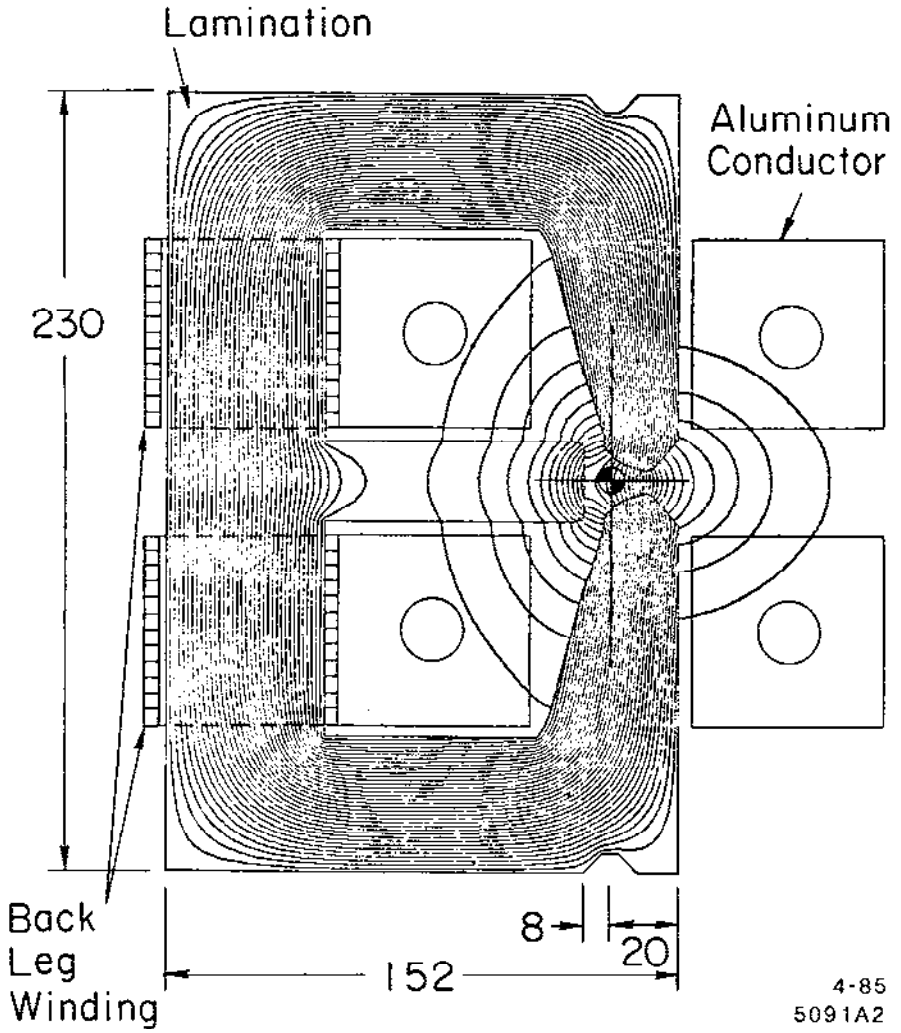

Fig. 2.15. Crossection of a SLC Arc Transport AG Magnet.

The calculation was done by Klaus Halbach and Bruce Humphries by first transforming the magnet into dipole geometry, using the conformal transformation.

$$Z_{\text{dipole}} = X + iY = z^2_{\text{quad}} = (x + iy)^2$$

$$\text{Hence} \qquad X = x^2 - y^2 \quad \text{and} \quad Y = 2xy$$

You can see that since xy = constant, the hyperbola transforms into $Y = \pm a^2$ (a constant) = $\pm$Gap/2. All the other points, including the good field region, end up somewhere else.

The transformed quadrupole (now a dipole) is now made as uniform as possible over the required good field region by the methods of shimming and anti-shimming described (see Ref. 40). In actual fact a certain amount of required positive or negative sextupole was added at this point since the arc system is a chain of achromats. For the positive case the result is shown in Figure 2.16.

Remember the program is very accurate in dipole geometry and mu infinite. Now we have to transform back to quadrupole geometry by $z = Z^{1/2}$.

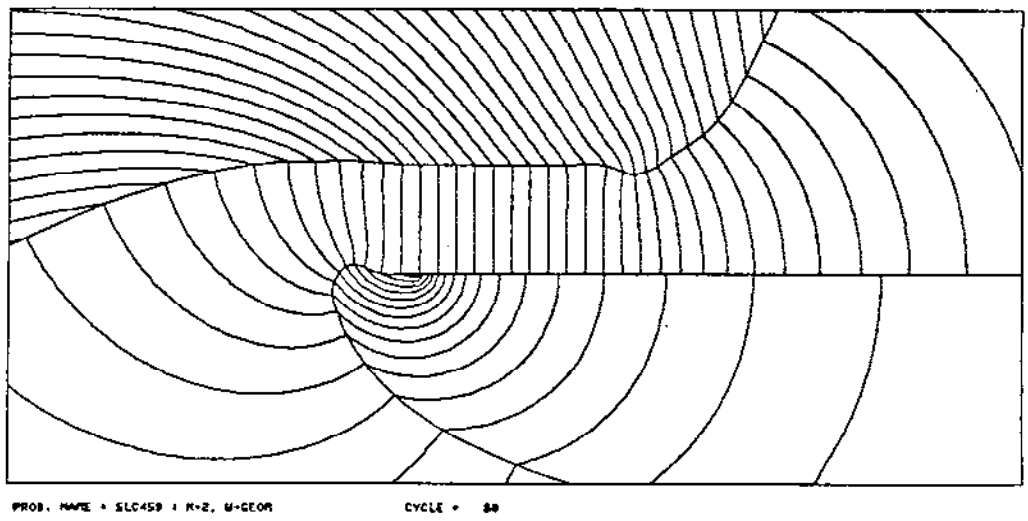

8-85

5221A39

Fig. 2.16. SLC Magnet Transformed into "Dipole" Geometry.

The x and y coordinates become:

$$z_{\text{quad}} = x + iy = Z_{\text{dipole}}^{1/2} = [X + iY]^{1/2}$$

$$\text{Hence} \qquad x = \left[\frac{(X^2 + Y^2)^{1/2} + X}{2}\right]^{1/2}$$

$$y = \left[\frac{(X^2 + Y^2)^{1/2} - X}{2}\right]^{1/2} \Rightarrow \frac{Y}{2x} \quad .$$

The final result for mu infinite is shown in Figure 2.17. If we have done the job correctly when the program is run with finite permeability, then the distribution in the good field region should not have changed. Measurements of the actual magnets showed no unwanted higher order terms in the good field region of ± 4 mm and a wide range of excitation for the negative sextupolar case (Ref. 41). The positive case showed some saturation effects but of insufficient magnitude to compromise operation.

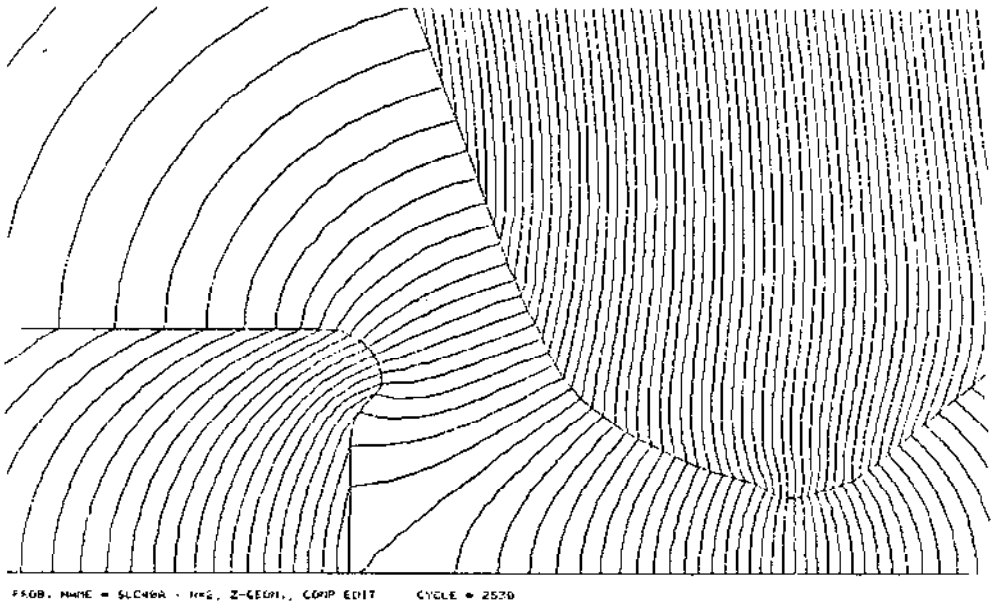

8-85 5221A40

Fig. 2.17. Final Profile with Noses for Positive Sextupolar Contribution.

The introduction of sextupolar terms into quadrupoles is not new. The resulting pole faces are then distorted as shown in Figure 2.18 (see also Ref. 42).

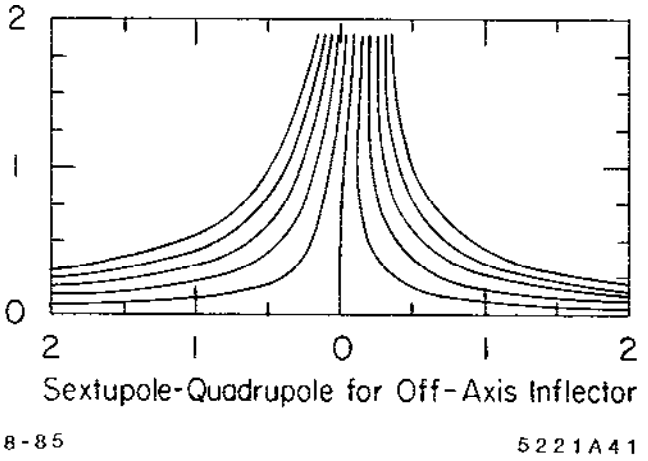

Fig. 2.18. Profile of Nomal Quadupole with Sextupole Addition.

(d) The superferric SSC collider dipole.

We have already referred to this magnet in Chapter 1 (Ref. 20). Figure 2.19 depicts a POISSON calculation of one corner of the configuration. Detailed perturbation calculations of the effects of errors in conductor placement have been carried out and are generally in good agreement with measurement up to the 3 tesla level. At this excitation these magnets can no longer be considered "iron dominated" since conductor placement now plays a significant role in field uniformity. 1 mil tolerances are called for!

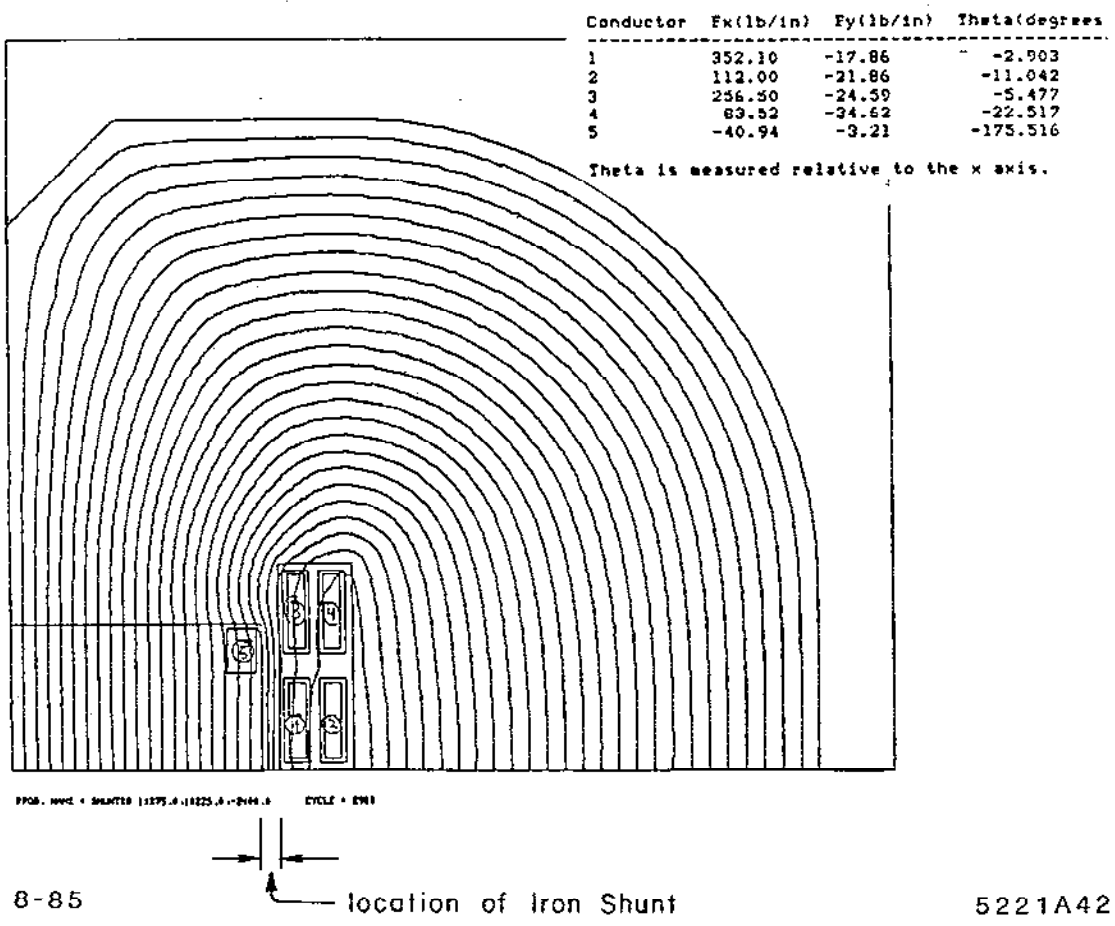

Fig. 2.19. TAC "Superferric" Profile at 3 Tesla (Note Presence of Iron Shunt Magnitude of POISSON Calculated Forces on Conductors).

2.5 Description of Fields in Harmonic Expansion

Around 1965, the measurement and diagnosis of quadrupoles underwent somewhat of a revolution with the use by J. Cobb et al. at SLAC (Ref. 43) of the fast rotating coil. This idea is based on the description of magnetic fields in terms of their harmonic expansion.

Imagine, if you will, a coil shown in Figure 2.20. Rotating with constant angular velocity – one side of the coil is placed colinear with the axis of the magnet, the other side sweeps out a circle of constant radius, r. The voltage that you will see on an oscilloscope is proportional to the rate of flux cut by the coil.

If the quadrupole is perfect, we should see a perfect sine or cosine wave at a frequency twice the revolution frequency.

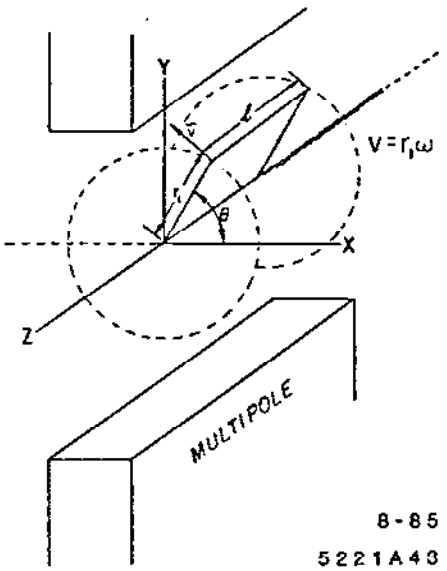

Fig. 2.20. The Geometry of a Harmonic Analysis Coil.

Since the real magnet has had its pole cut back for the coil, the magnet is not perfect, and there are satellite poles from the pole corners as shown in Figure 2.21. You can see that these satellites (there are 3 per pole) will give rise to a signal at 3 times the quadrupole frequency and will be superimposed on the main signal out of phase. We call this the 12 pole or dodecapole contribution. Its magnitude is a measure of how good the field quality is. More generally, we can write (Figure 2.22) a general expression for the field as a sum of the fundamental and higher order terms.

Now, you see the power of the method. By frequency and phase analyzing the signal by an electronic analyzer you can immediately determine the error fields in terms of the fundamental.

For example, if the amplitude of the 12 pole term is 0.1% of the 4 pole term at radius r_1, we can scale it to any other radius r_2 simply in the ratio

$$\frac{B(r_1)}{B(r_2)} = \left(\frac{r_1}{r_o}\right)^{6-1} \Big/ \left(\frac{r_2}{r_o}\right)^{2-1} = \left(\frac{r_1}{r_2}\right)^4$$

This means, of course, that allowed higher order pole contributions scale with very high powers and become important only near the aperture radius. The relative 20 pole, the next allowed pole scales as $(r/r_o)^8$, a fact that has led some wag to point out that "four rusty nails do a quadrupole make" provided the good field volume is sufficiently small. A good rule of thumb is that it is very hard to make a "bad" quad if only half its bore radius is used.

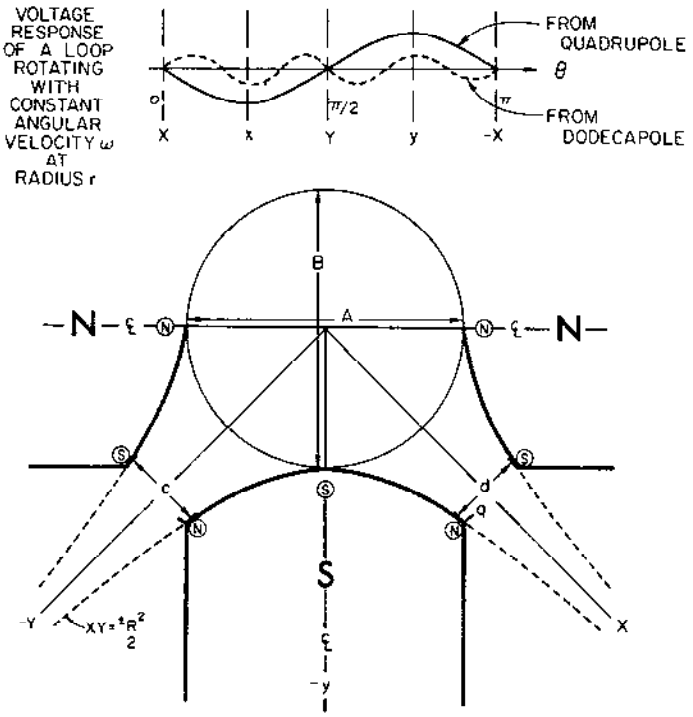

10-85 Quadrupole constructed with perfectly hyperbolic poles but poles truncated at points p and q. 379A11

Fig. 2.21. 4 Pole and 12 Pole Contribution from a Truncated Hyperbolic Pole.

This harmonic method just described gives the basis for diagnosing the illnesses that beset magnets. The magnitudes and phases tell you how to change the profile. Since the POISSON program can perform this analysis, the designer can first diagnose the magnets on paper.

Some of the illnesses are shown in Figures 23, 24, 25 and are listed in Ref. 43. The ones from incorrect pole shapes can produce only odd harmonics of the 4 pole, i.e., 12, 20, 28, etc. All others arise from "constructional asymmetries" caused only by incorrect stampings or that the magnet has not been assembled correctly. One cannot overemphasize the importance of establishing manufacturing practices that maintain constructural symmetry! The most general analytic treatment of errors is by Halbach, Ref. 44. How the measurements are actually carried out is treated in the next chapter.

THE FIELD EXPANSION

(in cylindrical coordinates)

$$B_r(r,\theta) = K_{22}\, r \sin 2\theta + K_{33}\, r^2 \sin(3\theta - \alpha_{33})$$

$$+ K_{44}\, r^3 \sin(4\theta - \alpha_{44}) + K_{55}\, r^4 (\quad)$$

$$+ K_{66}\, r^5 \sin(5\theta - \alpha_{55}) \ldots\ldots$$

or

$$B_r(r,\theta) = \sum_{n=1}^{\infty} K_{mn}\, r^{n-1} \sin(n\theta - \alpha_{mn})$$

$$B_\theta(r,\theta) = \sum_{n=1}^{\infty} K_{mr}\, r^{n-1} \cos(n\theta - \alpha_{mn})$$

We call

$n = 1$	Dipole
$n = 2$	Quadrupole
$n = 3$	Sextupole
$n = 4$	Octopole
$n = 5$	Decapole
$n = 6$	Dodecapole or 12 pole

For a quadrupole that has perfect constructional symmetry only odd harmonics of the 4 pole are allowed!

8-85 5221A45

Fig. 2.22. Terminology of the Field Expansion in Cylindrical Coordinates.

$$B_r = -\mu_o \sum_{n=2}^{\infty} \sum_{m=2}^{\infty} \nu_{mn} \left(\frac{k_{mn}}{k_{22}} (2K_{22}) \right) r^{n-1} \sin(n\theta - \alpha_{mn})$$

and similarly

$$B_\theta = -\mu_o \sum_{n=2}^{\infty} \sum_{m=2}^{\infty} \nu_{mn} \left(\frac{k_{mn}}{k_{22}} (2K_{22}) \right) r^{n-1} \cos(n\theta - \alpha_{mn}).$$

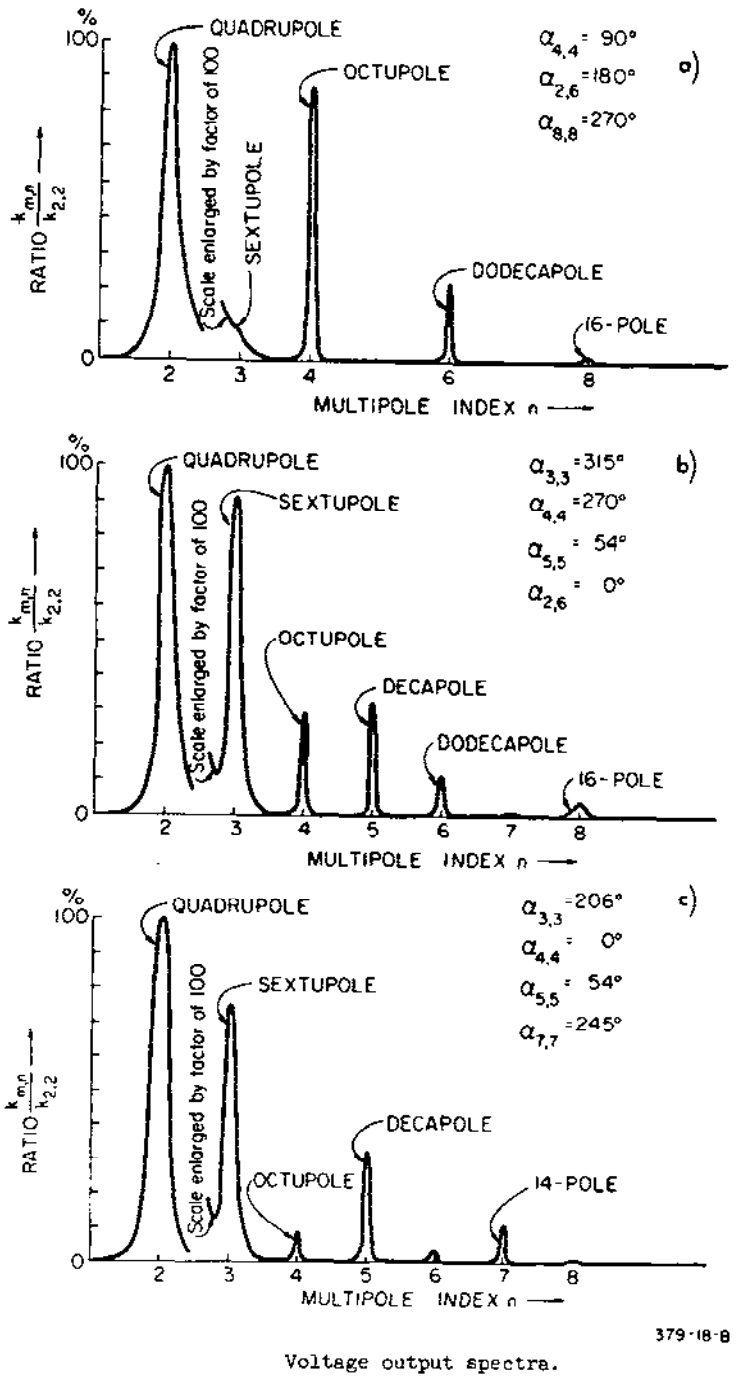

Voltage output spectra.

Fig. 2.23. Typical Observed Spectra.

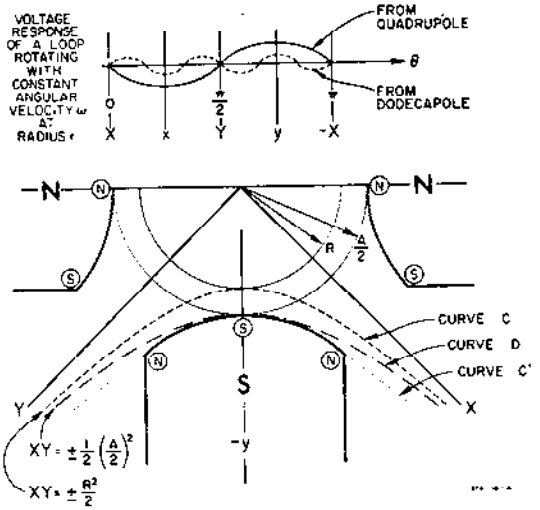

Quadrupole with all four poles moved radially away, by an equal amount, from the center of the aperture.

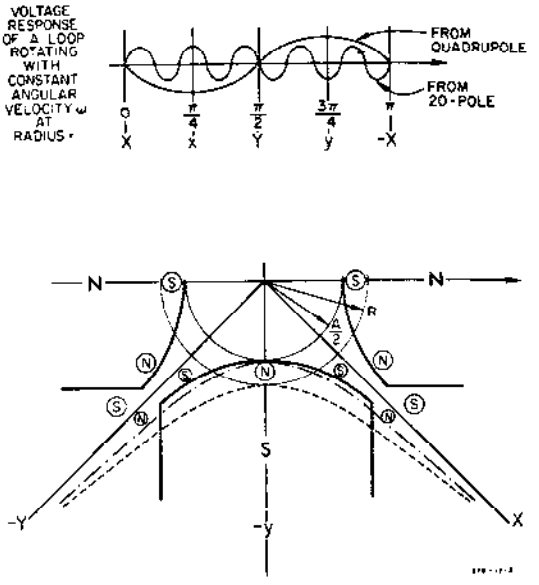

Quadrupole with all four poles moved radially toward the center of the aperture, by an equal amount.

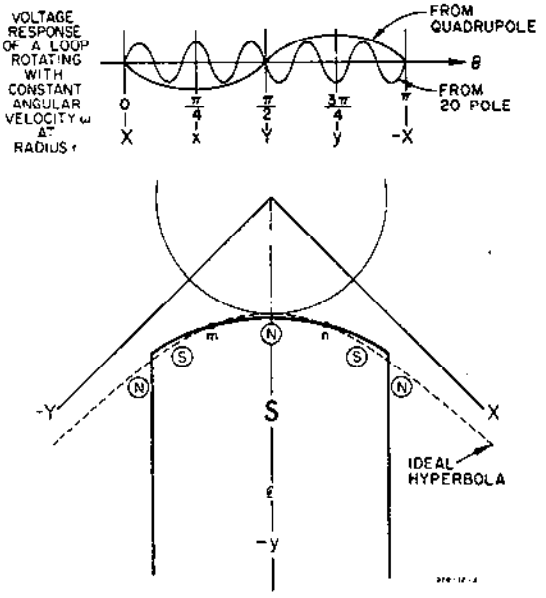

Quadrupole constructed with circular approximation to ideal hyperbolic shape circle and hyperbola coincide at points m and n .

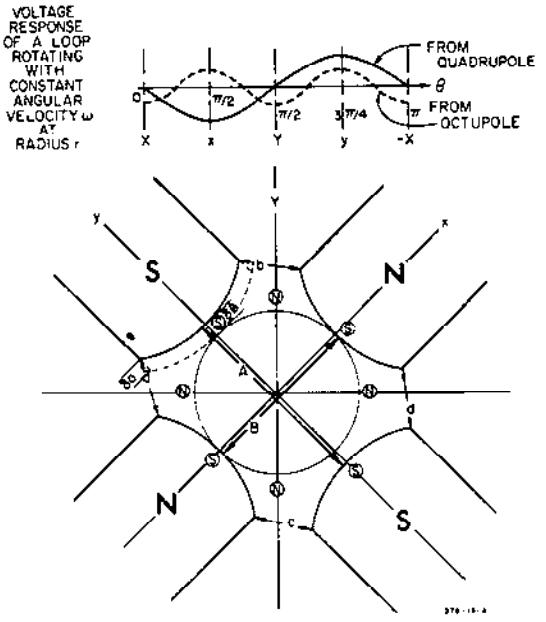

Octupole perturbation in a quadrupole field generated by geometrical asymmetry (a=b=c=d, but A ≠ B).

Fig. 2.24. Pictorials of Quadrupole Errors and Their Signals.

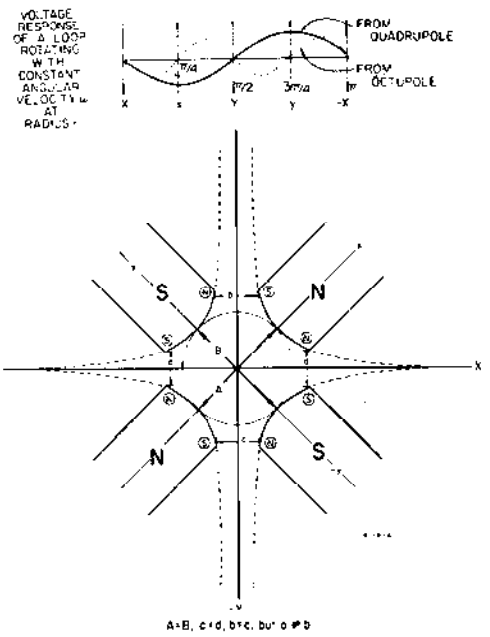

Octupole perturbation in a quadrupole field generated by geometrical asymmetry.

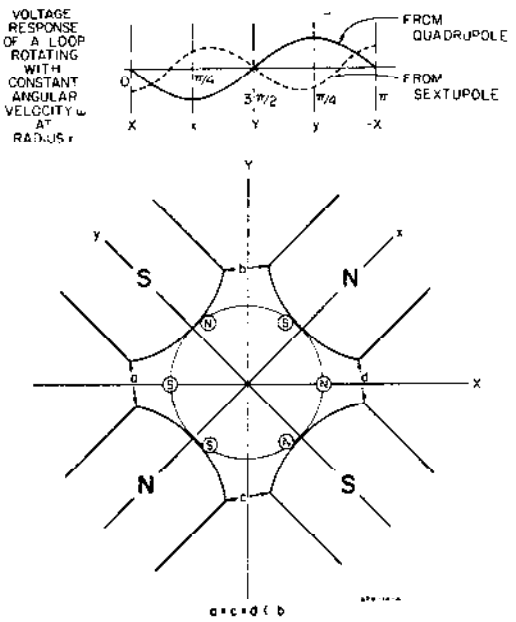

Sextupole field generated by asymmetric perturbation in a quadrupole.

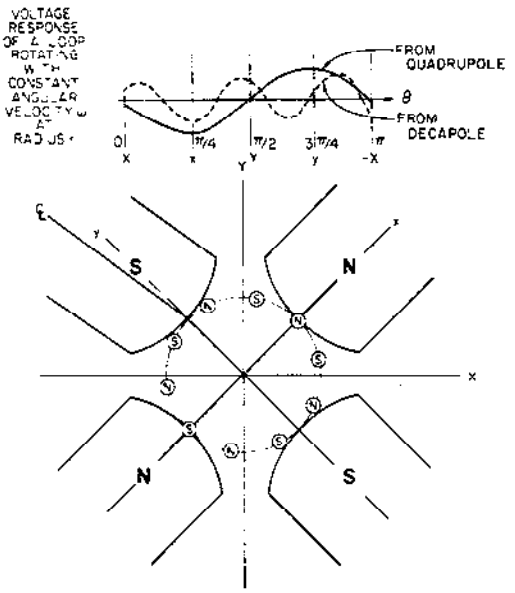

Decapole perturbation in a quadrupole field generated by geometrical asymmetry. (One pole with tilted centerline.)

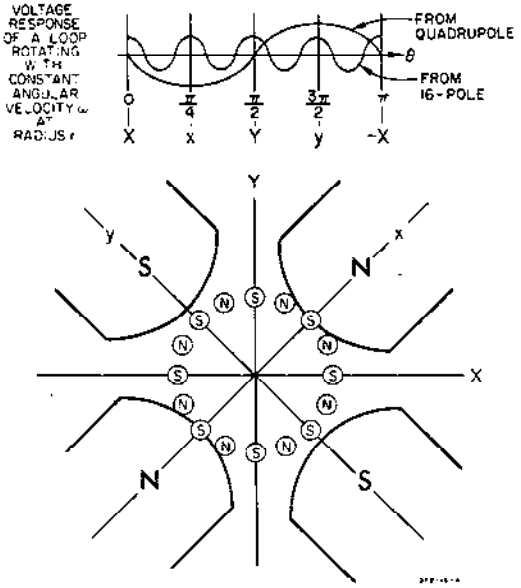

Sixteen-pole perturbation in a quadrupole field generated by geometrical asymmetry. (Poles along y-axis moved away from center of aperture.)

Fig. 2.25. More Pictorials.

2.6 End Effects

So far, everything we have said is two dimensional. Real magnets have ends which are felt by the traversing particles. What we need to do is repair not just the local errors but maintain the quality of the magnet *integrated over its total length* and this is done by shimming the ends. For a crude magnet ($1/10^3$) a simple cut across the end of the poles will do. For a very high quality magnet, better than $1/10^4$ more complicated procedures are used.

A square end will generally introduce substantial 12, 20 pole contributions. Figure 2.26 shows how the 4 pole and 12 pole fields appear at the ends of the magnet. If the poles are cut away, as shown, the integrated out of phase and in phase contributions of the 12 pole can be made equal so that the particles do not feel this higher order effect. The amount of cut "(d)" can be determined by an algorithm as detailed in Ref. 45. By adjusting the angle of the cut both 12 and 20 pole integrated contributions can be cancelled. You will appreciate that this trick also makes the quadrupole errors less sensitive to saturation effects since the end fields enter the steel more perpendicular to the steel.

Another method is to modify the pole contour in the center of the magnet to compensate for the end effects. This has been done extensively at CERN (Ref. 46).

Some of the highest quality quadrupoles known to me are the 24 PEP interaction region quads built at LBL (Refs. 47 and 48). The sum of all higher order pole field contributions were specified to be less than $1/10^4$ at the pole radius. Each pole has a removable pole shoe as shown in Figure 2.27(a). The harmonics of each magnet were measured and the shape of the end shoe calculated to compensate the error field. The shoes were then machined on a computer controlled milling machine, reinstalled, and the magnet was remeasured. Using the coefficients found in this way the required field tolerances were met. The 24 magnets (including the engineering) cost 1.4 million dollars. You may ask why not make the bore radius a little larger and not work so hard. The answer is that the optics of the storage ring required a certain gradient length product in a given length. The effort represents the current state of the art.

In spectrometer quads, of large aperture, sometimes the ends are made spherical. This, too, is very expensive. Mirror plates Figure 2.27(b) are often introduced to terminate the field so that it cannot interact with an adjacent magnet. The latter is described in Refs. 49 and 50. While we are on the subject of end correction, recently the entrance and exit fields of microtron magnets have been studied with TOSCA and the effects of the so called "end guards" evaluated (see Refs. 51 and 52).

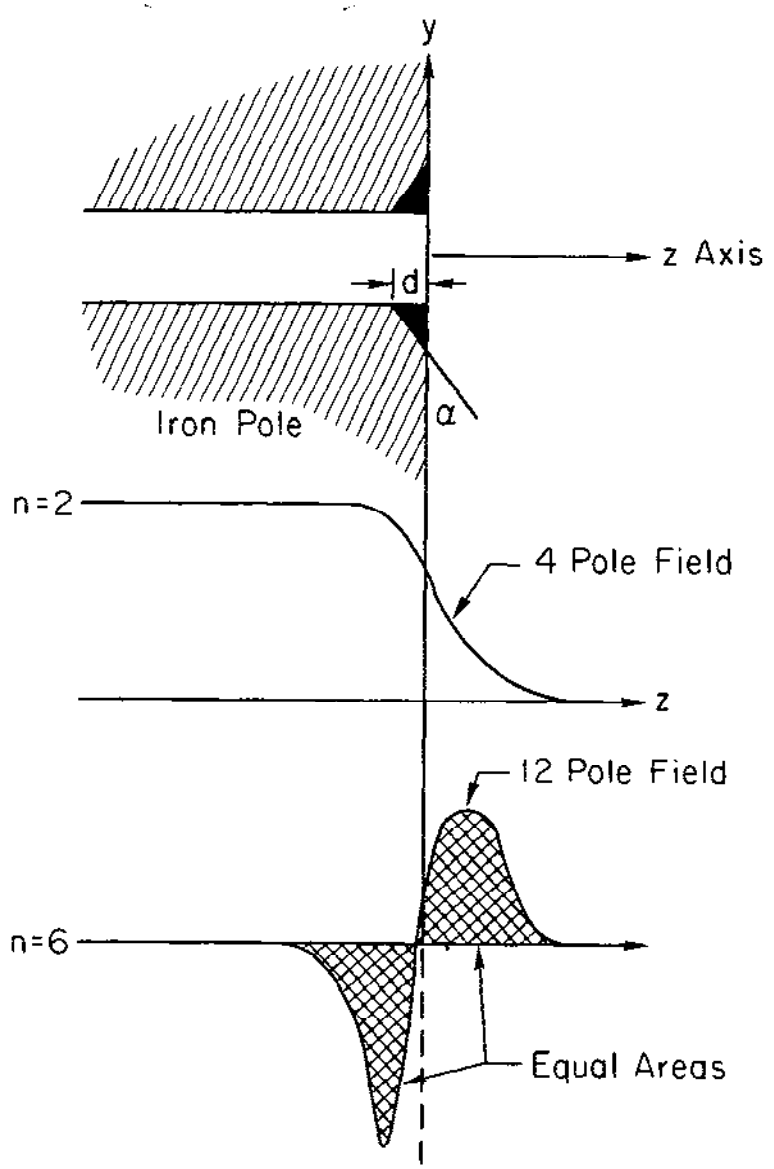

The cut of depth "d" and angle "α" can be adjusted to minimize both 12 pole and 20 pole integrated contributions.

8-85 5221A50

Fig. 2.26. A Simple Two Parameter "End Field" Correction.

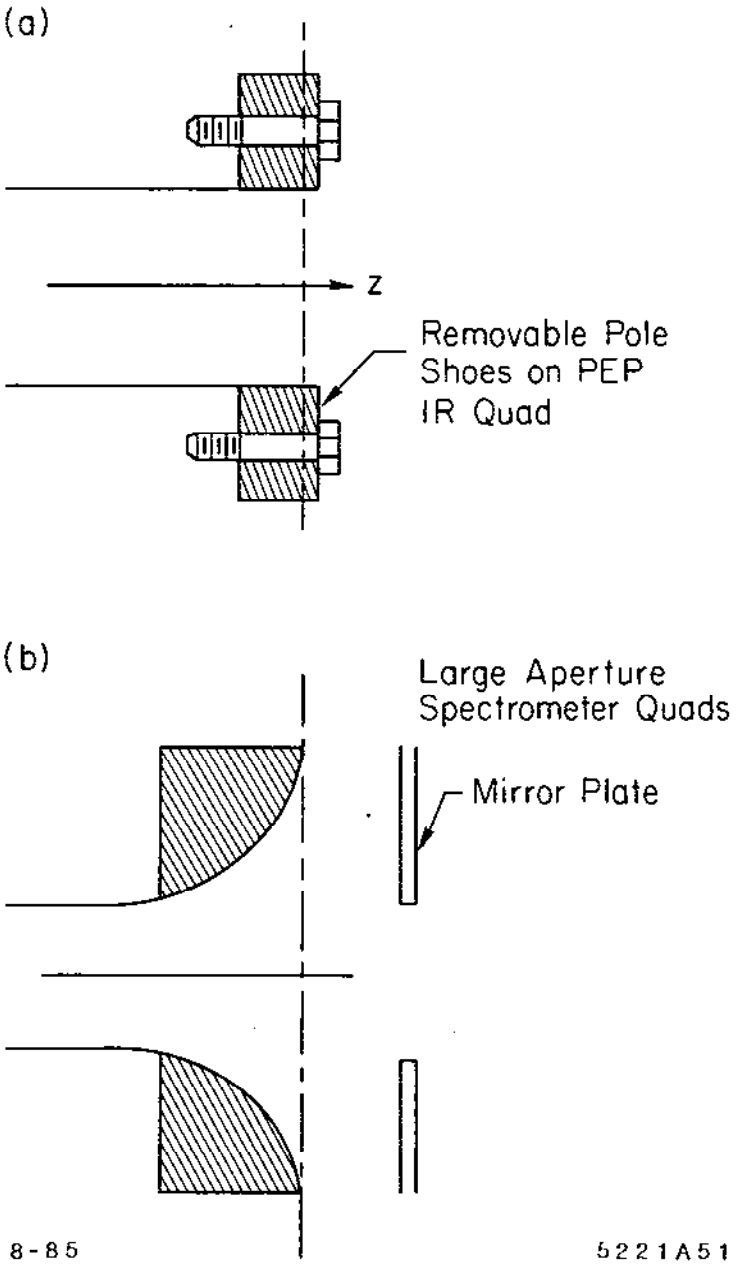

Fig. 2.27. Other Corrections (a) Removable Shoes, and (b) "Mirror Field" Termination.

2.7 Pole Face Windings

Some cycling accelerators need particular field shaping at injection energies to compensate errors that arise from remnant fields and eddy currents. Reference 53 describes how pole face windings are used.

REFERENCES – CHAPTER 2

22. NS-22 (1975) p. 1878. A. Chao, M.J. Lee and P. Morton (SLAC).
23. NS-24 (1977) p. 1197. R. Servranckx (SLAC).
24. Paper S2. A. Chao (LBL), PAC, Vancouver, 1985.
25. MT-5 (1975) p. 168. A.G.A.M. Armstrong et al. (Rutherford).
26. MT-5 (1975) p. 147. C. T. Carpenter, Imperial College London.
27. NS-20 (1973) p. 716. K. Endo et al. (KEK).
28. MT-4 (1972) p. 555. C.W. Trowbridge (Rutherford).
29. MT-4 (1972) p. 585. T.K. Khoe and R.J. Lari (Argonne).
30. MT-3 (1970) p. 198. A. Schleich and A. Segesseman (BBC-Zurich).
31. SLAC-56 (1966). E.A. Burfire, L.R. Anderson and H. Brechna.
32. SLAC-5l (1965). N.B. Herrmannsfeldt (SLAC).
33. UCRL 7784 (1964). A.M. Winslow.
34. UCRL 18439 (1968). J.S. Colonias.
35. PEP Note 326, Nov. 1979. R.A. Early (SLAC).
36. Paper H32. D.R. Walz and W.O. Brunk (SLAC), PAC, Vancouver, 1985.
37. Paper H33. R.A. Early and J.K. Cobb (SLAC), PAC, Vancouver, 1985.
38. A.G.A.M. Armstrong et al., COMPUMAG Grenoble, 1978.
39. Paper H34. G.E. Fischer et al. (SLAC), PAC, Vancouver, 1985.
40. MT-2 (1967) p. 47. K. Halbach (LBL).
41. Paper H35. W.T. Weng et al. (SLAC), PAC, Vancouver, l985.
42. NS-12 (1965) p. 842. W.B. Herrmannsfeldt and R.H. Miller (SLAC).
43. MT-1 (1965) p. 431. J. Cobb and R. Cole (SLAC).
44. K. Halbach, N.I.M., Vol. 74 (1969) p. 147 (LBL).
45. MT-4 (1972) p. 469. N.V. Hassenzahl (Los Alamos).
46. MT-3 (1970) p. 304. R. Perin (CERN).
47. NS-26 (1979) p. 4033. R. Avery et al. (LBL).
48. NS-26 (1979) p. 4030. R.M. Main et al. (LBL).

49. K. Halbach, N.I.M., Vol. 119 (1974) p. 327 (LBL).

50. K. Halbach, N.I.M., Vol. 119 (1974) p. 329 (LBL).

51. NS-30 (1983) p. 3288. R.L. Kustom (Argonne).

52. NS-30 (1983) p. 3611. K.M. Thompson, M.H. Foss and R.J. Lari (Argonne).

53. NS-20 (1973) p. 703. A. Asner, R. Holsinger and Ch. Iselin (CERN).

3. MAGNETIC MEASUREMENTS AND MORE ON HARMONIC ANALYSIS

3.1 INTRODUCTION

There are two main aspects to magnetic measurements, and I believe they are separable. The first question is: – "Does the final design perform to specifications and, if not, why not?" The second question is: – "Do all the magnets in an accelerator or beam line behave the same way?" In other words, I am separating the work of proving the design from the work of production quality control. The techniques may be similar, but the emphasis is quite different.

3.2 FIELD QUALITY CONTROL

Assuming that the "final" model is correct, let me list a few of the questions that need to be answered in production quality control.

(a) Is

$$\int_{-\infty}^{+\infty} B \cdot dz$$

for each bending magnet the same within a given error for a given current setting? In other words, do the bending strengths track with current. If not, unacceptable orbit distortions result.

(b) What is the absolute

$$\int B \cdot dl$$

for the collection of magnets? If other devices depend on this knowledge, say the injection energy, or final energy, this can be important. The values must be repeatable from day to day.

(c) Is

$$\int G \cdot dl$$

for each quadrupole the same? If not, the width of resonances are opened up.

(d) Is the absolute gradient correct? If not, the tune of the machine will be wrong or a focal plane is in the wrong place spoiling resolutions.

(e) Do the production quads have proper harmonic content? If not,they have been incorrectly assembled, or there may be a partially shorted coil.

(f) Do coils get too hot? If so, there is a blocked water passage.

(g) Are the magnets straight or twisted? If so, $x - y$ coupling occurs. You can think up your own list. The point I want to make is that when you are producing several magnets a day you must have a reliable magnetic quality control system, semi- automated, i.e., computer run with a capability of measuring and analyzing the data at high speed so that you can tell whether to accept or reject a magnet immediately. You don't have time to diagnose illnesses! The system and the running of it may cost perhaps 10% of the magnets themselves but, in my view, is essential for the successful operation of a large machine as well as catching fabrication errors before it is too late.

3.3 Magnetic Measurement Techniques

The many different methods of field measurement are reviewed in Refs. 54 through 57. I will comment on each method briefly to show in which situation it is most applicable.

3.3.1 Nuclear Magnetic Resonance

The most accurate method of field measurement depends on the anomalous magnetic moment of the proton, deuteron or electron. These values have been determined by others, and one can take the most recent values from the literature. For instance, the Larmour precession frequency of the proton, I believe, in 1984 was,

4257.7109 Hz/gauss (Free Proton)

This value must be corrected by 23 PPM for the proton in a water sample for diamagnetic and 2nd order paramagnetic screening by molecular electrons and other effects as shown in Refs. 58 and 59. In fact, the scientists at CERN carried out the most remarkable magnetic mapping of the muon storage ring to 10 PPM; their comments are worth reading.

The proton frequency at 17 kG is around 72 Megahertz. This is somewhat inconvenient electronically. Therefore, often the water sample is augmented with deuterium whose magnetic moment precesses at 653.59 Hz/gauss.

Lithium is also used at 1654.7 Hz/gauss. Needless to say, high precision measurements require well regulated power supplies. I will not go into the details of probe construction except to say that long leads generally degrade the signals

so that the local oscillator should be close to the probe and may, therefore, have to be controlled remotely. This is easily done by the use voltage controlled capacitors. It is very useful to have the oscillator track a slowly varying field automatically by means of a phase controlled feedback system.

There are three main disadvantages of the NMR.

1. The field must be quite uniform over the size of the sample. Therefore, gradient magnets and end fields cannot be measured.
2. The field cannot change in time rapidly.
3. One is measuring the field in only one place at a time. Over a long magnet this is tedious.

However, no laboratory can be without an NMR. It is the primary reference standard.

3.3.2 Hall Plates

The Hall effect is used to great advantage in making point measurements. The probes are small, don't require very elaborate electronics and can measure field directions. See Refs. 60 and 61.

Their disadvantages are:

1. They have zero offsets and are non-linear (1-2%). That means they must be calibrated carefully against NMR.
2. They are temperature sensitive – that means they must be put into a temperature regulated oven and controlled to $\pm 1°C$.
3. They require corrections if the field is very nonlinear.
4. They must be carefully aligned.
5. They suffer from magnetoresistive and thermal EMF effects.

Their worst disease is that they age and, if their exciting current is interrupted, require several days to stop drifting. Frequent calibration is, therefore, required. With care measurements can be made at about the $2/10^4$ level.

3.3.3 Static and Moving Coils

Perhaps the most useful technique of magnetic measurement is the use of coils.

Consider the Bending Magnet in Figure 3.1.

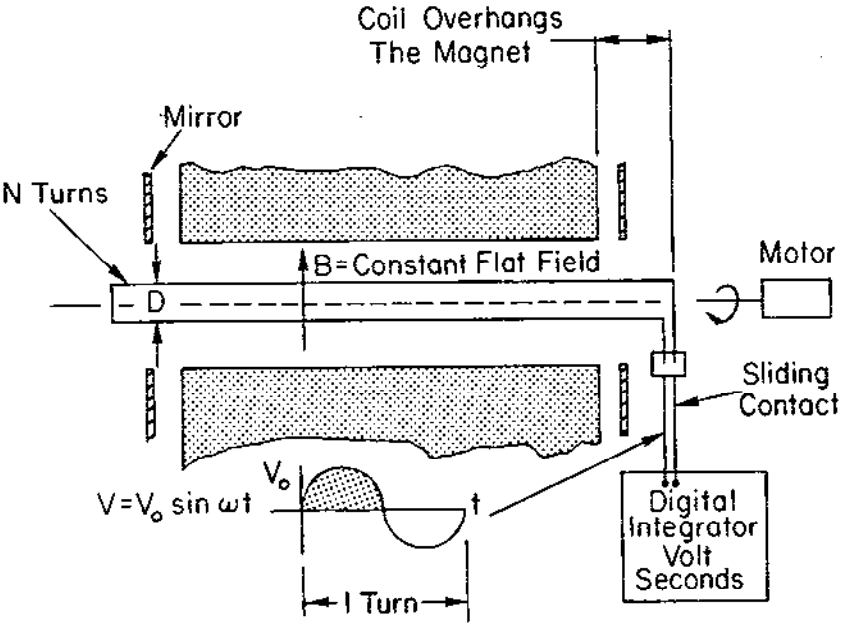

The voltage at the terminals is $V\,(\text{volts}) = -\dfrac{d\phi}{dt} = \dfrac{dB(\text{tesla})\,A(\text{m}^2)}{dt\ (\text{seconds})}$

$$\int B \cdot d\ell\ (\text{kG meters}) = \int V \cdot dt\ (\text{volt seconds}) \times \frac{10}{2 \times N(\text{turns}) \times D(\text{meters})}$$

Note:

1. This measurement is a direct absolute measure of the field a particle feels (when corrected for sagita of the orbit).
2. N and D are measured constants of the coil.
3. The integrator is made to count only + or − going signals.
4. Integrator must have an input impedance $\gg$ resistance of coil.

8-85 5221A52

Fig. 3.1. The Basic Integrated Dipole Measurement.

If the coil overhangs the magnet so that the ends are in a field free region, we measure directly what the particles feel

$$\int B \cdot dl$$

If the integration is only over the positive going signal we do not even need to measure the angle of rotation – the integrator cuts it for us.

How well can one measure the parameters of the system?

N is just the number of turns – you count them.

D is best calibrated by rotating the coil in a very well measured magnet which is mapped by NMR in the middle and with a hall probe at the ends. (If you use the same integrator for this as you do for the magnet to be measured you don't even have to calibrate the integrator or use a longer magnet.)

The integrator is calibrated with a precision voltage standard and internal precision clock as for example in a Hewlett Packard DVM (model 2401C). Or, the integrator could be any precision voltage to frequency converter coupled to a counter that can be turned on and off by a precision clock or the sign of the signal. (You realize of course that we have defeated some of the common-mode noise suppression of the integrator and opened ourselves to noise problems just as the voltage swings through zero. In practice taking averages over many turns solves some of these problems. Drift can be taken care of by linear subtraction in the data.)

The bearing on the shaft must be smooth and not bounce. The coil does not have to be exactly straight, but the dimension D should be uniform over the length of the coil.

This set up and its variations form the basis of nearly all machine magnet measurements at SLAC during production. With care, the equipment repeats with a rms of 3 to 5 parts in 10^5. Thermal effects on the coil must be taken care of. If the field is ramped in time, the coil is made stationary. Then, one measures the change

$$\Delta\left[\int B \cdot dl\right]_0^T$$

but one only knows the change in flux, not its absolute value. The starting value can be determined from peaking strips. Reference: J.M. Kelly, Review of Scientific Instruments 22, 256 (1951) or scan of the residual fields using Hall plates.

3.3.4 *More on Harmonic Measurements*

In the last chapter I stressed the importance of harmonic analysis. Since 1965, the methods and apparatus have been much refined by many authors. There are basically three types of systems:

1. The original scheme is shown in Figure 3.2 and is still used for diagnosing end fields. It is not as accurate as the newer methods. (For best signal and resolution keep the coil radius large and cross section square.) Motor coupling is important, Ref. 43.

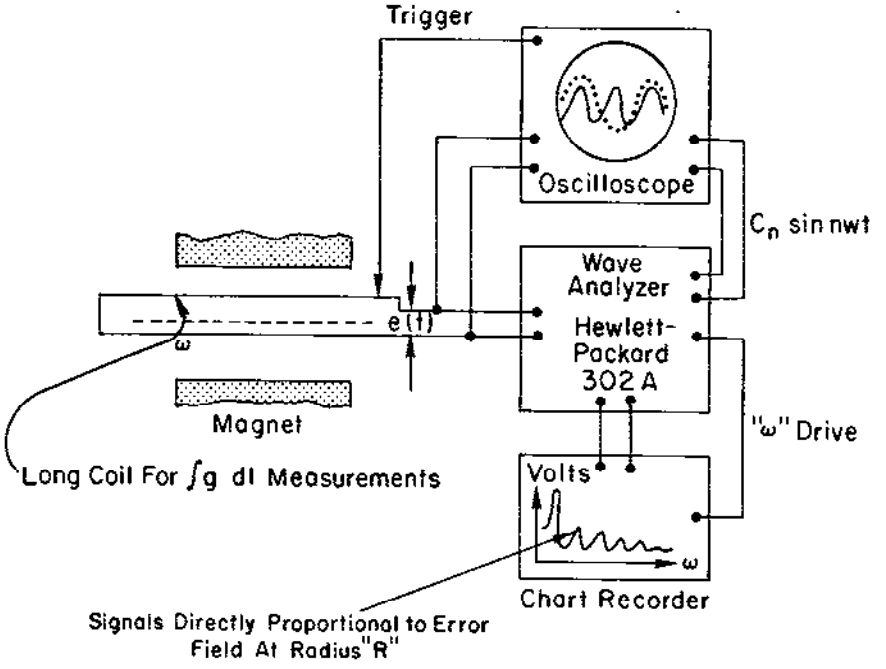

BLOCK DIAGRAM OF ANALOG SYSTEM

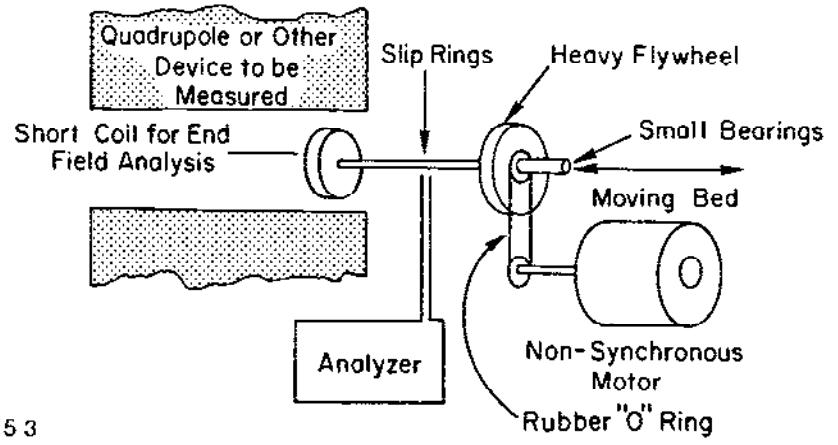

Fig. 3.2. Diagnosing an "End Field".

2. The second scheme is shown in Figure 3.3, Ref. 62.

3. The third system is shown in Figure 3.4. This was used on the PEP I.R. quads. Dr. Halbach suggested the use of "bucking" coils, (Ref. 63) in which the dominant signals, either dipole or quadrupole are balanced out by the way the coils are wound so that the error signals become visible. See also Refs. 64 and 65.

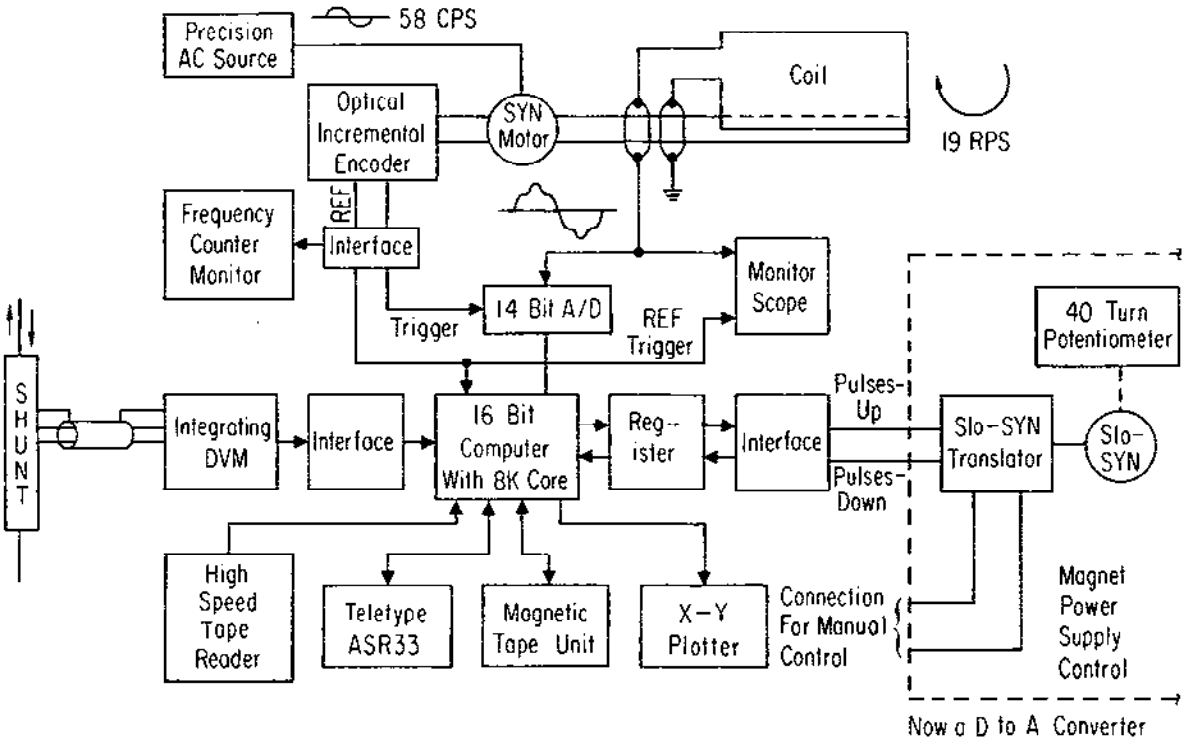

Notes:

1. The analyzer has been replaced by a 14 bit A to D converter which is keyed by a precision shaft encoder.
2. The digital data is stored.
3. The frequency analysis is performed by a Fast Fourier Transform program in the computer.
4. It is very important that the shaft speed is maintained constant and measured.
5. Because of relatively high shaft speed — coil lengths are limited to $\sim 1\frac{1}{2}$ meters.
6. Optical shaft encoder must have uniform graduations.
7. Motor torque reduced to minimum to prevent hunting.

9-85
5221B54

Fig. 3.3. Example of an Early Generic Measuring "System".

In method 2, after several hundred turns of averaging the data in storage, the FFT computation in a small computer took of the order of 5 minutes. This is fast enough, but the ultimate weapon is the modern dedicated FFT computer! There are several manufacturers that make these devices in the U.S., among them Hewlet-Packard (Model 3582) and Nicolet Scientific (Model 660) now sold by Wavetek. It is a delight to see the spectrum emerge on-line for instant diagnosis.

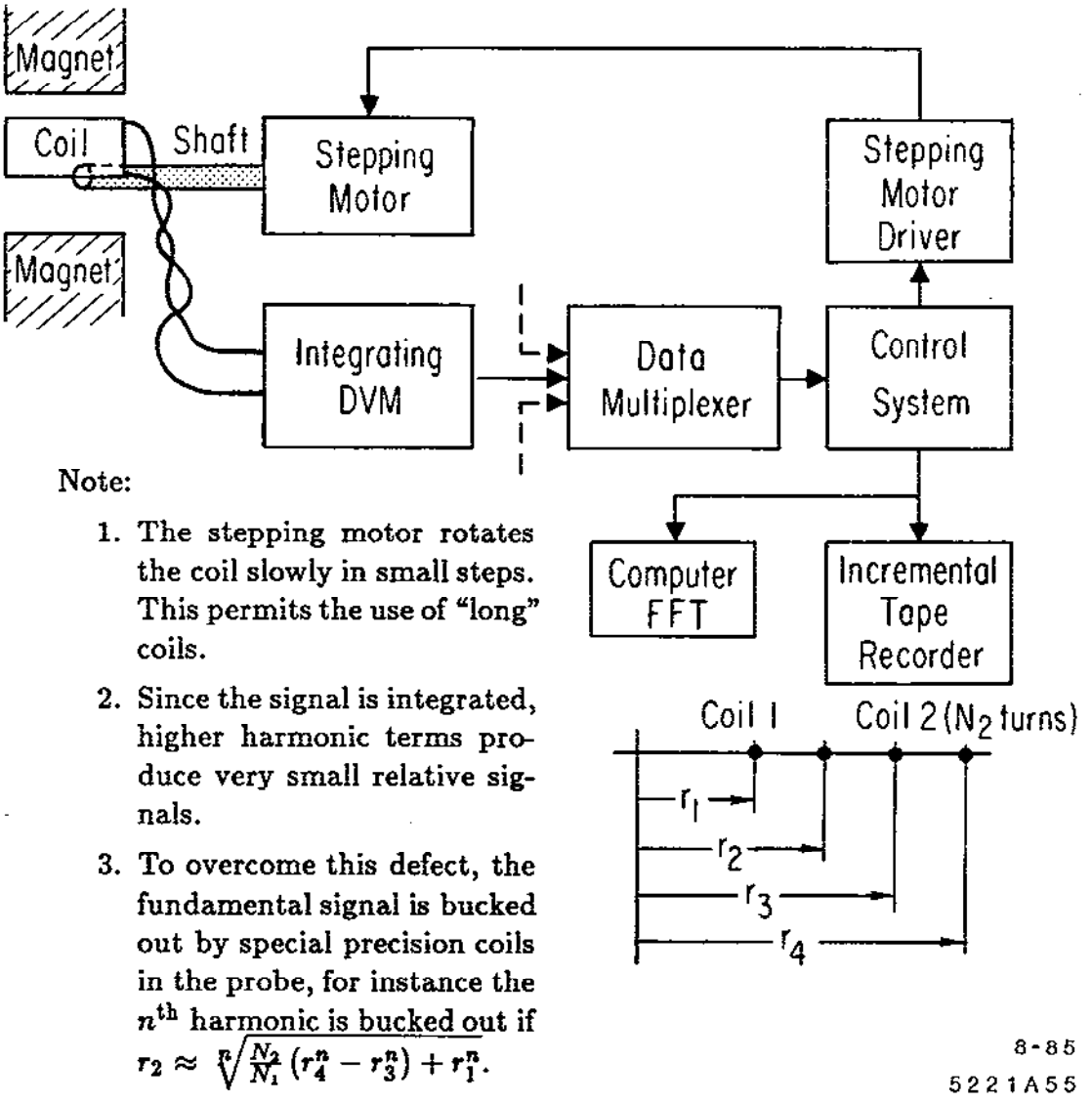

Note:

1. The stepping motor rotates the coil slowly in small steps. This permits the use of "long" coils.
2. Since the signal is integrated, higher harmonic terms produce very small relative signals.
3. To overcome this defect, the fundamental signal is bucked out by special precision coils in the probe, for instance the n^{th} harmonic is bucked out if $r_2 \approx \sqrt[n]{\frac{N_2}{N_1}(r_4^n - r_3^n) + r_1^n}$.

Fig. 3.4. Scheme for Very Small High Order Pole Contributions.

3.3.5 *The Floating Wire Technique*

In some spectrometer magnets with edge focusing the field is so complicated by edge effects to make particle tracking through a measured field map very time consuming. Physicists then resort to an old technique, that has recently been perfected to high accuracy ±.02% in which the particle's path is simulated by a current in a stretched wire.

In Figure 3.5 the equation of balance is derived. Modern applications, sensitivity and errors are discussed in Refs. 66 and 67. The method is not used very often in high energy work but makes a nice homework problem for students.

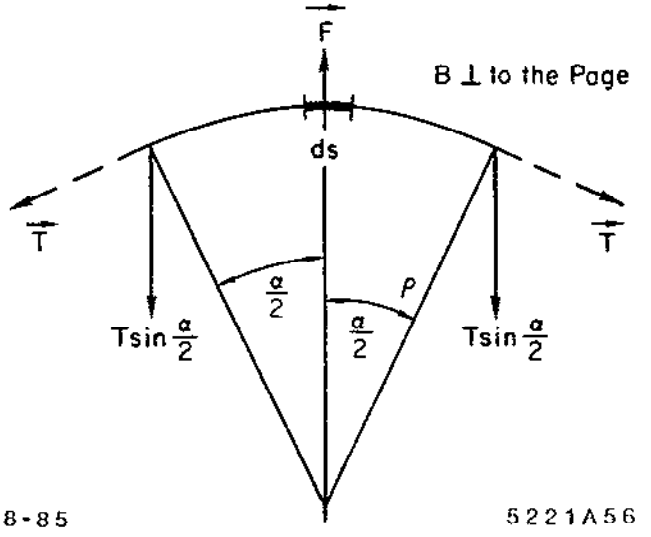

$$\vec{F} = q\left(\vec{v} \times \vec{B}\right) \qquad F = 2T \sin\frac{\alpha}{2}$$

For $\vec{v} \perp \vec{B}$

$$F = qvB = q\,\frac{s}{t}\,B = isB = i\rho\alpha B$$

For $\frac{\alpha}{2}$ small

$$F = T\alpha$$

$$\therefore \quad T\alpha = i\rho\alpha B$$

$$\text{or} \quad \frac{T}{i} = \text{“}B\rho\text{”} = \frac{pc}{e}$$

Fig. 3.5. The "Balance Equation" for the Schetched Wire.

3.4 Current Measurements

It is of no use to make good magnetic measurements if one cannot measure the current accurately. This may sound trivial, but it is not: 0.1% is easy, 0.01% harder, 0.001% very difficult.

3.4.1 Shunts

Suppose we use a shunt resistor and wish to measure a current of, say, 3000A by developing a voltage that can be compared to a standard voltage reference around 1 volt. Why so much voltage? The electrical environment around accelerators is notoriously noisy, and one would like to have a signal large enough so that, say, 0.01% is well above the noise.

In 1955, when my budget was very small, I built a resistor that is illustrated in Figure 3.6. I think you immediately see the problems with high current shunts. Some of the problems are:

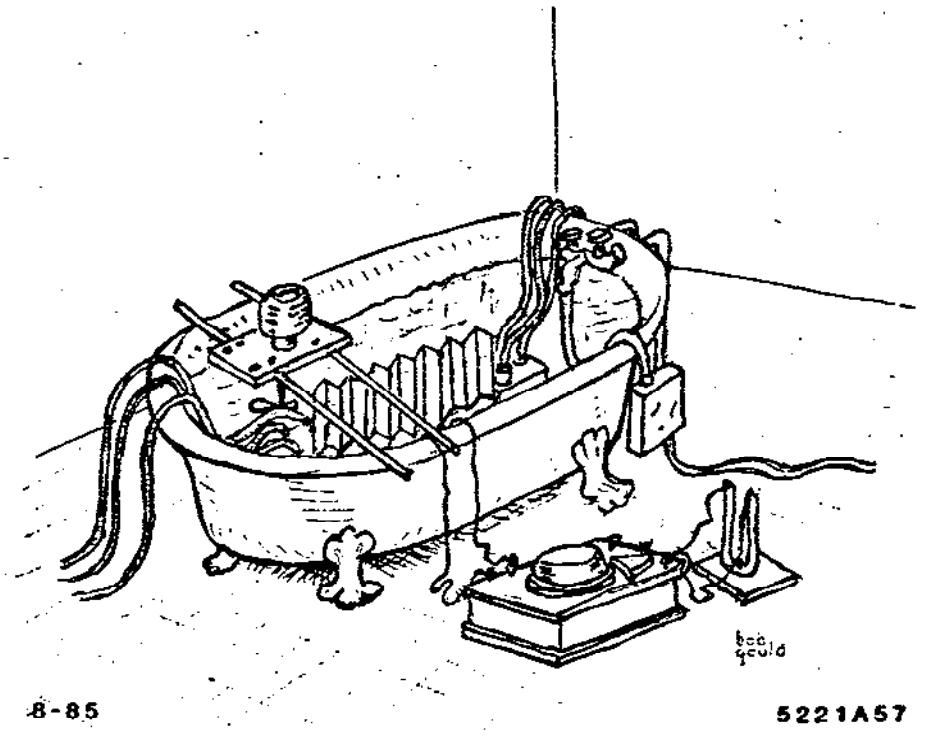

Fig. 3.6. How to Build a High Current Shunt (1954).

1. Even with manganin (13% Mn 87% Copper), designed for shunt application the temperature has to be controlled near 50°C.
2. The strip has to be mounted so that it is under no mechanical stress.
3. Thermal EMF's must be considered.
4. The inductance should be minimized.
5. The manganin must be aged for constant resistance.
6. There is a potential safety hazard due to lack of isolation between the high power equipment and the measuring electronics.

In 1971, Walter Praeg at Argonne developed a very elegant coaxial shunt which was used as a standard for a number of years. It is described in Ref. 68.

3.4.2 Transductors

Most of the shunt problems are overcome by use of Direct Current Current Transformers (DCCT). Invented in the 1930's, these devices have been improved ever since and are now almost exclusively used in all laboratories for the measurement of high currents, both DC and ramped DC.

At first glance it seems not possible to transform DC. Basically, the device is a magnetic amplifier. A good explanation of how they work can be found in Ref. 69, and I provide you with many other Refs. 70 through 76 that detail the improvements that have been made over the years.

The deceptively simple device is shown in Figure 3.7. Understanding it is not so simple. Follow the steps outlined. To overcome the notch in the DC output, a combination of cores is used either in parallel or in series, but this gets very complicated, and I will refer you to the literature.

Let me stress again the advantages:

1. Isolation from the magnet bus.
2. High output voltage.
3. Insensitivity to the drive voltage.
4. Small power dissipation.
5. With care – good stability over years.
6. Inherently good frequency response.
7. Fairly simple.

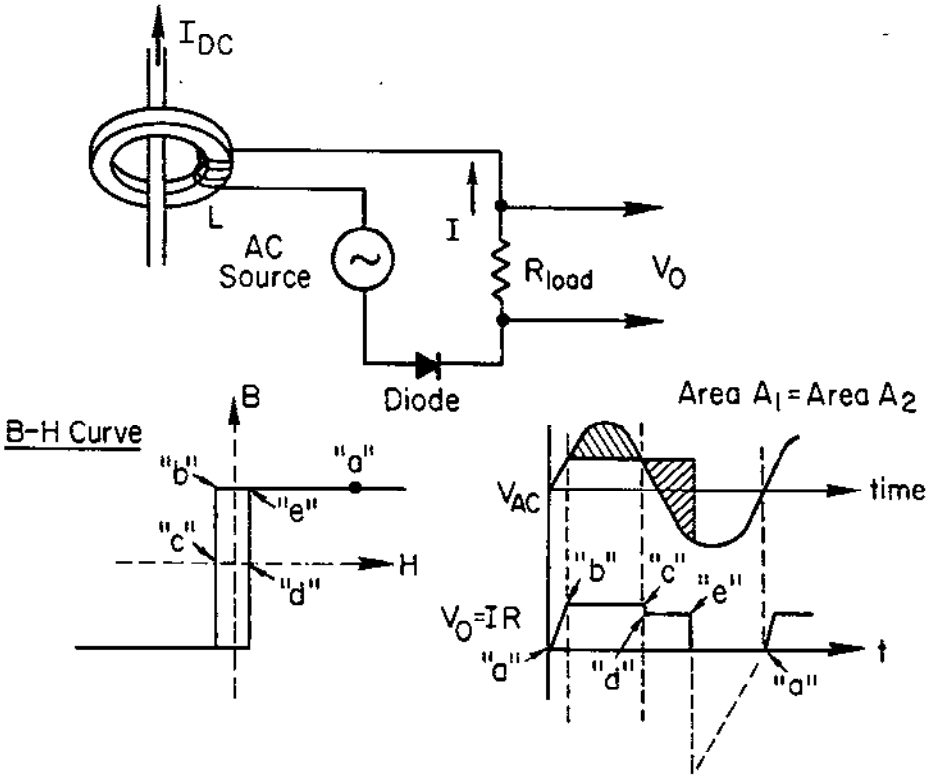

A. The DC current saturates the core to point "a".

B. The applied voltage V_{AC} drives the core toward point "b". Since L is small the current rises.

C. The core unsaturates points "b" and "c" holding the current constant. The flux change absorbed in the core in volt seconds is the Area A_1.

D. Between "c" and "d" a small step occurs in the current because the voltage across L becomes negative with respect to driving voltage but the current remains constant.

E. From "d" to "e" the core reverses, releasing its energy — current constant.

F. At "e" the core saturates L → 0, the current would go negative but is blocking by the diode.

9-85 5221A58

Fig. 3.7. Basics of a Simple Transductor.

Disadvantages:

1. Zero current offset.
2. Non-linearity.
3. Ripple (unless the electronics is very sophisticated).
4. Some sensitivity to stray fields. The disadvantages of offset and non-linearity are simple to overcome. If you operate a magnet system with the same device that you used to calibrate it, a knowledge of the "real" or absolute (in NBS terms) current is not necessary. Watch out for leakage currents to ground via "bad" water in the cooling system.

3.5 Repeatability of Calibrations

3.5.1 Hysterisis

THERE EXISTS NO SINGLE OR UNIQUE FUNCTIONAL RELATIONSHIP BETWEEN THE INDUCTION B AND THE DRIVING CURRENT I FOR AN IRON CORED MAGNET! Hysterisis in the core material causes the magnet to remember (like an elephant) where it has been in excitation. To make it forget, one must re-educate the magnet by giving it "history lessons".

For solid magnets and laminated magnets (whose laminations are not specifically insulated from each other) the conditioning shown in Figure 3.8 has proved generally satisfactory for most applications.

Some papers on this subject are Refs. 77 to 79.

In Figure 3.9 and 3.10 the effects of hysterisis on the PEP bends and some 1.0 meter long quads are shown. Notice that the strength varies several percent between upward and downward going current settings.

3.5.2 Reference Magnet

Since it is impossible to measure all the conceivable hysterisis paths that might occur in operation, it is very useful to employ an additional reference magnet in critical circuits.

During calibration, the magnet under test is wired in series with the reference magnet which is of identical construction. Both magnets are measured simultaneously. Of course, they go through the same cycle. This permits:

(1) A check on the measuring systems' repeatability.

(2) An evaluation of strength ratios of each magnet under test.

When all magnets are installed in the ring, the reference magnet is mounted in an accessible area and can be, if necessary, measured during operation. In principle, therefore, knowing the system ratio, we can determine the system

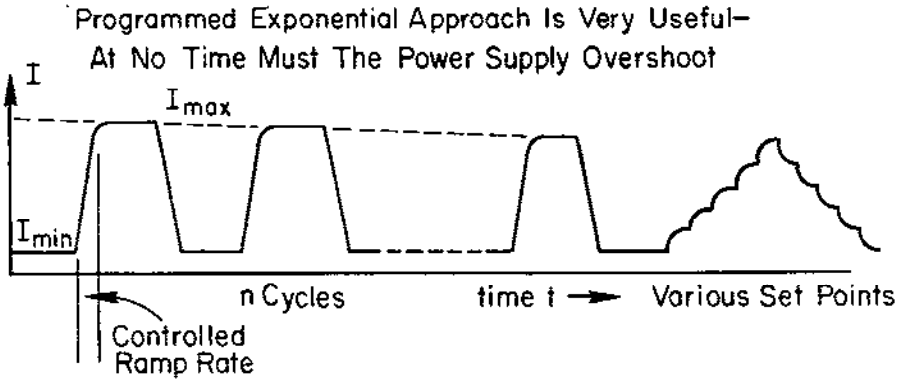

Notes:

1. It is not necessary to reverse the polarity.
2. The ramp rate can be as high as 1%/sec but should be the same each cycle and approaching set point.
3. I_{max} is preferrably enough to drive the core to 15 kG but lower values are also all right.
4. $I_{min} \sim 10\%$ of I_{max}.
5. Measurements can be made going up and going down but must be made in the same way each time and in the same way the machine is to be operated.
6. Solid core magnetic fields may take two minutes or more to settle before measurements, laminated magnets $\sim$ 30 sec.
7. For 0.01% repeatibility on laminated bending magnets $n \sim 7$ cycles, for ordinary quadrupoles $n \sim 3$ cycles.

9-85 5221A59

Fig. 3.8. A "Standarization" Procedure.

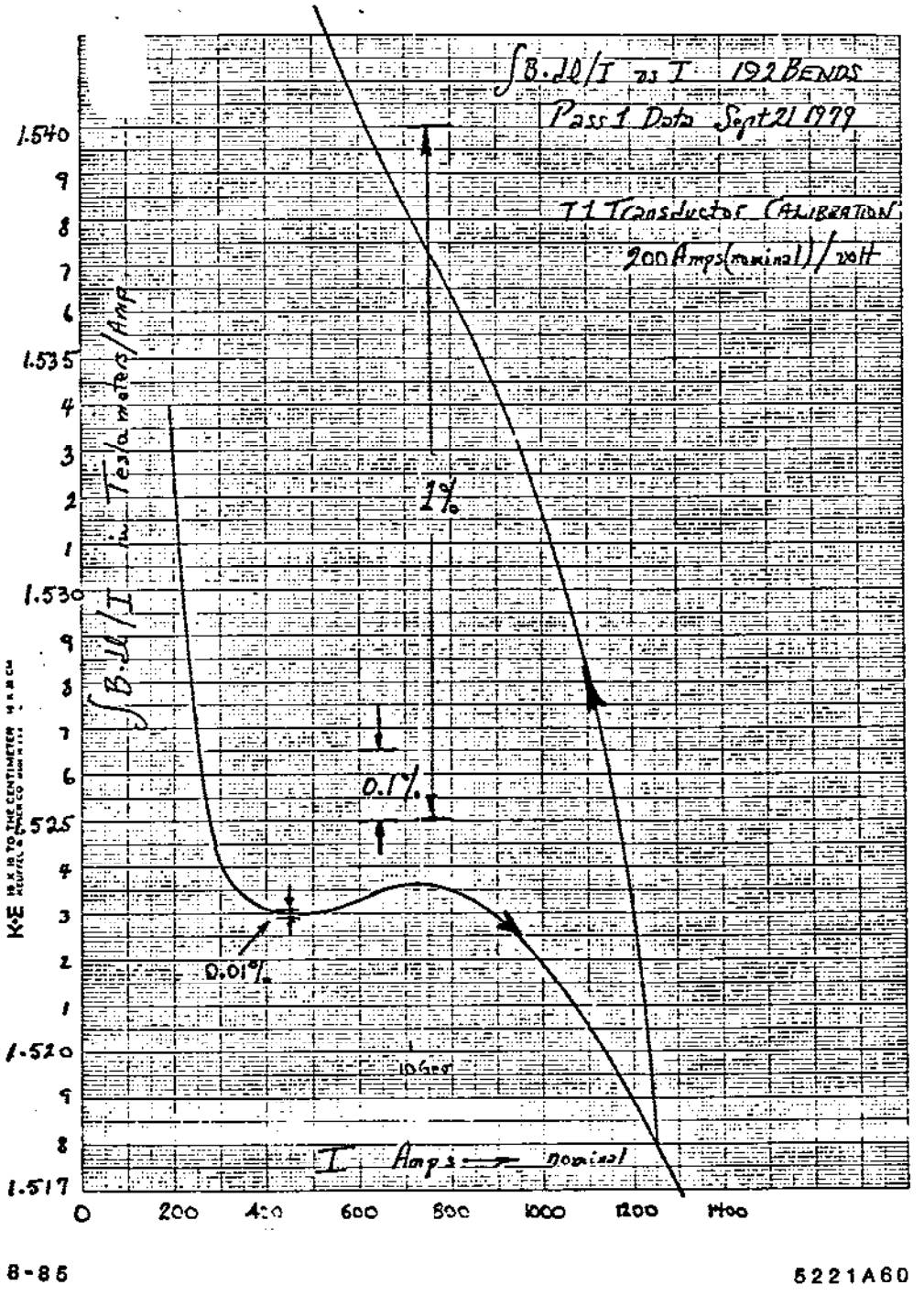

Fig. 3.9. Typical Hysteretic Behavior in a Laminated PEP Dipole (Armco Special CR Magnetic Steel).

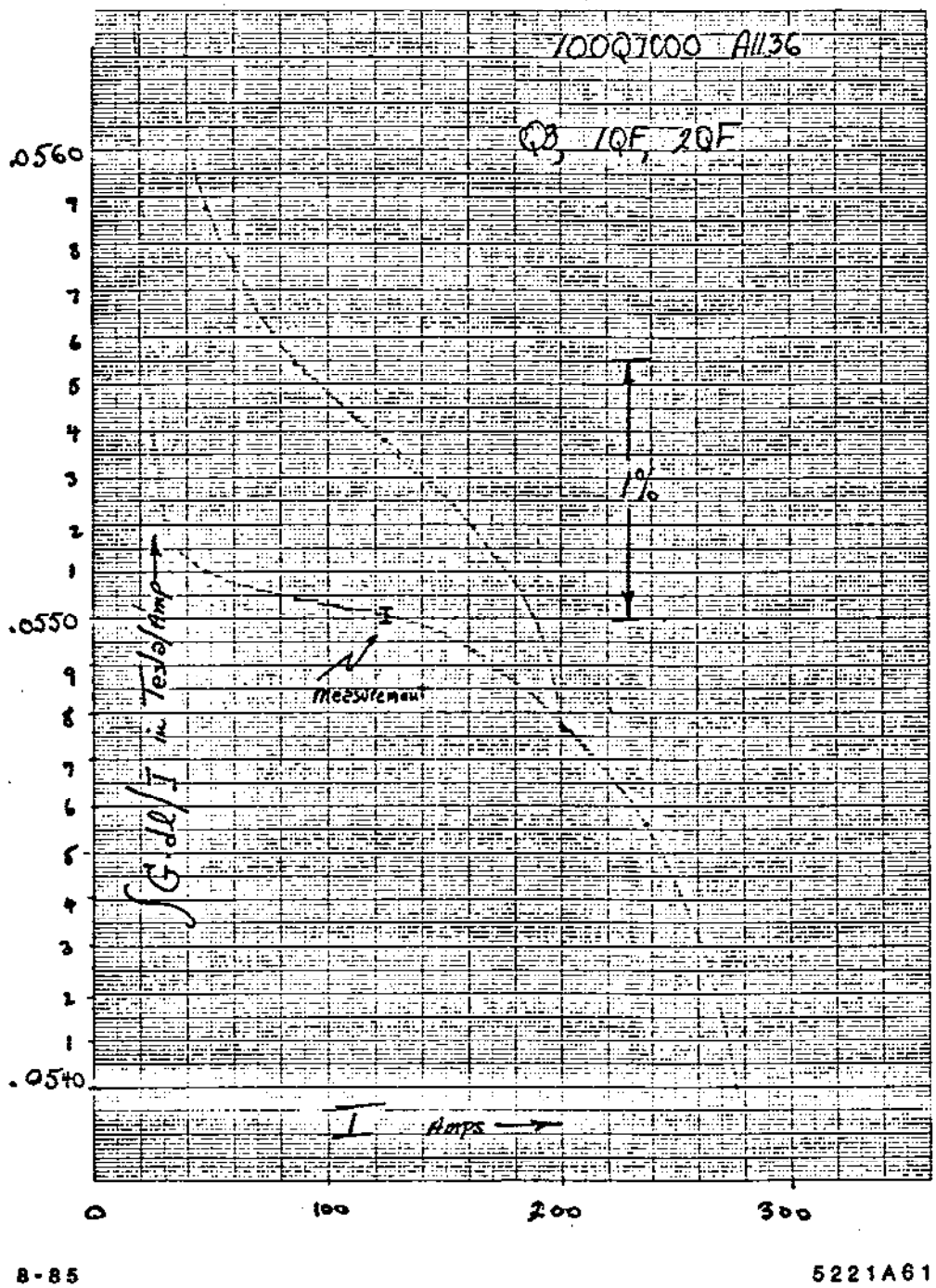

Fig. 3.10. Typical Hysteretic Behaviors at a PEP Quadrupole.

strength without any precise knowledge of the current flowing, and the hysterisis problem of setting magnets strings is solved.

3.6 Frequency Dependence of Inductance and Resistance

Power supply engineers need to know the characteristics of the load. The behavior of solid and laminated magnets' inductance and resistance as a function of frequency is shown next.

Figure 3.11 shows the measured and calculated response of some solid core magnets at CEA, Refs. 80 and 81. Eddy currents flowing in the poles exclude flux reducing the inductance. Eddy currents in the core and conductors increase with frequency the AC resistance of the magnet. Experiment and theory agree quite well.

More important today is, for example, the responses of NAL magnets which are laminated. Figure 3.12 shows the calculated transfer function in the presence of the vacuum chamber and the impedance presented to the power supply of the B_1 and B_2 bends. Notice these magnets exhibit a turn over at somewhat higher frequencies as one might expect.

Figure 3.13 shows the same sort of behavior for NAL quads, Ref. 82. Estimates of this kind are quite important to the power supply engineers in calculating their filter requirements as well as estimating whether or not the system as a whole can support transmission line modes.

The fairly thick aluminum vacuum chambers used at PEP filter out the high frequency chopper noise very effectively.

3.7 Miscellaneous Instruments

3.7.1 Permeameter

When buying hundreds or thousands of tons of steel, it is necessary to be able to quickly measure the quality and uniformity of the steel that is being shipped.

The CERN Permeameter is a particularly useful device and rapid in its operation. It is described in Ref. 83. Recently CERN has developed a "coercimeter" that does not even require sample cutoffs or rings but can be attached to the sheet steel as it comes off the roll. See Ref. 84.

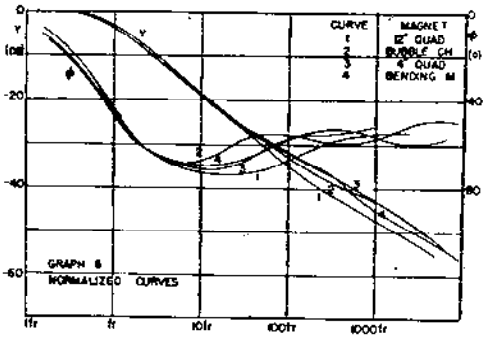

Figure 3.

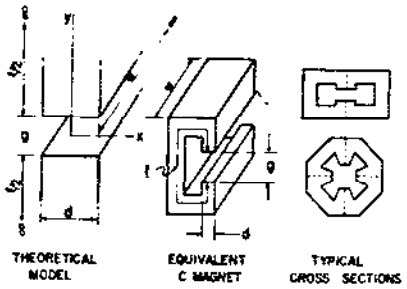

Figure 4.

L drops as flux is restricted
R rises due to eddy currents in conductors and iron

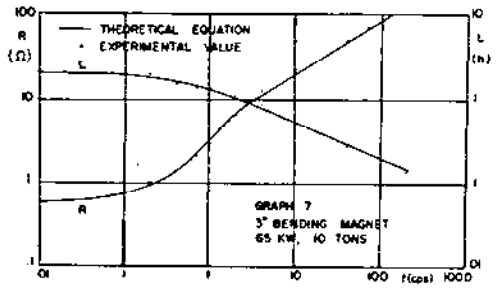

Figure 5.

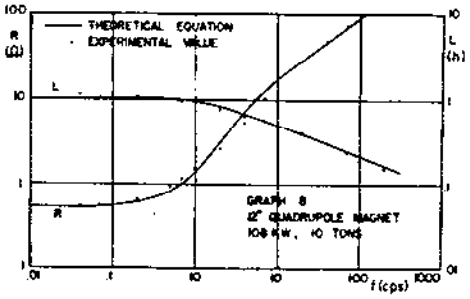

Figure 6.

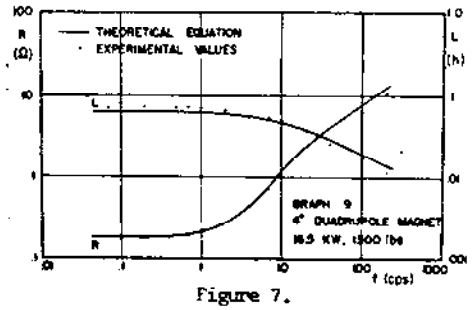

Figure 7.

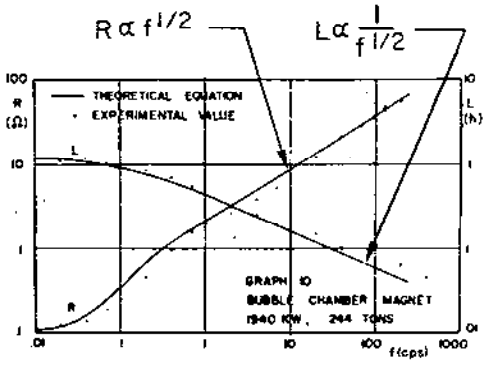

Figure 8.

8-85 Phase ϕ 90° —— 45° 5221A62

Fig. 3.11. Frequency Dependemce of Solid Core Magnets.

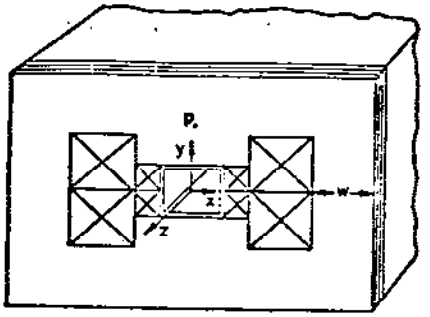

NAL BENDS

Including Vacuum Chamber

Fig.1 Dipole Cross Section

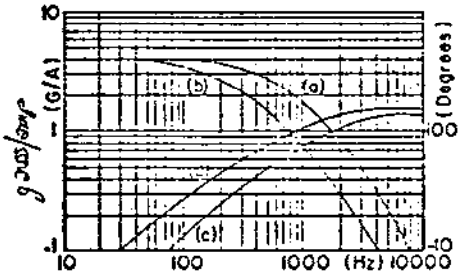

Fig.5 Transfer Function (B1)
(a) Magnitude (no shunt)
(b) Magnitude (10Ω shunt)
(c) Phase (no shunt)
(d) Phase (10Ω shunt)

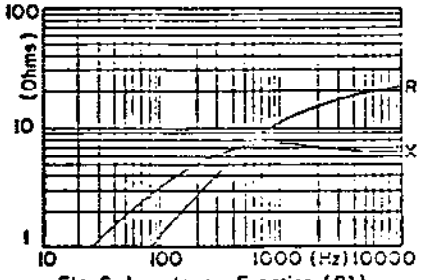

Fig.6 Impedance Function (B1)
(no shunt)
R_0 = .0059 Ω
L_0 = .0061 Hy

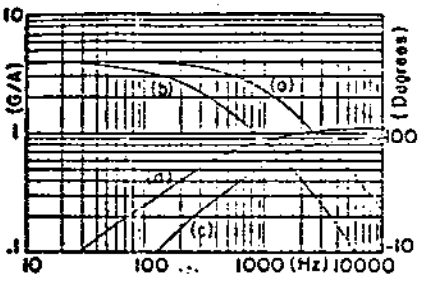

Fig.7 Transfer Function (B2)
(a) Magnitude (no shunt)
(b) Magnitude (10Ω shunt)
(c) Phase (no shunt)
(d) Phase (10Ω shunt)

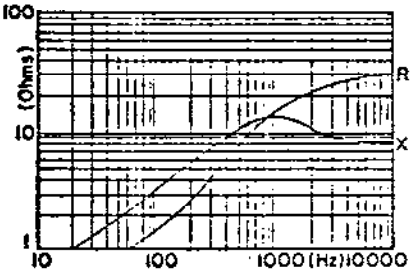

Fig.8 Impedance Function (B2)
(no shunt)
R_0 = .0073
L_0 = .0082 Hy

8-85

5221A63

Fig. 3.12. Frequency Dependence of NAL Bend Impedance Function.

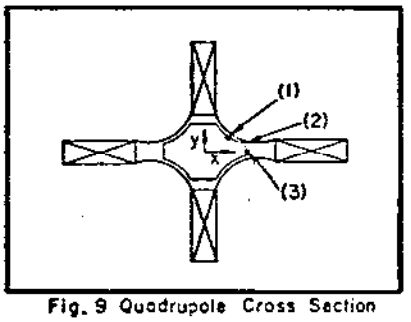

Fig. 9 Quadrupole Cross Section

NAL QUADS
Including Vacuum
Chamber

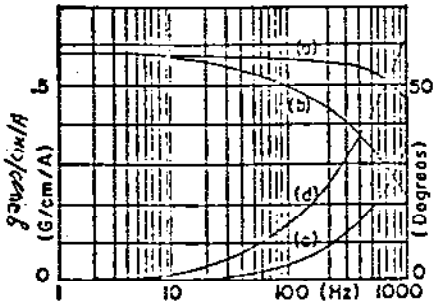

Fig.10 Transfer Function (7ft) QUAD
(a) Magnitude (no shunt)
(b) Magnitude (5Ω shunt)
(c) Phase (no shunt)
(d) Phase (5Ω shunt)

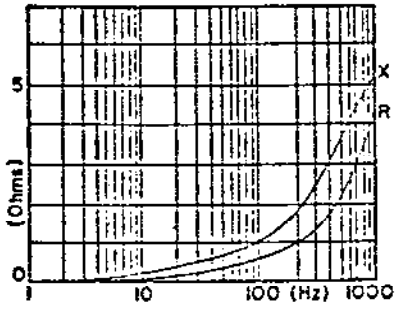

Fig.11 Impedance Function (7ft) QUAD
(no shunt)
R_0=.0049Ω
L_0=.0032 Hy

8-85
5221A64

Fig. 3.13. Frequency Dependency of NAL Quad Impedance.

3.7.2 Quadrupole Center Finder

In most of my experience, I have found that the magnetic center of a properly assembled quadrupole lies within .05 mm of its geometric center.

However, a clever device to check this was constructed at Frascati. It is described in Ref. 84.

3.7.3 Mappers

Most major laboratories have developed major general purpose mapping devices. The technology of a few of these may be found in Refs. 86, 87 and 88.

REFERENCES – CHAPTER 3

54. MT-6 (1977) p. 802. O. Runolfsson (CERN).
55. MT-4 (1972) p. 423. R. Yamada (FNAL).
56. MT-6 (1977) p. 826. W. Eschricht et al. (DESY).
57. MT-5 (1975) p. 74. T. Kasuga (KEK).
58. MT-2 (1967) p. 683. R. Armstrong Brawn (CERN).
59. MT-5 (1975) p. 133. K. Borer et al. (CERN).
60. MT-2 (1967) p. 693. P.A. Reeve et al. (Rutherford).
61. MT-3 (1970) p. 1492. B. Berkes (SIN Zurich).
62. MT-3 (1970) p. 1439. J.K. Cobb and D. Horelick (SLAC).
63. PEP Note 209, Feb. 1976. K. Halbach (LBL).
64. MT-5 (1975) p. 237. B. Langenbeck (GSI, Germany).
65. MT-5 (1975) p. 231. C. Wyss (CERN).
66. NS-26 (1979) p. 4003. M. Green et al. (LBL).
67. MT-1 (1965) p. 497. L.G. Ratner and R.J. Lari (Argonne).
68. NS-18 (1971) p. 375. W.F. Praeg (Argonne).
69. NS-20 (1973) p. 360. L.T. Jackson (LBL).
70. NS-22 (1975) p. 1234. J.A. Dinkel and A.R. Donaldson (FNAL).
71. NS-20 (1973) p. 411. R.E. Fuja and W.F. Praeg (Argonne).
72. NS-22 (1975) p. 1277. Q.A. Kerns (FNAL).
73. MT-2 (1967) p. 437. M.G.J. Frog, Brentford Electric, Crawley, Sussex, U.K.
74. MT-4 (1972) p. 674. M.G.J. Frog, Brentford Electric, Crawley, Sussex, U.K.

75. NS-18 (1971) p. 865. M.G.J. Frog, Brentford Electric Crawley, Susses, U.K.

76. W. Kramer, IEEE Trans. Comm. Elect. 83, p. 382 (1964).

77. MT-2 (1967) p. 297. J.K. Cobb and D.R. Jensen (SLAC).

78. NS-14 (1967) p. 473. E.J. Seppi et al. (SLAC).

79. K. Halbach, Nucl. Instrum. Methods 107, (1973) p. 529.

80. NS-12 (1965) p. 349. G. Gonzalez and A. Brambilla (CEA).

81. NS-14 (1967) p. 437. W.F. Praeg (Argonne).

82. MT-4 (1972) p. 627. S.C. Snowdon (FNAL).

83. MT-2 (1967) p. 735. K.N. Henrichsen (CERN).

84. MT-9 (1983) p. 965. J. Billan (CERN).

85. MT-2 (1967) p. 150. M. Placidi (Frascati).

86. MT-9 (1983) p. 937. K.N. Henrichsen (CERN).

87. MT-9 (1983) p. 943. M.I. Green and D.H. Nelson (LBL).

88. NS-30(1983) p. 3605. E.R. Lindstrom et al. (NBS).

4. SPECIAL PURPOSE MAGNETS

4.1 Introduction

So far we have discussed relatively straightforward magnet designs. In this chapter we will consider somewhat more unusual devices used for injection, extraction and correction. As stated at the outset the truly exotic will be discussed by the experts next week. We will also consider a generic collider detector magnet with respect to its problem with field uniformity.

4.2 Septum Magnets

Suppose we wish to have a strong field in a given volume which is located directly adjacent to a region that is to have zero field. The separation of regions can be effected by a current sheet or a thin iron sheet. Such schemes are used to bifurcate particles' paths.

4.2.1 *Current Sheet Types*

The principle of this design is shown in Figure 4.1. The "outside" field, calculated for an actual magnet at BNL is shown in Figure 4.2. The authors of Ref. 89 discuss the problems of cooling, forces on the thin septum, material choices and radiation resistance in detail. In Figure 4.3 we see how the outside field changes with the radial position of the conductor in the gap (Refs. 93 and 94). Notice how you can. compensate for constructural errors and tune a magnet this way. Effects due to iron saturation are often mitigated by the use of auxilliary back leg windings.

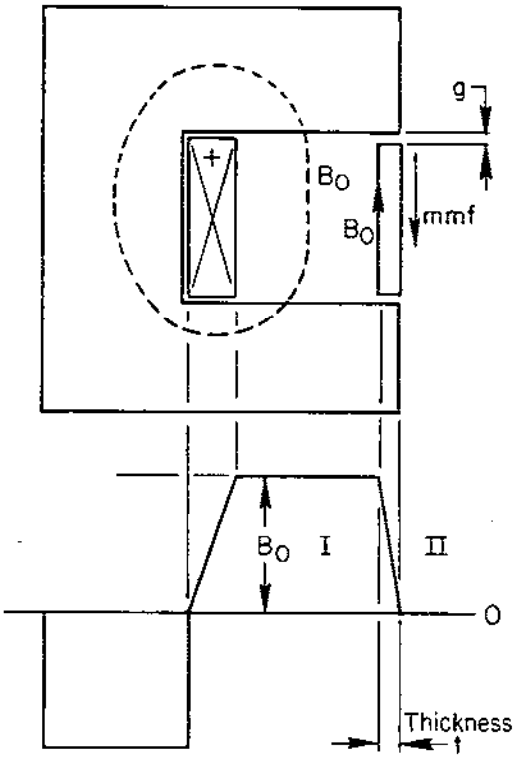

In Region II, in the absence of saturation and gap "g" between conductor and iron, the mmf of the conductor perfectly cancels the field of the main Region I.

In practice there will be leakage which can be partially compensated by displacing the septum.

The current density in the sheet is

$$J_{\text{Amp/mm}^2} = \frac{10000}{4\pi} \frac{B(\text{tesla})}{t(\text{mm})}$$

If $B = 1$ T, $t = 1$ mm, then $J = 800$ A/mm^2!

9-85 5221A65

4.1. The Principle of the "Current Sheet" Septum.

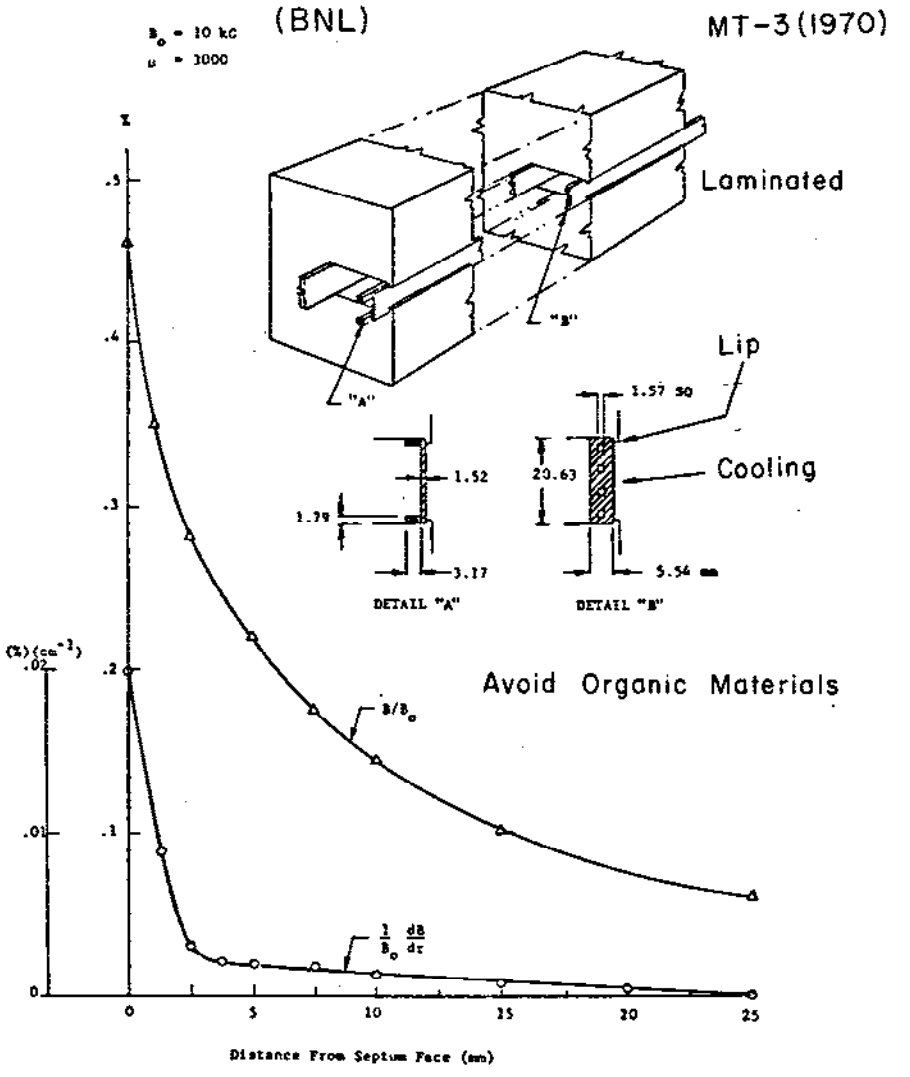

8-85 Ejector magnet for Fast Extracted Beam showing calculated fringing field. 5221A66

4.2. Fields in the "Field Free" Region of a Septum.

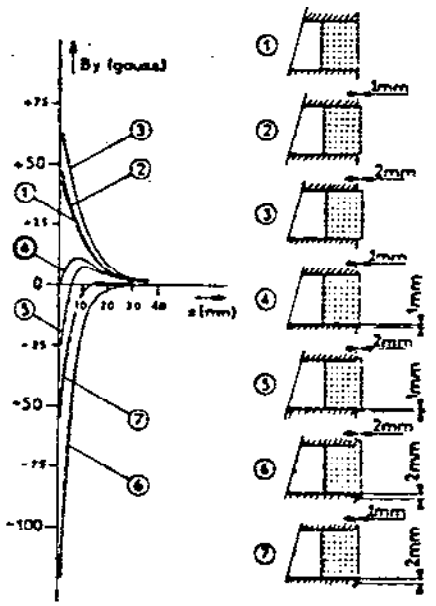

Fig.2 Calculated strayfield in the median plane of the MSE. Case 4 shows the septum geometry that has been chosen.

4.3. Stray Field as a Function of Conductor Placement.

Now that we have taken all this trouble to make the field zero outside the septum in two dimensions, what happens at the ends of the magnet? Figure 4.4 shows how badly the end fields can leak out. One can compensate this effect by moving the septum conductor radially, but this may not repair a gradient (Ref. 90). A better way is to arrange the return conductors in a very special way as invented by Halbach and described by R. L. Keizer in CERN Report 74-13, May 1974 and is shown in Figure 4.5, Ref. 91b. We saw that the current density in many applications is so high that the magnet must be pulsed. By using the magnet as a transformer, one can induce current to flow in the septum sheet if it is part of a short-circuited secondary winding Ref. 92. This is shown in Figure 4.6(a). A rather interesting geometry is shown in Figure 4.6(b). It shows how wild the current can become in some of these septum designs.

One of the nasty problems with pulsed septa having iron cores in storage ring applications is that after the current is turned off and the cancellation of fields no longer applies, the core field relaxes more slowly giving rise to stray fields an order of magnitude larger than permitted. Careful steel selection and additional vacuum chamber shielding is then required.

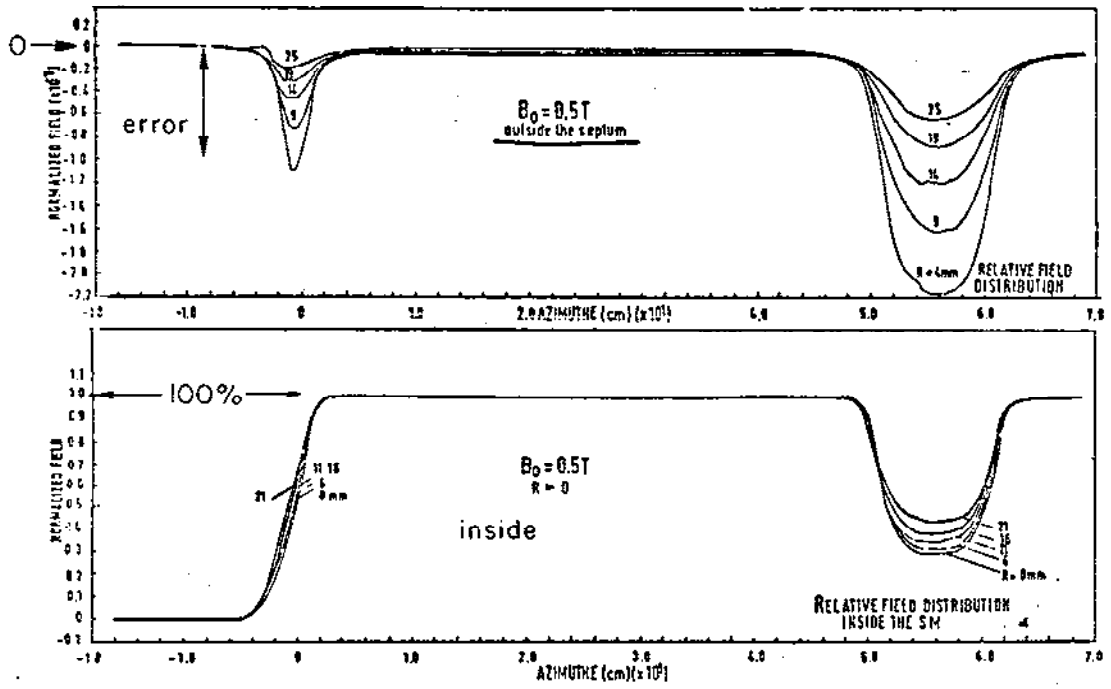

4.4. Error Fields at the Ends of Septum Magnet.

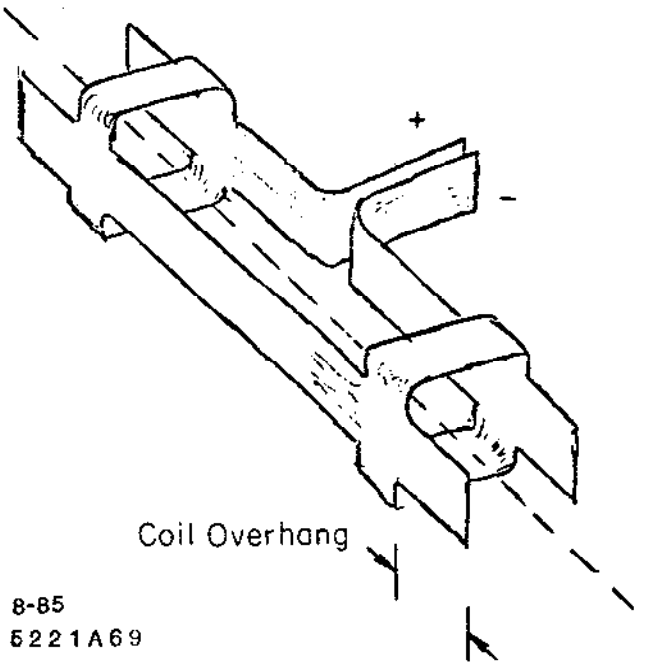

4.5. The "Coil Overhang" Solution to End Field Problem.

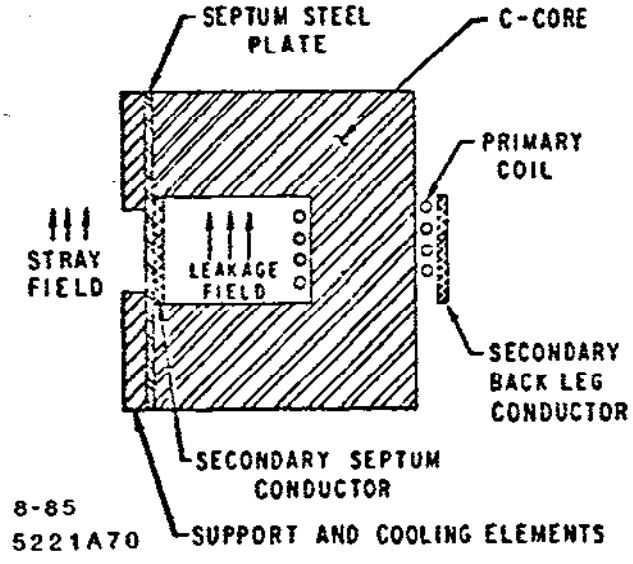

4.6. (a) A Septum with "Transformer" Coupling.

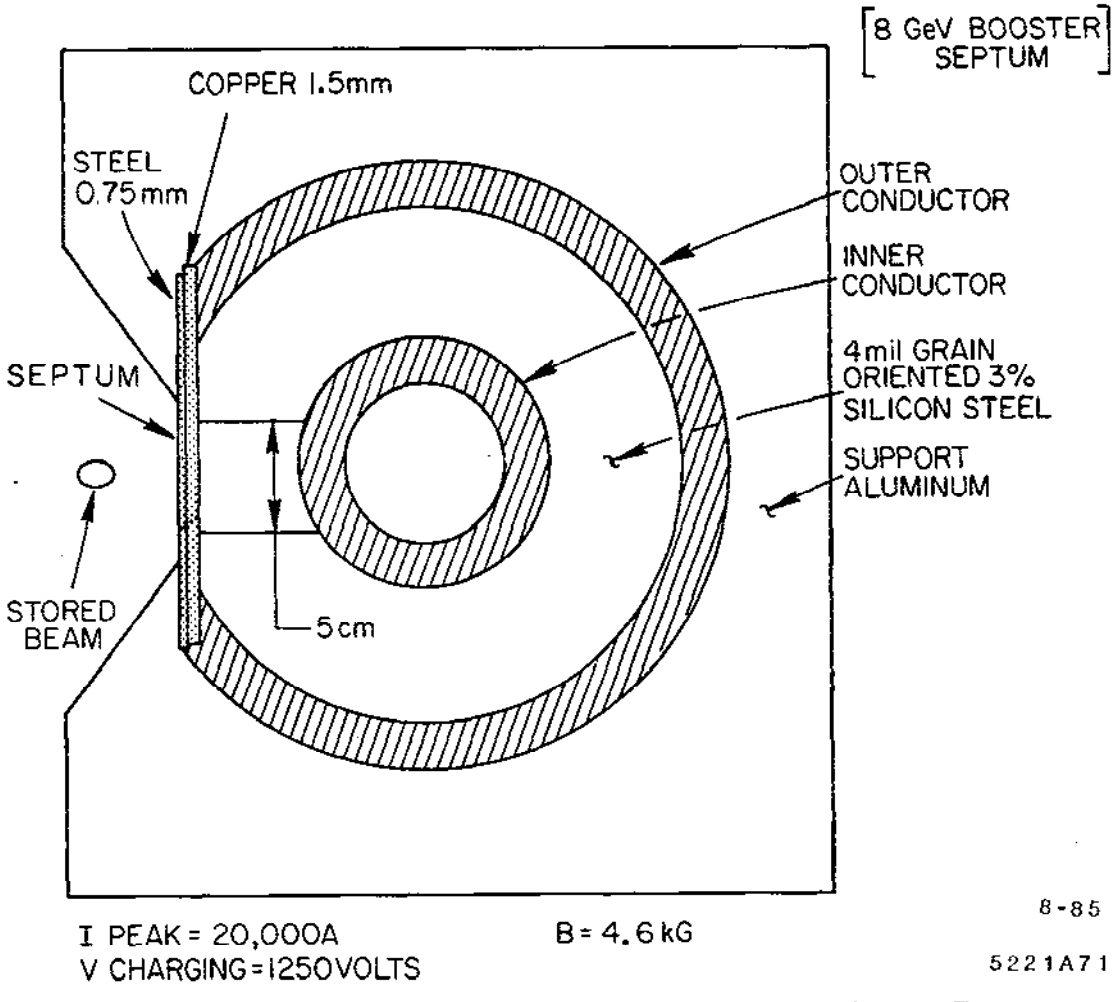

4.6. (b) A "Passive" Septum Coupled to a Coaxial Conductor Geometry.

Slow pulsed power supplies are often of the form shown in Figure 4.7. To give you a feeling for typical parameters, as illustrative of a medium size device, I have inserted some values for a 10.4 uh magnet that pulses at a rate of 180-pps using resonant charging and energy recovery.

Other pulsed magnet considerations are listed in Refs. 95 and 96. Of particular note is the analysis of eddy current effects at the ends of pulsed magnets which very often get very hot because the field is no longer in line with the plane of the lamination (Ref. 97).

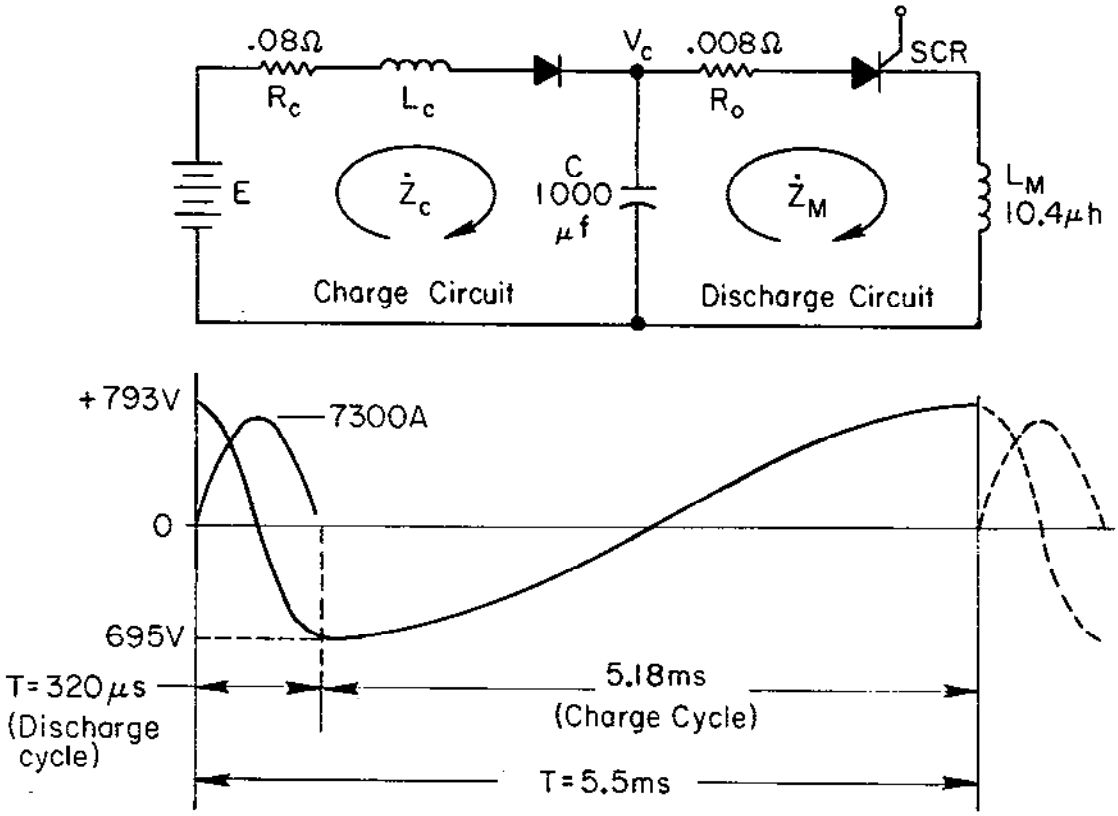

Discharge Circuit			Charge Circuit		
I_m	=	7300 A	E	=	88.5 volts
I_{rms}	=	270 A	$I_{c\ max}$	=	518 A
V_c	=	773 volts	$I_{c\ rms}$	=	348 A
Q	=	12	$DC_{input\ power}$	=	26.3 kW
L_{magnet}	=	10.4 μhenry	L_c	=	2.5 mhenry
			Q	=	20

8-85 5221A72

4.7. Parameters of a Medium Size Pulse Power Supply.

4.2.2 Iron Septa

The geometry shown in Figure 4.8 shows the principle of the Lambertson septum. The field is now perpendicular to the septum, and since the coils can be large, the design does not suffer the usual current density limitations. In practical cases B_0 is limited to about 10 kG before the iron saturates and stray fields result. An extra magnetic shield is often used.

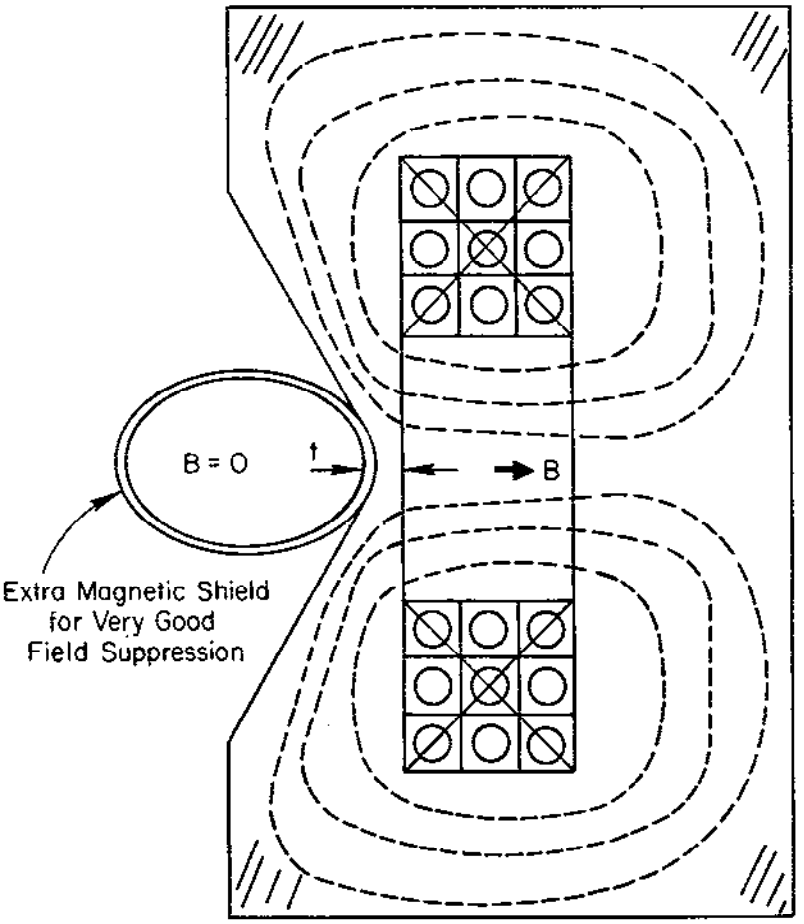

Notes:

1. Field is perpendicular to septum.
2. No current density limitation.
3. B_0 is generally limited to less than thick 10 kG.

8-85 5221A73

4.8. Principle of the Iron "Lambertson" Septum.

Iron septa can take many unusual forms. Some of the most novel examples are shown in Figure 4.9 in which the external proton beam from the CERN SPS is split into two or three separate channels (Refs. 98-100).

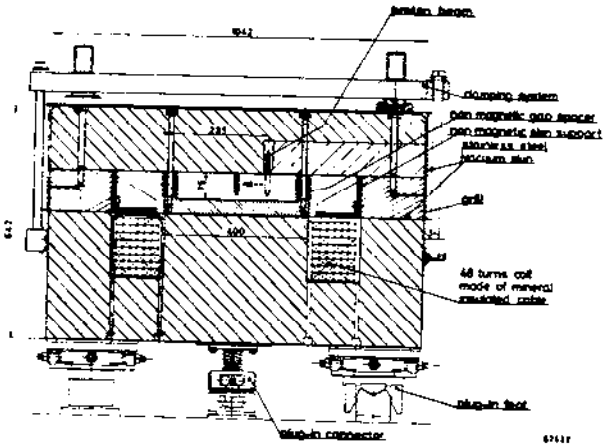

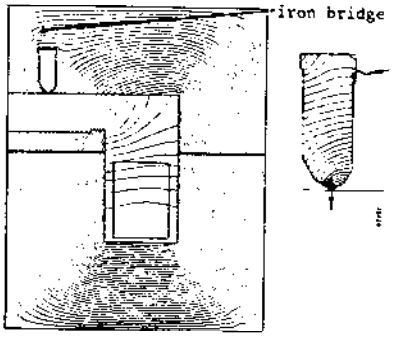

Calculated flux pattern of one half of the single-septum magnet at 8 kGauss

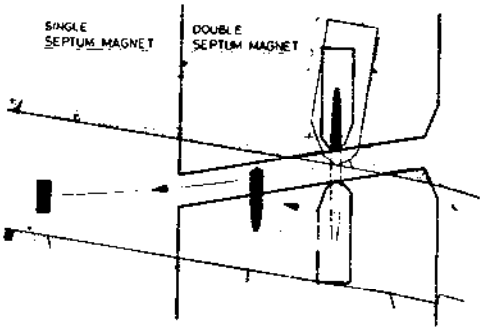

Septa used to split beams after they have been extracted from the CERN SPS.

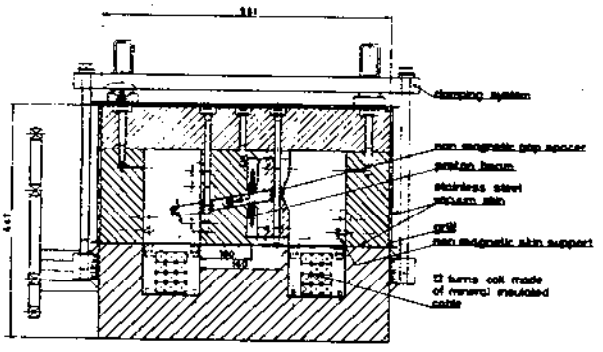

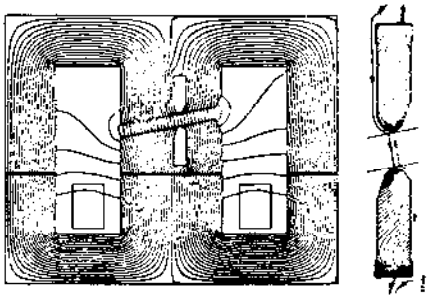

Calculated flux pattern of the double-septum magnet at 8 kGauss

Cross section of the double-septum magnet (length 3600 mm, weight 6.2 tons)

8-85
5221A74

4.9. Double Iron Septa at the CERN SPS.

4.3 MULTIPOLE MAGNETS

Accelerators or storage rings sometimes need higher order pole correction magnets to cancel residual polarities introduced by the main magnets. These may be rotated quadrupoles to compensate linear coupling, sextupoles for chromaticity, octupoles to introduce Landau damping, etc.

A single magnet that can introduce all of these, with arbitrary magnitude and angle is shown in Figure 4.10 and Refs. 101 to 104. It is a multipole with 12 iron poles. The coil currents are controlled to produce the desired fields. The magnet needs to have a fairly large aperture with respect to the beam aperture because near the poles the fields tend to be badly distorted. This makes the device weak, but fortunately in accelerator applications the required strengths are also weak.

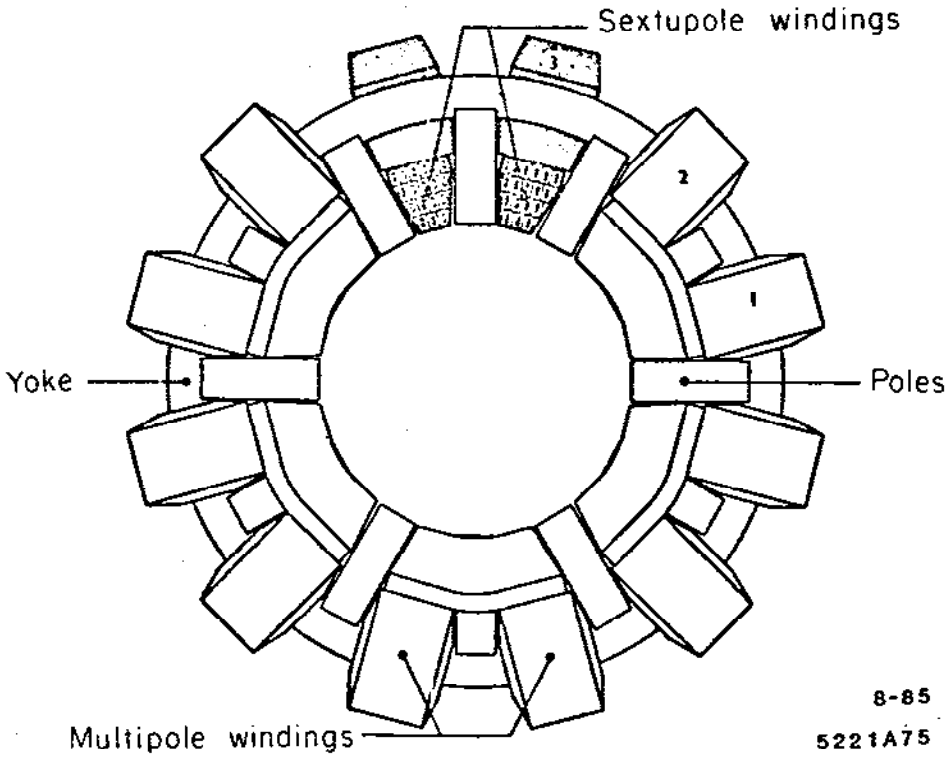

4.10. A "Multipole" Correction Magnet.

4.4 Detector Magnet

I have time to show you only one of many devices. As an example I have chosen the SLAC Mark-II storage ring detector magnet as it was originally configured for operation at SPEAR.

In storage ring experiments it is important to cover as much of the solid angle around the collision point as possible, preferably without disturbing the trajectories of the beams.

A solenoidal magnetic field is appropriate to analyze the reaction products, particularly if they leave the interaction point at large angles. Figure 4.11 shows an exploded view of the device. A 5 kG field coaxial with the colliding beams is produced in a volume 3 meters in diameter and 4 meters long. The flux of the central field is returned by upper and lower flux bars and end caps as shown which, exclusive of the iron plates of the muon detectors, weigh some 350 tons. Power in the then "thin" (in radiation lengths) coil was about 3 megawatts.

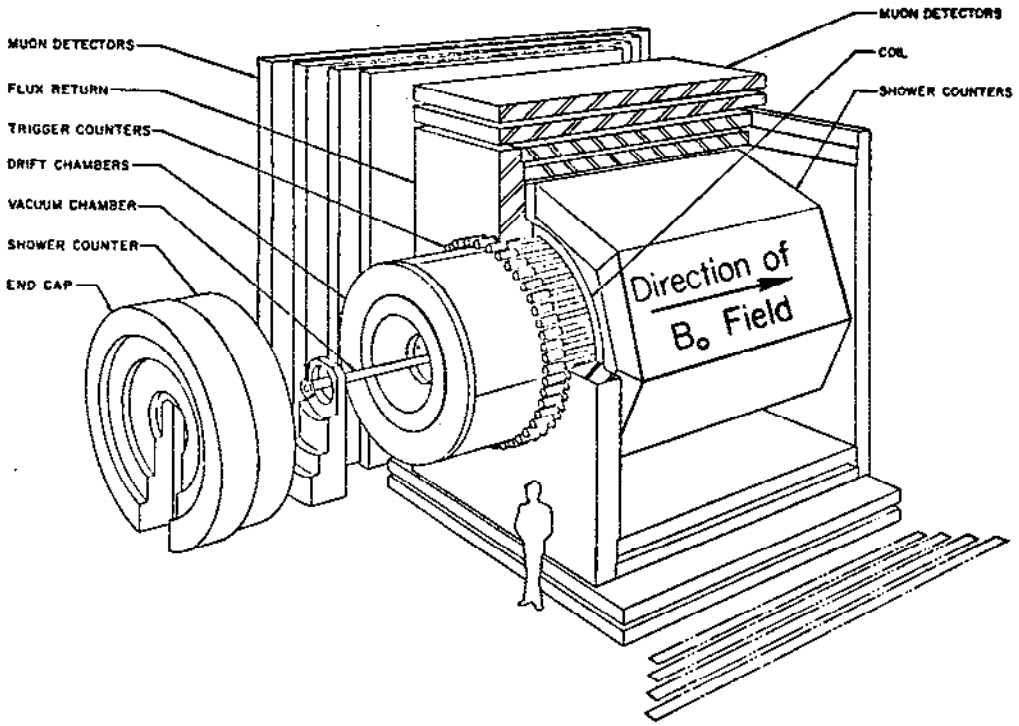

4.11. Exploded View of the Mark II Detector Magnet.

A POISSON calculated field plot in cylindrical geometry of half the magnet is shown in Figure 4.12. Notice how parallel the field lines are, indicating a very uniform field. That they are not equally spaced results from the fact that they represent lines of constant vector potential in cylindrical geometry. The point of showing this example is as follows: To achieve uniformity in the central field

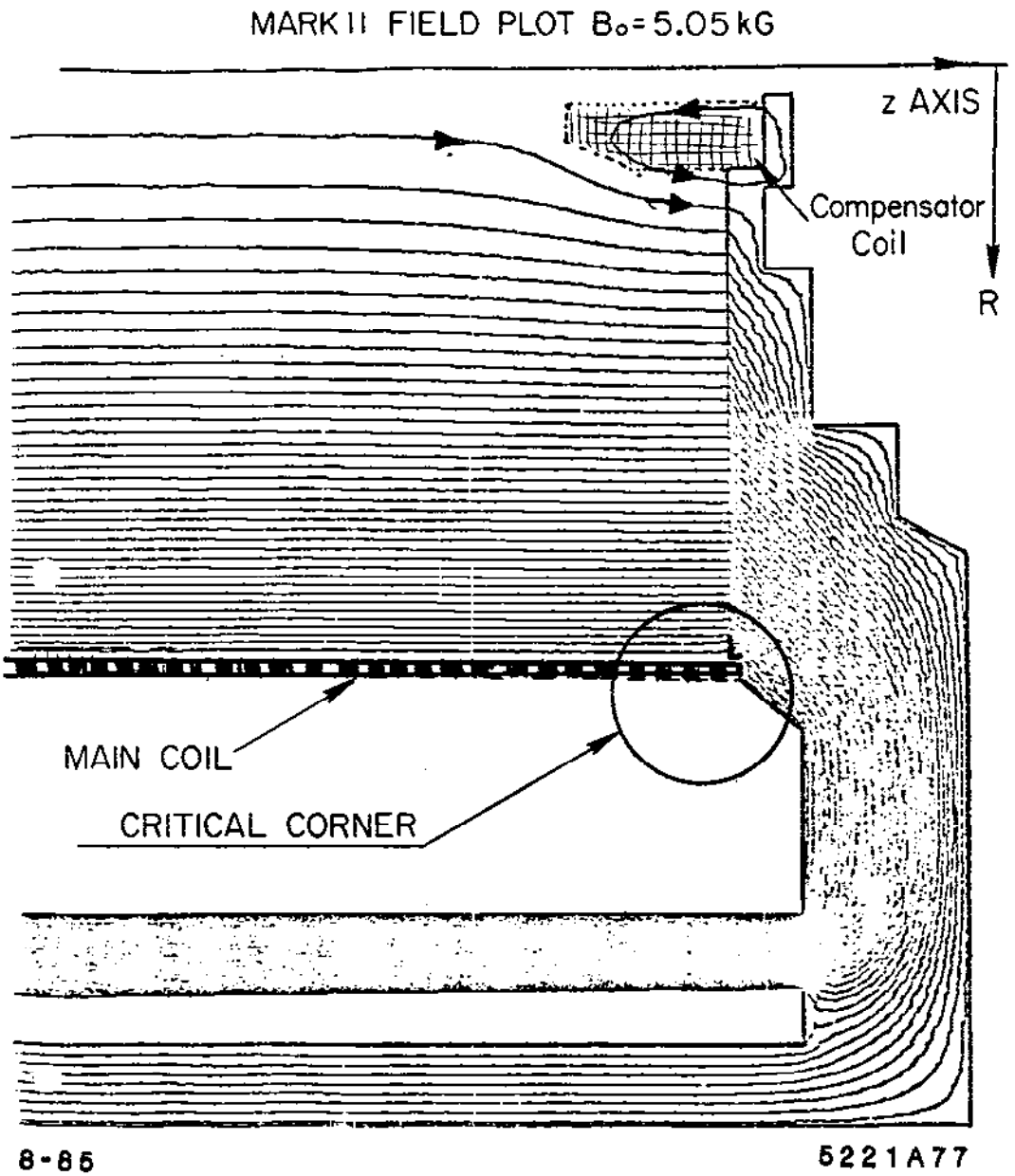

4.12. Mark II Field Distribution Calculated in Cylindrical Coordinates.

volume, it is terribly important to bring the main coil as close to the iron faces of the ends as possible. This forces the field lines to flow parallel to the coil and enter the steel normal to the iron and not leak sideways, an imperfection that would produce radial field components. If the coil were a superconducting one, the vacuum vessel and superinsulation would prevent such close coupling. It is also important that the effective coil to steel distance at both ends of the magnet be exactly the same. Were this not so, axial asymmetries result in the main field and substantial unbalanced axial forces occur between the coil and iron.

The perturbation on the axis at the ends of the magnet was caused by coils that compensate the main field so that the total integrated field through the magnet is compensated to exactly zero. The magnetic axis of such coils requires careful alignment. At the SLC these coils are no longer required.

REFERENCES – CHAPTER 4

89. MT-3 (1970) p. 1501. J.J. Grisoli and H.C. H. Hsieh (BNL).
90. MT-3 (1970) p. 1518. F. Fabiani et al. (CERN).
91. R. L. Keizer, Cern Report 74-13 (1974).
92. NS-26 (1979) p. 4024. M. Foss et al. (Argonne).
93. MT-6 (1977) p. 504. Y. Baconnier (CERN).
94. NS-20 (1973) p. 719. R. Carrigan (NAL).
95. MT-5 (1975) p. 125. W.F. Praeg (Argonne).
96. NS-22 (1975) p. 1548. W.O. Brunk and D.R. Walz (SLAC).
97. MT-3 (1970) p. 279. A. Asner et al. (CERN).
98. NS-24 (1977) p. 1571. L. Evans et al. (CERN).
99. MT-6 (1977) p. 498. L. Evans et al. (CERN).
100. NS-18 (1971) p. 984. C.H. Rode et al. (NAL).
101. MT-6 (1977) p. 528. N. Marks, Daresburg, U.K.
102. MT-5 (1975) p. 22. N. Marks, Daresburg, U.K.
103. H.D. Ferguson, J. Spencer and K. Halbach, N.I.M. 134 (1976) p. 409 (LAL, LBL).
104. NS-24 (1977) p. 1266. A. Ando et al. (KEK).

5. MATERIALS, MANUFACTURING PRACTICES, AN EXERCISE PROBLEM

5.1 MATERIALS

For general references to get you started, see Ref. 105.

5.1.1 Steel

Figure 5.1 shows the B-H curve for a large variety of steels. The student of iron magnets should consult the classic reference "Ferromagnetism" by R. M. Bozorth (Van Nostrand 1951).

We will concern ourselves with only two types of steel: ingot iron for large solid core magnets; sheet steel for laminated accelerator magnets (1 to 3 mm thick) and leave electrical transformer steels (.1 mm thick) for pulsed magnet applications to others.

(a) Ingot Iron

Steel from Basic Oxygen Furnaces (the oxygen is used to burn out carbon) is ladled into ingot molds. Usually the top 1/3 of the ingot must later be thrown away because its carbon content is much higher than that at the bottom. The size of a typical heat (pouring) of steel in the U.S. is about 200 Tons.

For magnets a carbon content of .06% $\pm$ .02% is particularly convenient because the magnetic properties of this steel are the least sensitive to carbon content in this range.

For large blocks, a few % of silicon is often added to prevent blow holes. Heavy slabs are hot rolled. Figure 5.2 shows a typical B-H curve for AISI 1010 steel i.e. of 0.1% carbon content. Notice the variation of permeability (mu) with excitation. Figure 5.3 shows how the low induction properties change with post rolling heat treatment (annealing). In the last few years, special very low carbon cast steels have become available from Hoesh-Estel, Dortmund, Germany, Ref. 106.

(b) Steel for Laminated Accelerator Magnets

Laminated fabrication (as opposed to machining) of steel cores requires flat sheet stock which is cut to shape in a punch and die operation. Two types of steel are currently in use: special decarburized steel made expressly for accelerator magnets, and relatively ordinary 1006-1010 sheet used for car bodies, refrigerators and washing machines.

To understand the properties of these products it may be useful to briefly review how they are made by referring to Figure 5.4. For magnet applications the game is to obtain a predictably low carbon content of UNIFORM chemistry from lot to lot. Notice that even if the top of the ingot is discarded, the rim

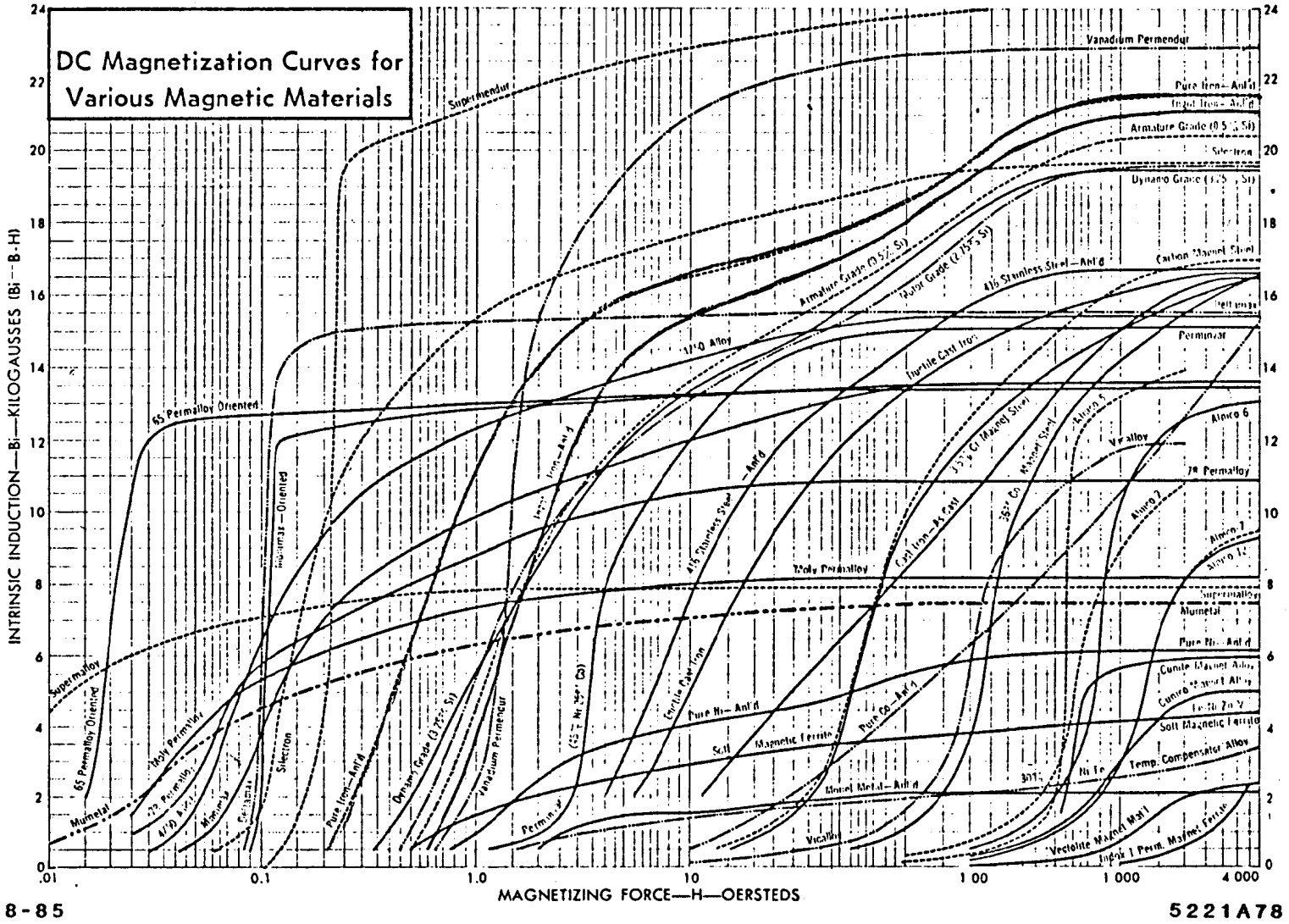

5.1. B-H Curves for Various Ferromagnetic Materials.

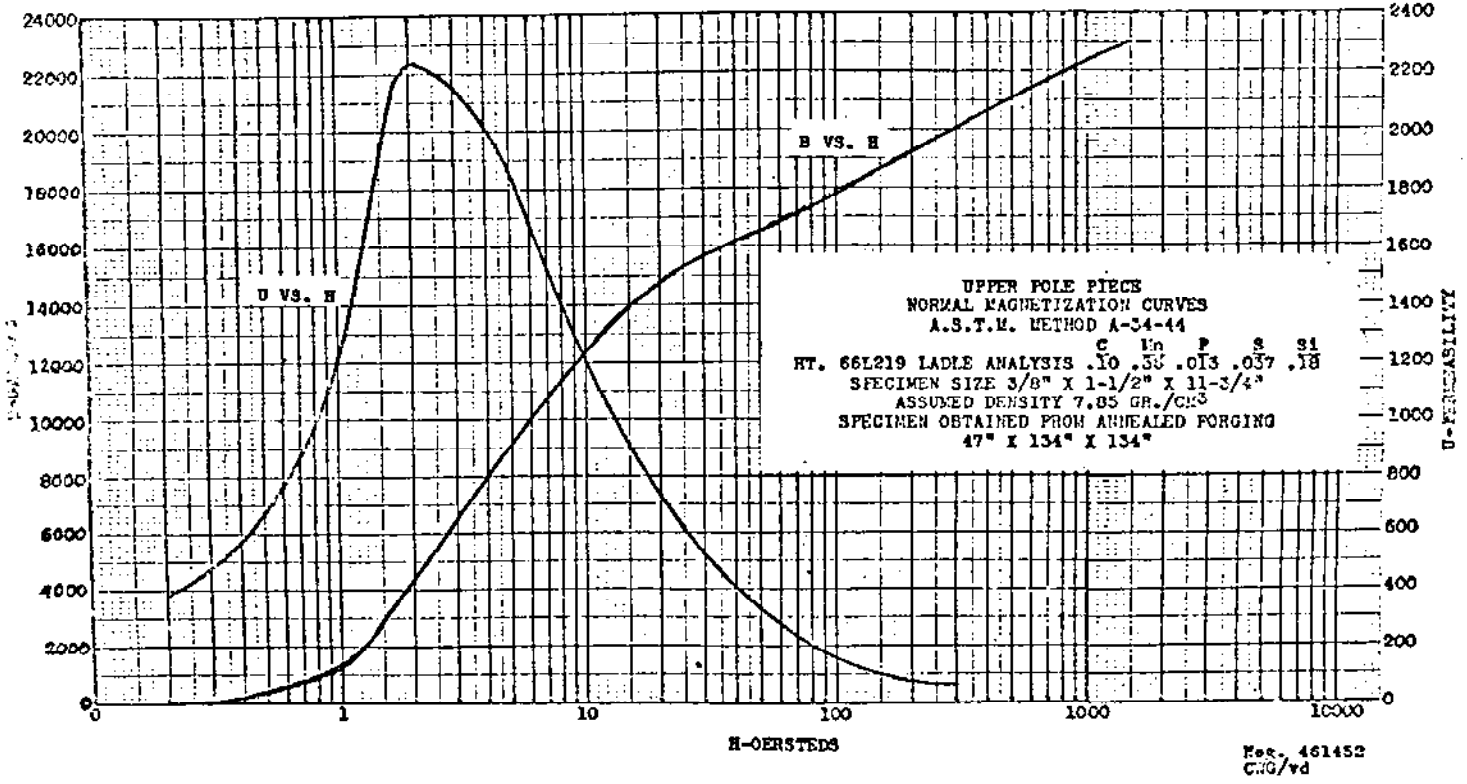

8-85

5221A79

Fig. 5.2. Typical B-H of a Large 1010 Steel Forging.

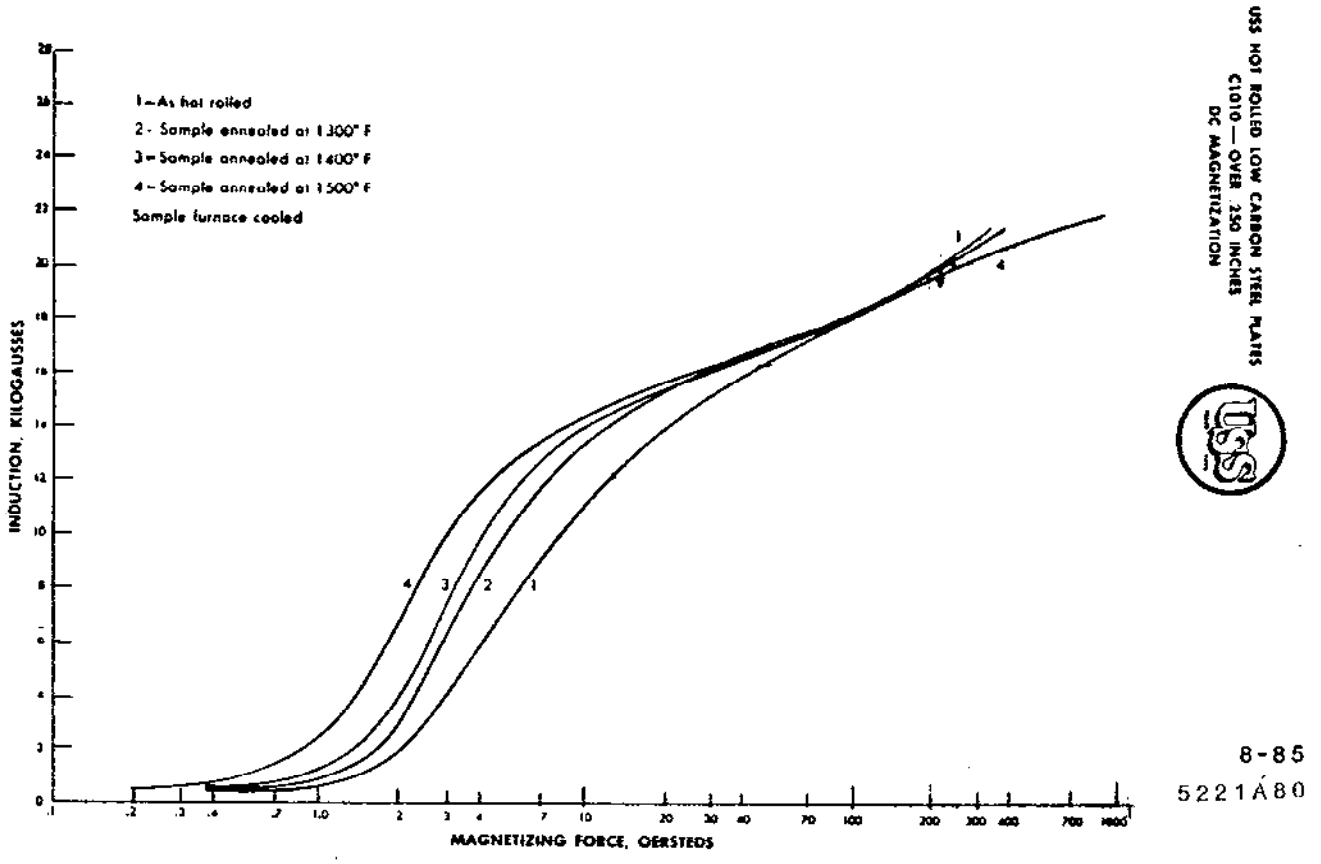

5.3. The Effect of Annealing on Hot Rolled 1010 Steel.

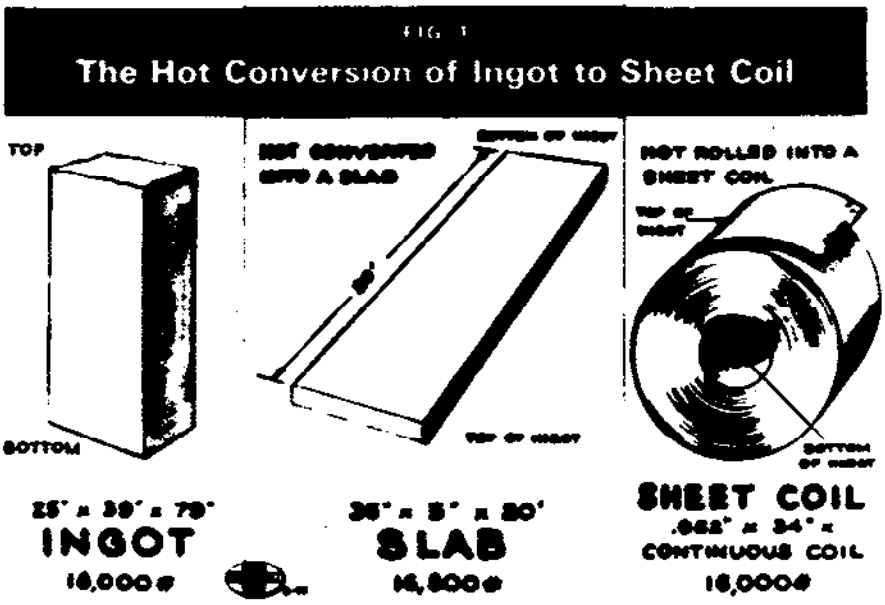

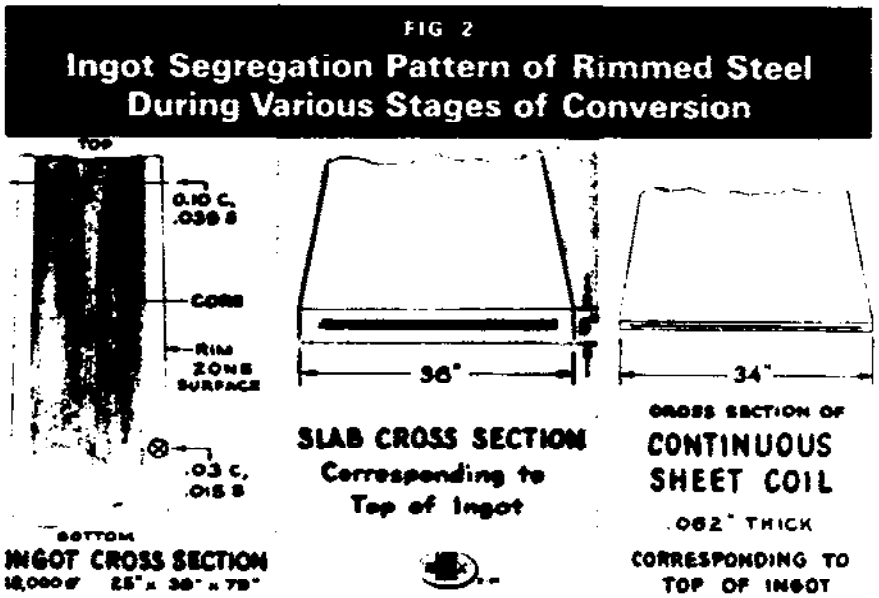

5.4. Rimmed Steel Rolling.

of the ingot remains on the outside of the material throughout the subsequent rolling stages. Carbon segregation is minimized in so called "killed" steels in which a certain amount of aluminum or silicon is added at the pour. These actions will make a more uniform steel but appear (from our measurements) to lower the desirable magnetic properties somewhat. The slab, which has been either cast or hot rolled, is reduced in thickness in a hot rolling operation to a controlled thickness about 1/4 to 3/8 of an inch and coiled on a roll to cool.

Such coils, called "hot band" in the trade,may be purchased at this point by a so called rerolling mill for further processing. To make 16 gauge material, the coils will be carefully cold rolled to about .070″ recoiled and then be placed in an annealing oven. The steel will be rather soft after this treatment (Rockwell B scale 20 in some cases) and difficult to stamp accurately. The final so called "temper pass" provides the final reduction to $.062 \pm .001''$ and can be made soft, medium or hard depending on the application. We have found that Temper 3 hardness (Rockwell B scale 70) distorted the least in a single hit stamping operation. The steel is recoiled and sent to the slitting mill where the sides are trimmed and the correct width is obtained. We have found it best to have the strip leveled (that is flattened) and cut to shipping length so that the stamping house does not have to straighten the material. Since it is easier to ship and stamp from a coil than from sheet stock this is a bit more expensive but has proven essential for us.

Every step in the process affects the magnetic properties in some way so adherence to rigid quality control standards and traceability is essential.

ARMCO INC. Eastern Steel Division in Middletown Ohio makes a specialty product they call "Special Cold Rolled Magnet Steel". During an annealing stage the material is passed, in open sheet form, through an oven whose atmosphere is designed to remove carbon. To some extent this can occur only near the surface but since the sheet is thin the reduction is very good. This material has been used for the FNAL main ring, the PEP storage ring and other machines. The manufacturing ranges of its low coercive force and relatively soft hardness are shown in Figures 5.5 and 5.6. The B-H curve is displayed in Figure 5.7. This is a high field material having a permeability between 180 and 181 at a magnetizing force of 100 Oe (7960 A/m). The temperature variation of mu and effects of intense neutron irradiation are listed in Refs. 107 and 108. Do look up an important contribution on this material at liquid helium temperatures by the BNL group in Ref. 109.

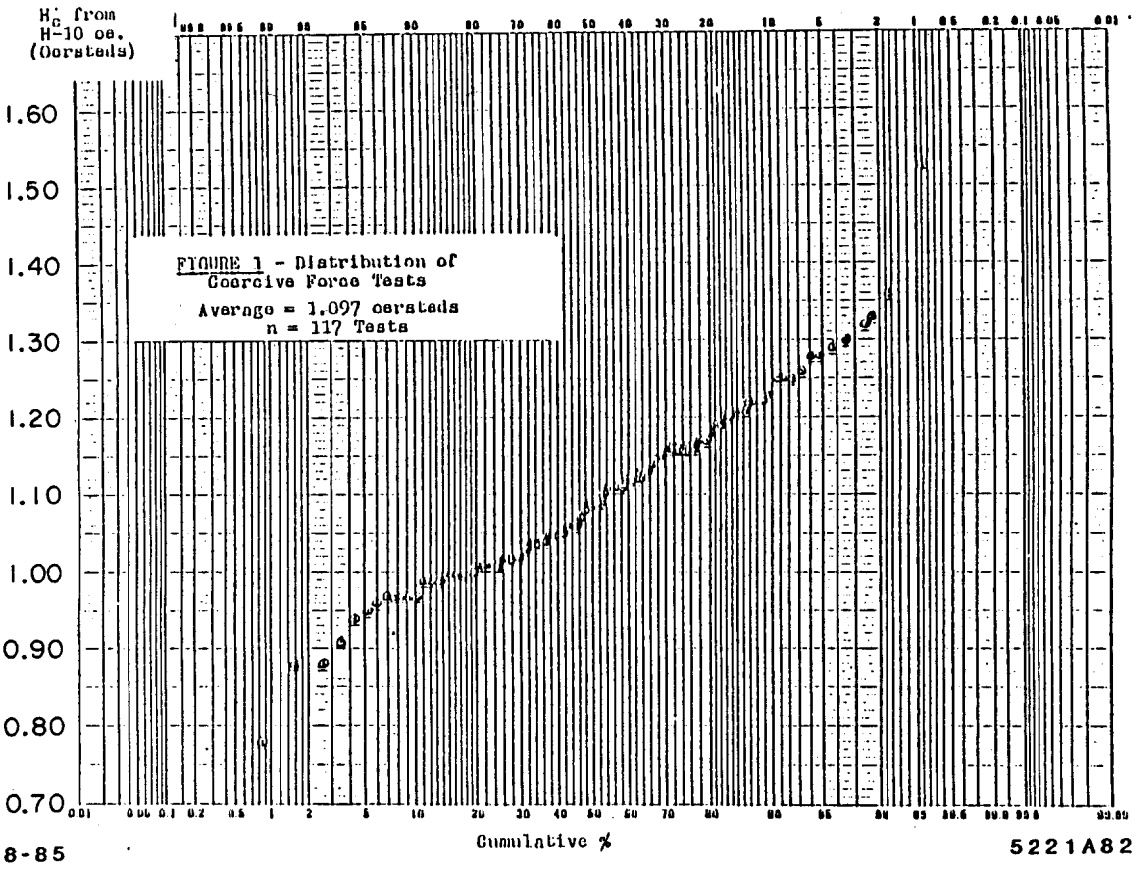

Fig. 5.5. The Distribution of H_c Among Production Lots (Armco CR Special Magnet Iron).

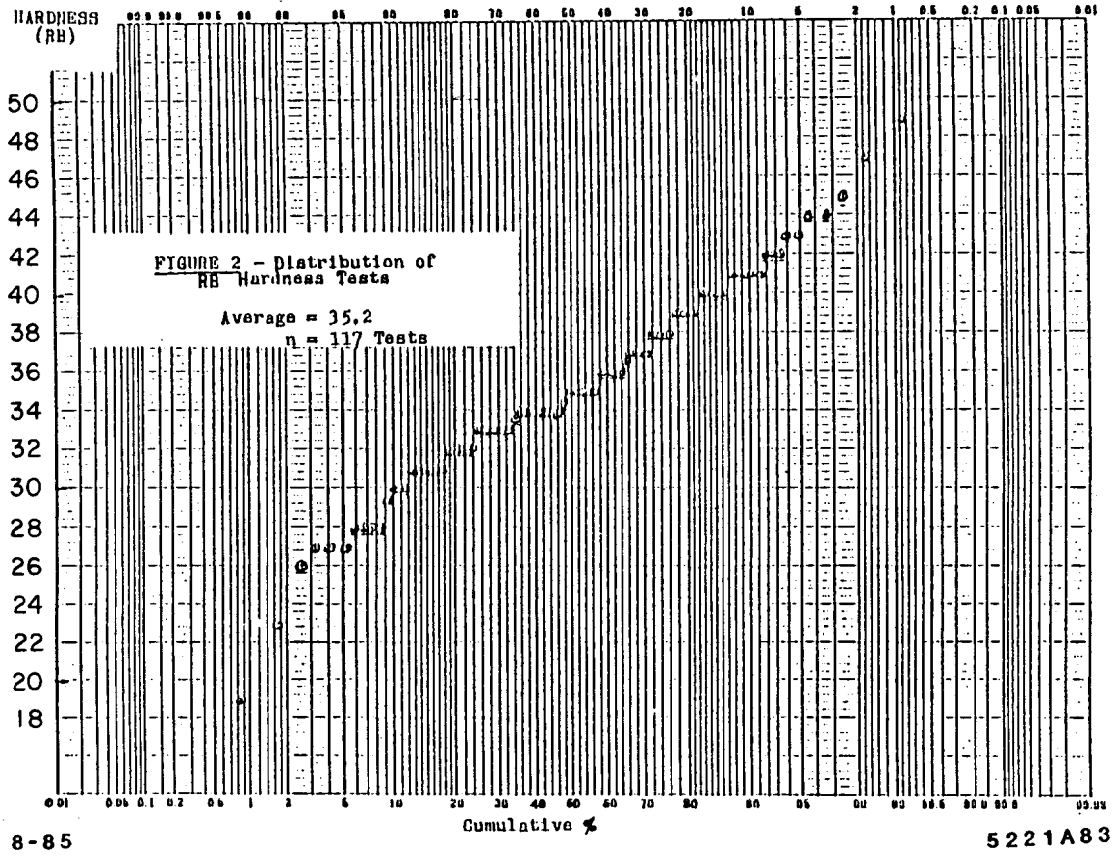

Fig. 5.6. The Distribution of RB Hardness among Production Lots (Armco CR Special Magnet Iron).

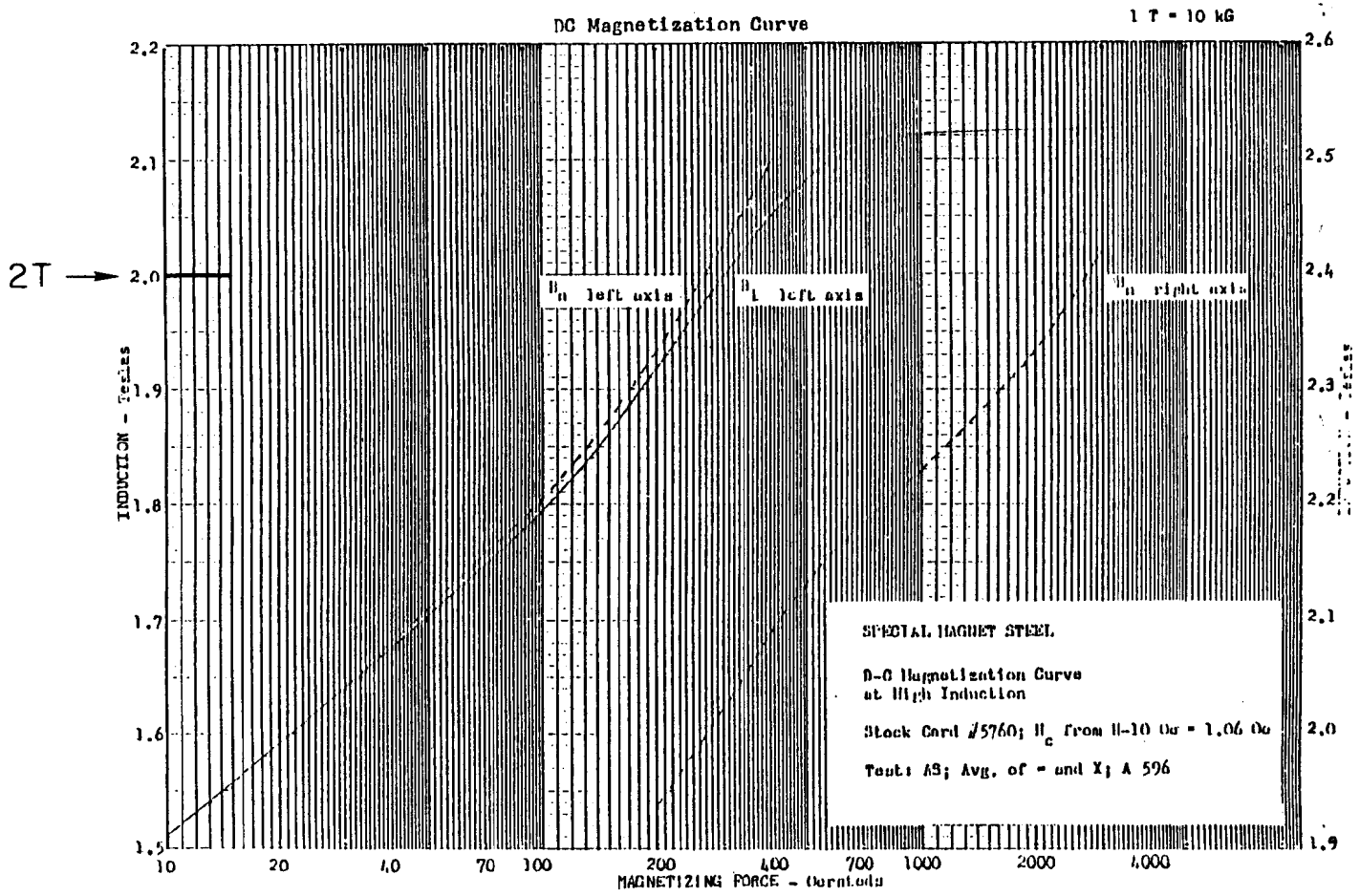

Fig. 5.7. DC B-H Curve for Armco Special Magnet Iron.

5.1.2 *Conductor Materials*

1. The resistivity of international electrical grade annealed copper (99.91% pure) at 20°C is, I believe,

$$\rho = 1.724 \times 10^{-6}\ \Omega\text{cm}[1 + .00393(t - 20°\text{C})]$$

   Remember, therefore, for a coil running at 40°C to add about 8% to resistance.

2. The International Aluminum Standard at 20°C is

$$\rho = 2.827 \times 10^{-6}\ \Omega\text{cm}[1 + .00403(t - 20°\text{C})]$$

   At 40° the ratio of resistivities of Al/Cu is 1.65.

However, the price per pound of copper is, perhaps, 3 times that of aluminum, and since the density ratio is 3.27, the increased price of larger coil and core (to keep the power consumption the same) may well be offset by using aluminum.

Aluminum coils are also much easier to fabricate because the material has less tendency to work harden or keystone.

However, coil connections must be heliarc welded, and extra precautions must be taken to ensure good mechanical connections. A special paste (Alcoa No. 2EJC) is used to prevent voltages across connections. The use of aluminum is described in Refs. 110 and 111. Aluminum can be hard anodized to provide a very hard (but brittle) radiation-resistant surface insulation (up to 750 V breakdown). The surface must be treated after the coil is wound, because the conductor cannot be bent very much after anodizing without breaking the insulation Ref. 112. Aluminum is available in extrusion form of almost any length.

5.1.3 *Conductor Insulation*

In the accelerator magnet field the outstanding problem of coil insulation is radiation damage, which, when combined with magnetic and thermal stresses, leads to coil failure. These problems have lead to the development of specially formulated epoxy impregnated fiber insulation systems. The use of mineral insulator, hard anodized surfaces and even the use of cement are described in Refs. 113 through 122.

It appears safe to say that the studies of M.H. Van de Voorde and co-workers at CERN are the most extensive and systematic of any I have seen. His article "Selection Guide for Organic Materials in Nuclear Engineering", CERN Report, CERN 72-7, has been the Master Guide in this field for ten years. This work has been extended by H. Schonbacher and A. Stolarzlzycka in two more recent volumes, CERN 79-4 and CERN 79-8. Write to CERN to obtain copies of their work.

Vande Voorde	Literature Guide to Radiation Resistance
CERN-70-10	Epoxy
CERN-ISR-MAG/68-59	Hoses
CERN 68-13	Epoxy Electrical 1968
CERN ISR MAG/68/44	Epoxy Mechanical
CERN-69-12	Materials
CERN-70-5	Polymers - High Energy Accelerators
CERN-ISR-MA/73-36	Dosimetry
CERN LAB II-RA/72-10	Electronic Components
CERN ISR-MAG/67-3	Epoxy
CERN ISR-MAG/PS-6464	Paints
CERN-ISR MAG/67-19	Glass Reinforced
CERN-ISR MAG/68-14	Lubricants
CERN ISR MAG/PS/6455	Textiles
CERN MPS/66-22	Water-Radiolysis
CERN ISR/MA/75-38	Polymers at Cryogenic Temperature
CERN 72-7	Selection Guide for Organic Materials in Nuclear Engineering

10-85 5221A97

Fig. 5.8. Index to the Radiation Resistance of Misc. Materials.

In examining Figure 5.9 you will see that most thermosetting resins do not survive a dose of 10^9 rads. How they fail you must read about on your own.

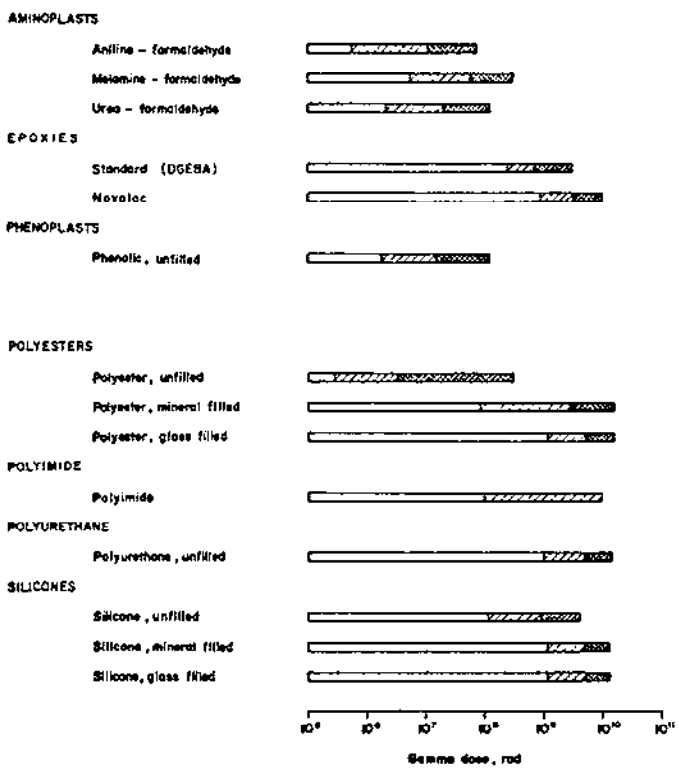

Fig. 5.9. Relative Radiation Resistance of Thermosetting Resins.

If doses above 10^9 rads are going to be encountered, non-organic materials are used (Ref. 122). Loading the epoxy with aluminum oxide powder (grain size 10 microns) has been found at SLAC to be an effective method of radiation "hardening" the insulation (Ref. 115).

Figures 5.10, 5.11 on thermoplastics and elastomers show a material selection guide for cable insulation and hoses. Beware of Teflon and certain types of rubber!

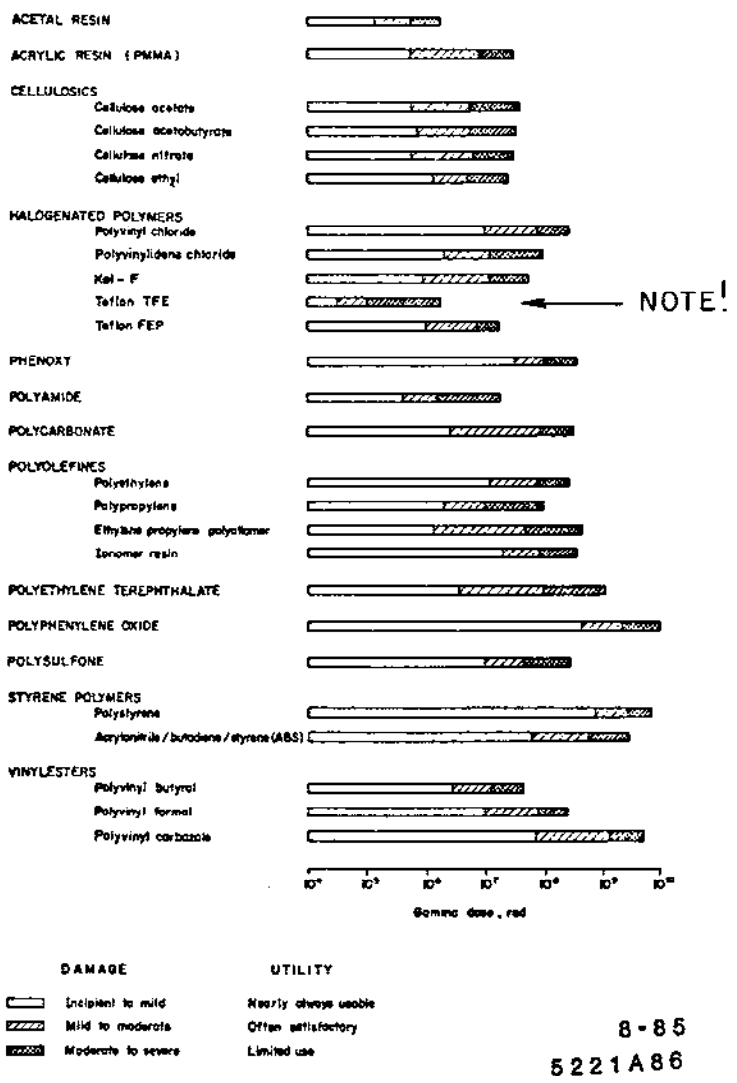

Fig. 5.10. Radiation Stability of Thermoplastic Resins.

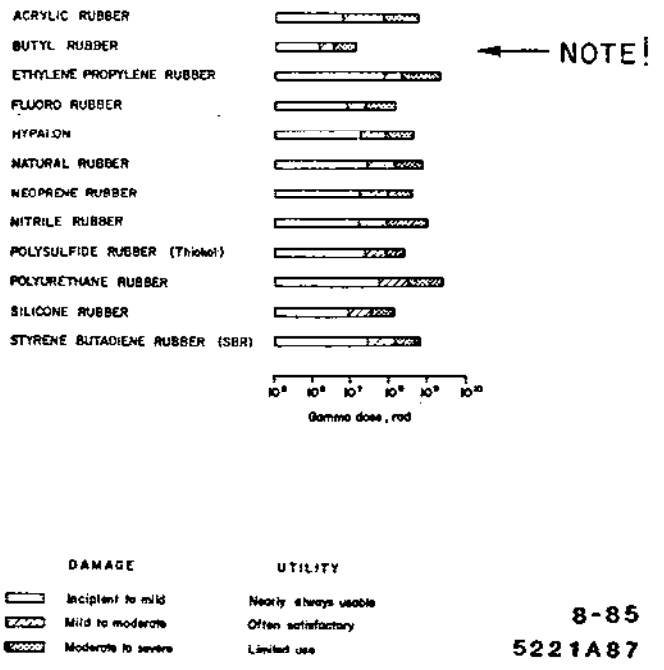

Fig. 5.11. Radiation Stability of Elastomers.

5.1.4 Water

Complex chemistry problems arise when high voltage magnets are cooled with water. The treatment of water is essential and is described in Ref. 123. Economic considerations are discussed in Ref. 124. Generally, the resistivity of the water should be maintained at greater than 5×10^6 ohm-cm, the pH between 6 and 6.5, with dissolved oxygen at or below 0.1 ppm.

Needless to say, filters are essential to remove foreign matter (metal chips, dirt, grease, etc.) from obstructing the small cooling passages of coils.

5.2 Manufacturing Practices

5.2.1 Core Construction

The many articles listed in the previous chapters detail many of the construction techniques employed for core assembly. A particularly interesting example, however, is the description of how the ISR cores were made, because it stresses the stringent requirements of uniformity from core to core in this machine. I suspect no machine in the world has had as much care lavished on it as this one. See Ref. 125, CERN ISR-MA/76-6.

(a) Uniformity

We have already seen how the properties of the steel depend on from what part of the ingot the material is taken. The problem is often greater among the various steel ladle pourings.

Not only is it cheaper to make a large ensemble of magnets of complicated profile by laminating them, the magnets themselves can be made more "identical" to each other by randomizing the laminations from among the total amount of steel purchased.

Statistical methods are used to determine how detailed the randomizing process needs to be. Some comments:

1. Plan enough lead time so that you are not forced to build magnets on a production schedule before you have a fair fraction of the total amount of steel required.
2. The assembly techniques must be worked out on sufficiently large numbers of models before you start production because any changes in procedure thereafter may produce magnets of differing character.
3. Remember also that the effective $\int B \cdot dl$ of a saturated magnet depends not only on its length, but also on its linear weight density.

(b) Stampings

As machine energies increase magnets become smaller and smaller in bore and tolerances on parts become harder to meet. As stated earlier we now need laminations whose critical dimensions have tolerances in the .0001" domain. Conventional stamping techniques, which used to call for die clearances of several % of material thickness, will no longer suffice. Two things have happened: a) The introduction of the "fine blanking" process in which die clearance is virtually absent and the metal is more or less extruded by the punch, and b)The introduction of the computer controlled wire EDM machines which have revolutionized the speed and accuracy (hence the cost) of making conventional die sets with very close fits. Small die clearance means more sharpenings (perhaps every 20K strikes but yields better surfaces). Both techniques when properly applied seem capable of providing the community with parts of sufficient accuracy. I will not regale you with the horror stories that abound when one first tries to learn how to weld together a straight magnet.

(c) Cement Magnets

We cannot leave this subject without mentioning the newest wrinkle in the trade. The LEP magnets run at very low fields at injection (0.023T). So low in fact that the problem of non-uniformity of residual field becomes severe. This problem was solved by the CERN designers by reducing the packing fraction of the laminations to 27% filling the 4 mm void between the laminations with fine grained sand and cement mortar so that the assembly acts mechanically as a prestressed concrete beam but in which the induction in the steel leaves is higher than it would otherwise have been. See Figure 5.12. Also, cement is no doubt cheaper than steel. The heroic measures that had to be developed to put this elegant idea into practice can be found in Ref. 126.

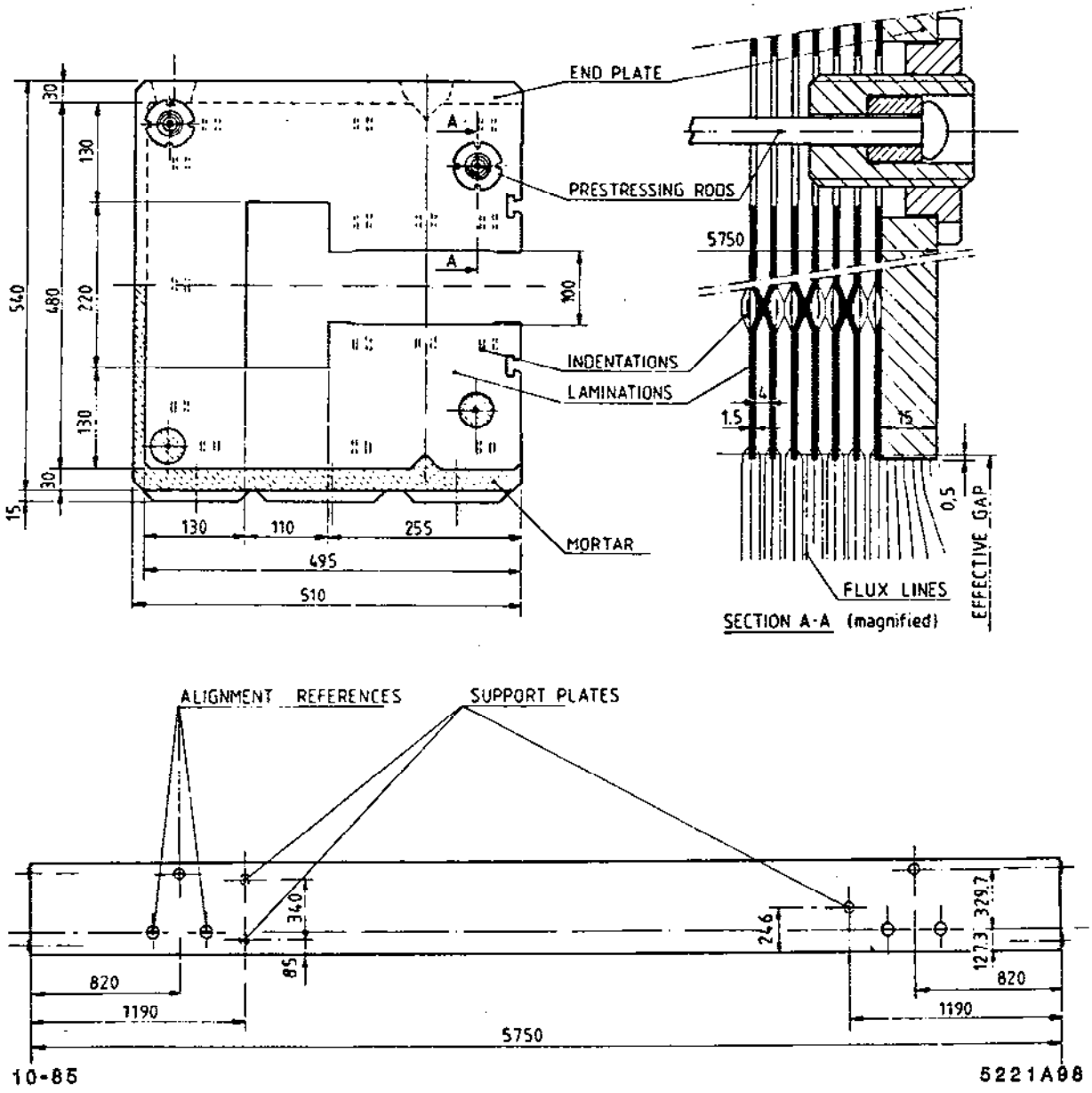

Fig. 5.12. Steel – Concrete Core of LEP Dipole.

5.2.2 Coil Construction

Conventional coils are normally wound with the conductor insulated with an epoxy impregnated layer of wrap which cures when the whole coil is potted in an evacuable form and baked. An automatic device to wrap the multiple layers of insulation, glass or cotton tape, etc., on the conductor is shown in Figure 5.13. It travels along a table with the wire passing through its middle.

The development of tooling and fixtures of this kind is important to keep manufacturing costs under control.

Coil winding shops generally mount the winding forms on platforms that were gun mounts so that the conductors can be layed into precise locations with mallets. You will appreciate that statement when you see the "dog eared" coils that become a necessity when lattice opticians forget that magnets have ends. See Figure 5.14. The tighter the radius the coil winder has to accommodate (he does it with a huge rubber mallet), the more the conductor keystones, the more likely that the insulation is damaged and turn to turn short circuits result.

Some older unusual practices are described in Refs. 127 to 128. but in 1979 three laboratories, SLAC, CERN and DESY decided (apparently independently) that for large machines one should abandon the concept of a coil altogether and simply string the magnets on a common bus – like beads on a string. This is actually being carried out for the SLC Arc Transport, and the LEP and HERA (e^-) rings. Look mother – no coil ends! See Figure 5.15.

(a) Coil Testing

Conventional coils should be tested BEFORE they are installed in a magnet. This is often done by "ringing" them; a process nothing other than making them the L of a high frequency LC oscillator and measuring their Q. Applied voltages should be high enough to cause weak spots to break down but not high enough to cause an otherwise healthy coil to fail. A turn to turn short shows up on the otherwise smooth oscillatory waveform as noise. The procedure is somewhat empirical since it does not test the long term thermal working of the coil, a fact that reminds me that I failed to remind you in Chapter 1 that the conductor should usually have a hole in it for water cooling.

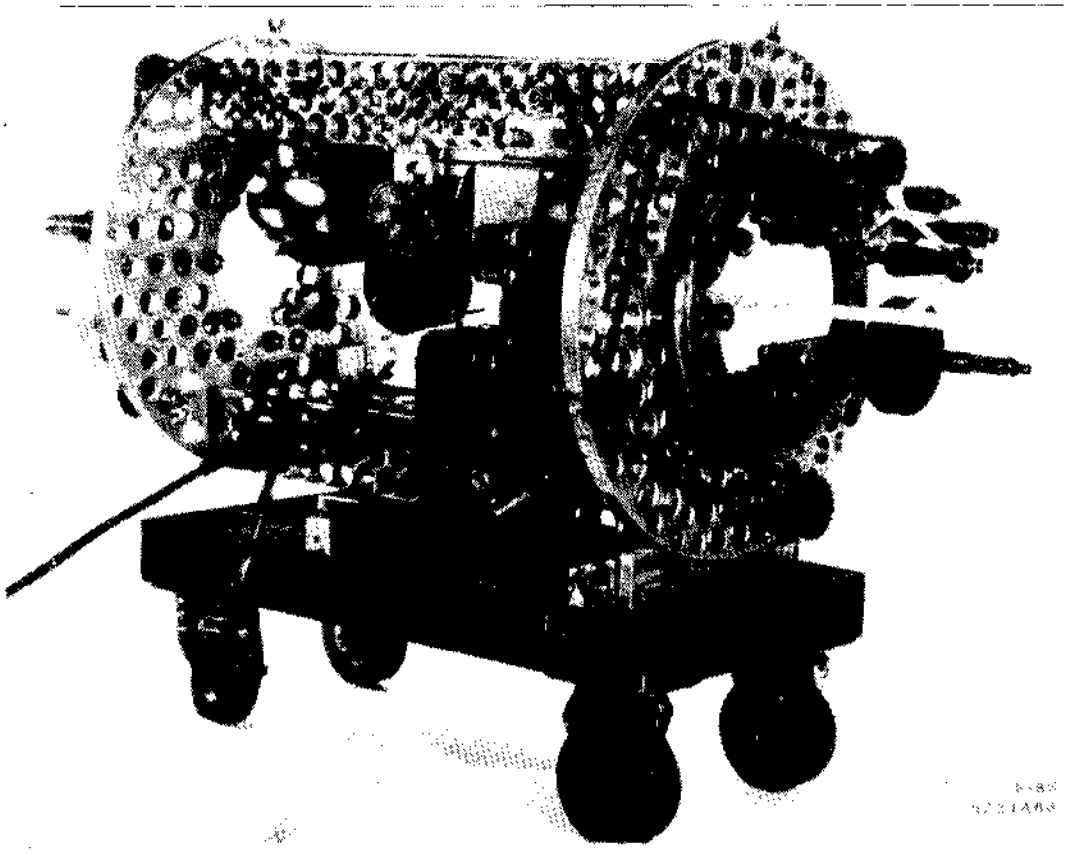

Fig. 5.13. An Automatic Insulation Tape Winder.

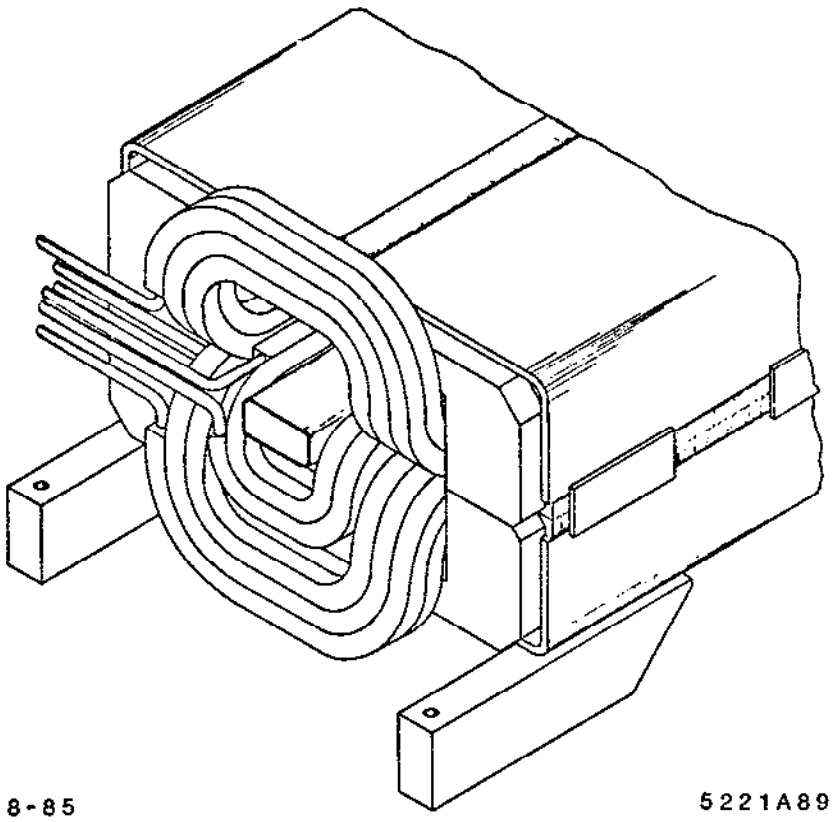

Fig. 5.14. Example of "Dog Eared" Coil Ends.

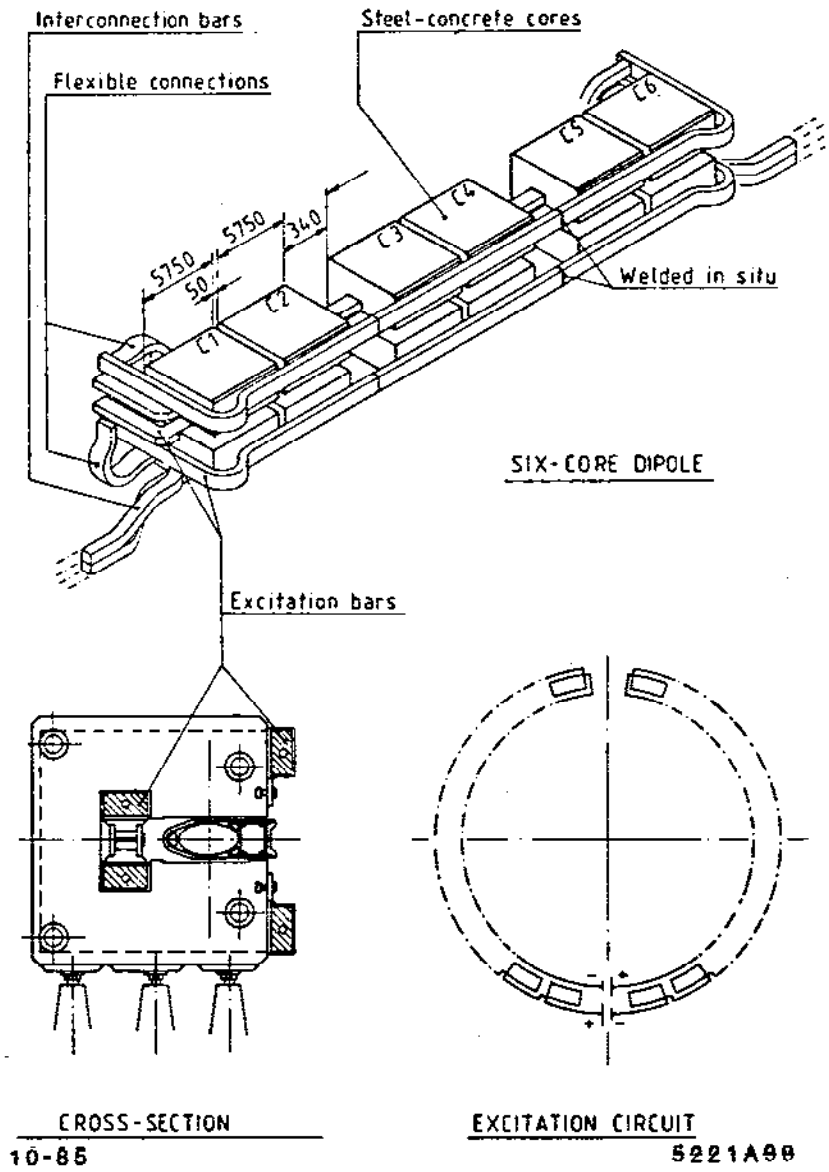

Fig. 5.15. LEP Six-Core Dipole Conductor Design that Minimizes "Coil Ends".

5.3 An Exercise Problem

Now that you have heard thirty-five years of magnet practice go by in two hours you should have become accomplished magnet designers and I would like to provide you with a small test problem. To all who hand in a solution (SLAC Bin No. 12), I will return comments. To aid you in this task I have provided you with the boy physicists crib sheet in wallet card form (Figure 5.16) and some ancient UCRL Engineering Design Data sheets (Figures 5.17 and 5.18) which are as useful today as the day they were written.

A WALLET CARD OF FORMULAS AND UNITS

I. Lorentz Force:

$$\vec{F} = q \pm (\vec{v} \times \vec{B})$$

$$d\vec{F} = I\, d\vec{l} \times \vec{B}$$

$$\frac{F}{l} = \frac{\mu_o}{4\pi} \frac{2 I I'}{a} \quad \text{newtons/meter}$$

II. Magnetic Rigidity

P (ev/c) = 300 (B gauss ρ cm)
P (Gev/c) = 0.3 (B *tesla* ρ meters)
In which 3 = 2.99792458

III. Bending angle

$$\Theta\ rad = \frac{\int B \cdot dl}{(B\rho)}$$

IV. Biot and Savart

$$d\vec{B} = \frac{\mu_o}{4\pi} \frac{I\, d\vec{l} \times \vec{r}}{r^2}$$

$$B_{\text{line current}} = \frac{\mu_o}{4\pi} \frac{2 I}{a}$$

$$B_{\text{solenoidal}} = \mu_o \frac{N I}{l}$$

Amperes Law:

$$\oint B \cdot dl = N I = \oint B/\mu \, . dl = \frac{B\, l_{gap}}{\mu_o} + \frac{B\, l_{iron}}{\mu_o} \frac{\mu_o}{\mu_{iron}}$$

$$\therefore N I = 2.02\ B\ (\text{gauss})\ \text{Gap}\ (\text{inches})$$

VI. Reluctance: In *MMF*, the counter part of resistance.

$$R = \frac{l}{\mu A}$$

VII. Inductance:

$$L\ (\text{henries}) = \frac{N \Phi\ (\text{webers})}{I\ (\text{amperes})}$$

$$\Phi = \int B.da \quad (\text{weber/m}^2)(\text{m}^2)$$

VIII. Energy stored:

$$W\ (\text{joules}) = \tfrac{1}{2} L I^2 = \tfrac{1}{2} \int \mu H^2\, dv$$

IX. Faradays Law:

$$E\ (\text{volts}) = -\frac{N\, \partial \Phi}{\partial t} = -\frac{N\, \partial BA}{\partial t}$$

X. Time constant:

$$\tau\ (\text{secs}) = \frac{\sum L_i \quad (\text{henries})}{\sum R_i \quad (\text{ohms})}$$

XI. Water Temperature Rise:

$$\Delta T\ (\text{deg C}) = \frac{3.8 \times P\ (KW)}{Q\ (\text{gal/min})}$$

XII. Skin Depth:

$$\delta\ (\text{cm}) = \sqrt{(\rho/\mu\omega)} = \frac{6.6 \text{ for Copper}}{\sqrt{f\ (Hz)}}$$

$$\sim 7/\sqrt{f}\ \text{cm for Iron}$$

XIII. Radiation Dose:

1 Rad = 100 ergs/gram deposited
= 6.3×10^7 mev/gram
~ $10^9 \gamma$ ~ 3.5×10^7 min.ioniz./cm²

Force: Newton = 10^5 dynes = weight of 1 apple, 1 Kg force = 2.2 # = 9.8 Newtons
Magnetic Field H: 1 Amp turn/meter = $4\pi/10^3$ Oersteds
Magnetic Induction B: 1 Weber/m² = 10^4 Gauss = 1 Tesla
Flux: Φ 1 Weber = 1 volt second
Inductance L: 1 Henry = 1 volt second/Ampere
Energy: 1 joule = 1 watt second = 10^7 ergs
Permeability of free space: $\mu_o = 4\pi \times 10^{-7}$ webers/amp.meter or henry.meter

8-85 5221A90

Fig. 5.16. A Wallet Card of Magnet Related Formulas.

RADIATION LABORATORY · UNIVERSITY OF CALIFORNIA · BERKELEY

DESIGN DATA

DATE 6/5/52 | U.W. NO. 56 | PAGE 1

SUBJECT: MAGNET DESIGN INFORMATION

PREPARED: A. Schmidt, D.T. Scalise

CHECKED BY: M. Kane, L. E. Brown

CONDUCTOR PROPERTIES

CONDUCTOR	Specific Weight Lbs./Cu.In.	RESISTIVITY = ρ (Microhm inches) at 20C.	at 40C.	$0C \leq t \leq 120C$	Heat Conductivity at 20 C. (Watts/in.°C)	Specific Heat at 20 C. (Watt Sec/Lbs.°C)	Linear Coef. of Thermal Expansion. (per°C.)
ALUMINUM Internat'l Al. Std.(99.58% Al)	.098	1.11	1.20	$\rho = .00453(t+225)$	5.4	430	23.9×10^{-6}
COPPER Internat'l Annealed Cu. Std.(99.91% Cu)	.321	.679	.732	$\rho = .00267(t+234)$	9.76	175	16.8×10^{-6}
SILVER (99.98% Ag)	.380	.64	.69	$\rho = .0025(t+236)$	10.52	106	18.8×10^{-6}

FORMULAS INDEPENDENT OF MATERIAL

(Ampere turns for gap) = 2.02 x (gauss) x (inches gap)

(Pounds force on conductor) = (1/1750) x (kilogauss) x (amperes) x (inches length)

(Pounds forces between pole faces) = (1/1.735) x (kilogauss)^2 x (sq. inches area)

CONDUCTOR FORMULAS DEPENDING ON MATERIAL AND TEMPERATURE

	Coefficients at 40 C.		Coef. at any temperature proportional to
(kilowatts) x (tons) =	(.059) Al, (.118) Cu, (.131) Ag	$\times$ (Mega-amp. turns)^2 x (inches mean turn length)^2	ρw
(Amperes)/(sq.inch) =	(202) Al, (469) Cu, (525) Ag	$\times \sqrt{\frac{\text{(kilowatts)}}{\text{(tons)}}}$	$\sqrt{\frac{w}{\rho}}$
(Sq. inches Cross Section) =	(4.95) Al, (2.13) Cu, (1.90) Ag	$\times \frac{\sqrt{\text{(kilowatts) x (tons)}}}{\text{(volts) x (parallel paths)}}$	$\sqrt{\frac{\rho}{w}}$
(Sq. inches Cross Section) =	(1.20) Al, (.732) Cu, (.69) Ag	$\times \frac{\text{(Mega-amp. turns) x (inches mean turn length)}}{\text{(volts) x (parallel paths)}}$	ρ
FOR RECTANGULAR CONDUCTOR LOSING HEAT FROM TWO EDGES			
(Degrees C. rise at center) =	(.028) Al, (.0094) Cu, (.0082) Ag	$\times (10^{-6}) \times$ (inches width)^2 x (amperes/sq. in.)^2	$\frac{\rho}{k}$
(watts)/(sq. in. edge surface) =	(.60) Al, (.366) Cu, (.345) Ag	$\times (10^{-6}) \times$ (inches width) x (amperes/sq. in.)^2	ρ

SYMBOLS: ρ = resistivity; w = specific weight; k = heat conductivity

REFERENCES: UCRL Chart I-1027; Chem. Physics Handbook, Circular 31 Bureau of Standards

DTS:plc

8-85

6221A91

Fig. 5.17. A "UCRL" Design Data Sheet of 1952.

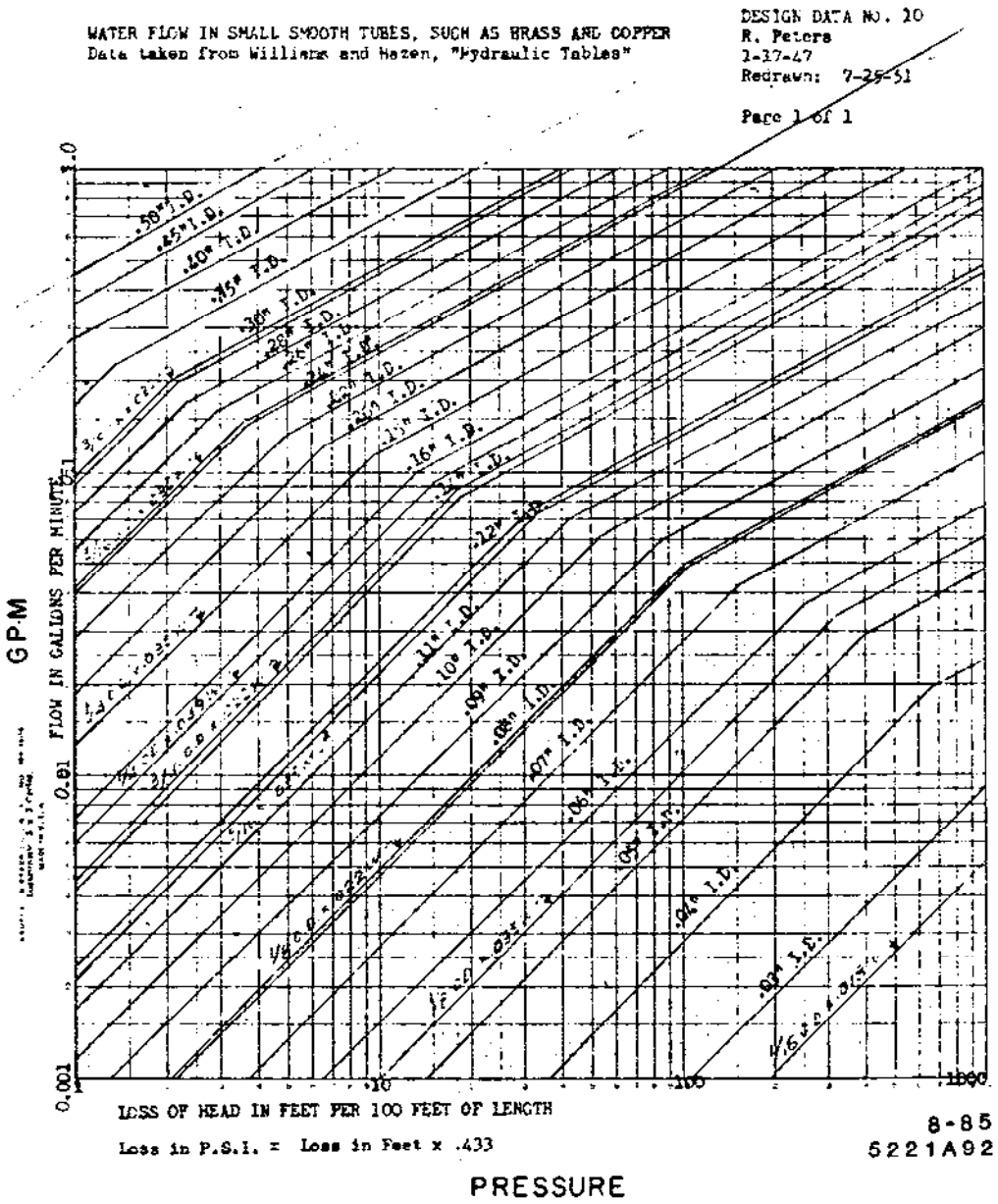

Fig. 5.18. Pressure – Flow of Water in Small Smooth Tubes (a UCRL Design Data Sheet of 1951).

Problem:

Four DC steering magnets are required for some injection lines, each to produce an angular deflection of 4 milliradians for 15 GeV/c electrons. The space reserved, along the beam line, for each magnet is 1.2 meters. The vacuum tube is circular and has an outside diameter of 46 mm. The field uniformity requirement on $\int B \cdot dl$ versus x is approx. $\pm 3/1000$. The available power supply for each magnet is capable of delivering 36 volts at 30 Amps and is located 300

meters from the magnets. Provide a conceptual design for these magnets (H type) and make a very rough cost estimate.

REFERENCES – CHAPTER 5

105. MT-2 (1967) p. 305. H. Brechna (SLAC).
106. Hoesch Estal, Eberhardstrasse 12, D-4600 Dortmund 1, West Germany. Tel. (0231) 8443292.
107. MT-3 (1970) p. 45. A. McInturff and J. Claus (BNL).
108. MT-3 (1970) p.1205. H. Vogel (LAL).
109. NS-30 (1983) p.3472. Tannenbaum et al. (BNL).
110. NS-16 (1969) p. 777. E. Roskowski (SLAC).
111. NS-14 (1967) p. 398. M. Green (LBL).
112. NS-20 (1973) p. 708. H.M. Holbud and J. Shill (Columbia U., N.Y.).
113. MT-2 (1967) p. 341. G. Pluym and M.H. Van de Voorde (CERN).
114. NS-12 (1965) p. 683. H. Brechna (SLAC).
115. H. Brechna, SLAC Report-40, March 1965.
116. NS-16 (1969) p. 611. A. Harvey and S.A. Walker (LAL, Pyrotenax).
117. MT-4 (1972) p. 456. A. Harvey (LAL).
118. MT-3 (1970) p. 677. D.R. Willis and D. Wilson (Lintott, Susses, U.K.).
119. MT-3 (1970) p. 1224. A.T. Gresham et al. (Rutherford).
120. NS-22 (1975) p. 1100. R. Grouiran (CERN).
121. NS-22 (1975) p. 1042. M.T. Wilson (LAL).
122. NS-30 (1983) p. 3617. R. Griegs et al. (LANL).
123. NS-18 (1971) p. 887. W.O. Brunk, C.A. Harris and D.B. Robbins (SLAC).
124. NS-16 (1969) p. 650. G. Homsy and W. Jones (CEA).
    NS-16 (1969) p. 654. E. Eno et al. (LBL).
125. T.M. Taylor, CERN ISR-MA/76-6 (1976).
126. NS-30 (1983) p. 3614. J.P. Gourber et al. (CERN).
127. MT-4 (1972) p. 349. R. Main and R. Yourd (LBL).
128. MT-6 (1972) p. 134. A.A. Koch et al. (BBC Zurich).